Answers to Anonymous Referee #1

We thank anonymous referee #1 for his/her helpful comments and suggestions. We revised the manuscript according to his/her comments and the comments of anonymous referee #2. In the following answer to the referee we decided to give

- *referee comments in italic*
- our answers in normal format and
- **textual changes in the manuscript in bold format.**

We revised our manuscript according to the comments of anonymous referee #1 and #2, of which the main changes are as follows:

(1) Revision of the theory section: the equations for the sub-adiabatic model do now consider the sub-adiabatic state as the general case and can be transformed to the adiabatic case by setting $f_{ad} = 1$.

(2) The order of the theory and data section was reversed, so that the reader first gets a clear picture of the methods that are used and of the observed data that are available from the satellite and ground perspective. The following results section starts with an overview of parameters observed and used for the retrievals of key parameters which then can be compared to each other.

(3) A comprehensive revision of the introduction to introduce the goals earlier, and give a more focused overview of previous studies that use similar instruments and methods.

(4) We added an overview table of parameters considered in other studies that applied the sub-adiabatic model, to give a better comparison and motivation to what is done in this work.

(5) We omitted the presentation of method OE2, which led to some confusion. Instead we added a comparison of the adiabatic factor as derived from ground based observations using (a) the observed cloud geometrical depth from radar and ceilometer as well as the liquid water path from the microwave radiometer and (b) the observed radar profile and the adiabatic radar profile which can be calculated from the results of the OE1 method.

(6) To avoid confusion by introducing a "virtual adiabatic cloud geometrical depth" calculated from the ground-base microwave radiometer, we splitted the comparison of satellite and ground into Q_L and H. This means the following new structure of the results section: (a) comparison of ground-based parameters: f_{ad} and f_{ad}^{OE} (b) comparison of ground-based parameters: N_d^{FI} and N_d^{OE} (c) comparison of ground- and satellite-based parameters: Q_L (d) comparison of ground- and satellite-based parameters: H (e) comparison of ground- and satellite-based parameters: N_d

(7) We completely redid the figures for this study and hope that these are easier to read now.

We adress more specific remarks in the following:

(C1) *I would encourage the authors to include a more explicit overview of the* f_{ad} *values reported in the literature, of how it is represented in retrievals of* N_d *and* H*, and to provide a more direct comparison to the other studies that have focused on* H *and* N_d *retrievals. I will use the example of the southeast Pacific because I am most familiar with that literature, but I would encourage the authors to be as fully comprehensive as possible.*

(A1.1) To give a better overview of f_{ad} in literature and how it is represented in the retrievals of N_d and H from passive satellite remote sensing, we added a table to our manuscript.

(A1.2) To give a more direct comparison to other studies findings regarding H and N_d retrievals, we added the following sentences to our discussion in the results section:

regarding H: **The correlations for temporally averaged data are within the range of values that were obtained by Roebeling et al. (2008b), Min et al. (2012) and Painemal and Zuidema (2010). Roebeling et al. (2008b) found correlations of 0.71 between SEVIRI and Cloudnet for a homogeneous stratocumulus cloud layer. Min et al. (2012) found correlations of 0.62 between in-situ and MODIS retrieved H, and could show a better agreement of H when the adiabatic factor is explicitely calculated and considered. Painemal and Zuidema (2010) found correlations of 0.54 (0.7 for $H < 400\,\mathrm{m}$ with cloud fraction$> 90\,\%$) comparing radiosonde-derived cloud geometrical depth to respective MODIS observations. In their study Painemal and Zuidema (2010) reported that satellite values were higher compared to the ground-based ones. The reason for this can potentially be explained by a bias of MODIS-retrieved r_e but also in the choice of the adiabatic factor in the retrieval of H. Satellite derived H increases if we choose $f_{ad} < 1$ instead of $f_{ad} = 1$.**

(...)

For the cases investigated here, we saw a better agreement in H for available MODIS retrievals compared to SEVIRI if $f_{ad} = 1$ is choosen. Indeed, clouds are actually sub-adiabatic while the retrieval assumes adiabatic clouds. This could counteract a high bias in MODIS r_e that is reported in previous studies (Marshak et al., 2006). For the four cases considered in this study, the number of collocated observations with MODIS is not sufficient in order to determine which effect is predominant for the bias. Therefore a larger dataset would be desirable for a more in-depth investigation.

regarding N_d:

The importance of r_e for the retrieval of N_d from passive satellite imagers has already been pointed out by previuos studies. Those which were mainly based on MODIS (Painemal and Zuidema, 2010, 2011; Ahmad et al., 2013; Zeng et al., 2014). Painemal and Zuidema (2010) report a high bias of MODIS-derived r_e, but also state that the choice of the other parameters in the retrieval (namely k, Γ_ad) is able to compensate for this effect so that still a good agreement between MODIS retrieved and in-situ values could be achieved. A high bias of r_e occurs for broken cloud conditions (Marshak et al., 2006). Zeng et al. (2014) also saw a good agreement for MODIS derived N_d (using $f_\mathrm{ad} = 0.8$) with CALIOP (Cloud-Aerosol Lidar with Orthogonal Polarization), although they found a high bias in r_e compared to POLDER (Polarization and Directionality of the Earth Reflectance).

Ahmad et al. (2013) also points out the importance of the effective radius for the N_d retrieval. As mentioned before, for our study only few MODIS observation points are available, but we already see that discrepancies in r_e in comparison to SEVIRI are a major source of uncertainty for N_d.

(C2) *For example, Painemal, D., and Zuidema, 2010, ACP, found an overestimate in H_{sat} when compared to ship-board measurements, that they attributed to an overestimate in the satellite re (see their appendix). This is similar to the current studys findings, in that this studys H_{sat} is lower than that measured from the ground - which they attribute to an underestimate in satellite re. So both the Painemal and Zuidema and the current student highlight the importance of the satellite-derived re, with the solar zenith angle differences (I think) resulting in the opposite sense of the bias.*

(A2) See answer A1.2.

(C3) *Regarding N_d, there is some disagreement in the literature on how best to calculate N_d from satellite that is related to f_{ad}. The authors cite Bennartz, 2007 - its N_d calculation assumed an f_{ad} of 0.8. Painemal and Zuidema 2011 (JGR) p. 8 discuss how f_{ad} is represented in their Nd calculation vs. that by George and Wood (2011), and Painemal and Zuidema 2013 (ACP) eqn 9 provide another approach for calculating N_d that allows for a fluctuating f_{ad}. I would encourage the authors to be more explicit on how their study fits in with these and other similar studies, and then use the opportunity to opine on what they think is the best approach for satellite retrievals over Germany.*

(A3.1) According to suggestions of referee #2 we restructured the section about the sub-adiabatic cloud model and introduce the general set of equations considering explicitely the adiabatic factor. We explained more explicitely that in our study for calculating N_d (and H) we use $f_{ad} = 1$ in a first step and try to include the adiabatic factor calculated from ground-based observations in a second step.

(A3.2) For a comparison on the adiabatic factor choosen in other studies we added a table. On the discussion of the importance of the adiabatic factor for the retrieval of H and N_d see also answer A1.2.

Specific comments

(C4) *abstract: the optimal estimation technique only considers variations in f_{ad}. please clarify. also mention location, and the 4 dates (these provide some information on the synoptics). mention that the current SEVIRI retrieval underestimates re relative to ground and MODIS measurements (rather than sensitive to satellite re retrieval).*

(A4.1) For a discussion about the OE method see answer A12.

(A4.2) We added location and dates in the abstract: **We investigate four different cases (27 October 2011, 1 June 2012, 27 September 2012 and 21 April 2013) of temporally homogeneous and inhomogeneous liquid cloud layers observed over Germany.**

(A4.3) We changed the last sentence in the abstract to: **For all evaluated cases, the current SEVIRI retrieval seems to underestimate the effective radius relative to ground-based and MODIS measurements for unfavourable solar zenith angles of**

above approximately $60°$. This deviation strongly propagates to the derived cloud droplet number concentration.

(C5) *introduction: many previous studies are cited. at this point the reader is not yet clear on what the authors are doing. please group the studies that have similar goals but use different instruments (eg lidar, solar radiometers) separately, then discuss the papers that have applied similar instrumental datasets to this study. Briefly but more explicitly summarize previous findings relevant to the current study on f_{ad} and major uncertainties. Mentioning location of the previous findings and contrasting to the cloudnet site used here can be one way to establish originality. which previous studies are most similar to what the authors pursue here? mention the cloudnet site location explicitly and the 4 dates. mention the OE approach constrains itself to the f_{ad} model only, and justify why, including why radiometric noise is not being considered. also, how does this study differentiate itself from the cloudnet products? a table might be a nice way to present the results from previous studies (and this one).*

(A5.1) We restructured the introduction and added a table for easier comparison of values considered by other authors within the sub-adiabatic model. Location of the Cloudnet site and the 4 dates are now explicitely mentioned. We stated the main goal of the paper at an earlier position in the introduction. We decided for the following structure for the revised introduction: The introduction now first motivates the importance for investigating key parameters for the first indirect effect. We afterwards state the overall goal of the study. Then we list a shorter and more focused overview of ground-based retrieval methods for these key parameters. Afterwards we outlined the importance of the adiabatic model for the satellite retrieval. Herein also its major uncertainties are shortly mentioned. Finally, a short outlook on the remaining part of the paper is given.

(A5.2) To also give a stronger motivation for our study we added the following sentence to the introduction: **To our knowledge such evaluations from the SEVIRI instrument for the indirect aerosol effects' key parameters have been rarely carried out (e.g. in Roebeling et al. (2008a))**

(A5.3) The main difference to the standard Cloudnet products lies in the estimation of N_d which is not provided by Cloudnet. We added the following sentence: **Since Cloudnet does not provide N_d, we developed and apply an optimal estimation technique to obtain N_d, based on the method introduced by Fox and Illingworth (1997), similarly also applied in Rémillard et al. (2013).**

(A5.4) For discussion of the OE method see answer A12.

(C6) *2.1 first paragraph could well go in the introduction. be more specific about the instruments and dates.*

(A7) We listed the ground-based instruments more specifically and moved the first paragraph to the introduction.

(C7) *2.1 bottom of p. 5134. why were no soundings used? the simulated cloud top heights do not match those observed by the radar well according to fig. 1 but I see little discussion of this anywhere.*

(A7) Indeed, there is a disagreement of cloud top height from SEVIRI and the ground-based radar. The reason for the disagreement is multifold. On 21 April 2013 there is a semitransparent cirrus cloud layer present at around 10km. While the radar-based cloud top height refers only to the liquid cloud layer, the effective brightness temperature in the 10.8 channel used for the SEVIRI method is altered due to the semitransparent cirrus cloud.

On 27 October 2011 we hypothize that a inversion layer is present at Leipzig. For the Leipzig site no soundings are available. The closest available sounding is at the DWD site Lindenberg. The 12 UTC sounding shows an inversion layer at around 1000m, consistent with the cloud top height obtained from the radar. But there is also a second less pronounced inversion layer present at around 3000m. This ambuigity is known to result in biases for cloud top height (Derrien et al., 2005).

On 01 June 2012 and 27 September 2012 the cloud top height agrees reasonable well when temporally longer overcast periods occur. In the remaining periods broken clouds occur that can not be resolved by the satellites spatial resolution. Therefore the brightness temperature within one satellite pixel stems from clouds and surface within this pixel, leading to warmer brightness temperatures and therefore lower cloud top heights.

We added the following short discussion to the paper: **While for some time periods a good agreement can be seen, also periods with large discrepancies are found. Differences may result from semitransparent cirrus cloud layers (21 April 2013), inversion layers (27 October 2011) or broken cloud conditions (1 June 2012 and 27 September 2012). In the following we sum up the synoptic conditions for each case.**

(C8) *2.2 line 5: the most interesting cloud deck - please make this more specific/objective.*

(A8) We rephrased the sentence: **For this study, we focus on four ideal cases to gain a better understanding of the microphysical processes within the cloud by ruling out side-effects accompanying complicated cloud scenes such as multi-layer clouds as well as possible. We consider single-layer cloud systems which are entirely liquid and non-drizzling as ideal. We chose cases in a way that cloud layers are well-observed by all ground-based instruments and by MODIS and SEVIRI.**

(C9) *2.2 how was the drizzle/no-drizzle threshold specified? how sensitive are your results to this threshold? at the other end, how sensitive is the radar?*

(A9.1) For our study we used the Cloudnet target classification of rain/drizzle which uses the Doppler velocity to identify falling droplets. According to typical thresholds used in other studies we checked the threshold of a maximum column radar reflectivity Z_{max} = -20dBZ.

Rémillard et al. (2013) believed that if Z_{max} stays below -20dBZ drizzle contribution is minimal. Martucci and O'Dowd (2011) found mean radar reflectivity of -8dBZ in drizzle case, and mean radar reflectivity of -44dBZ in non-drizzle case, while Mace and Sassen (2000) demonstrated high frequency of light drizzle with radar reflectivity above -20dBZ (cumulative propability of around 20% at 0dBZ).

None of our profiles not already excluded by the Cloudnet target classification did exceed this value. The daily maximum values for all Z_{max} values are Z_{max} (21 April 2013) = -29.0 dBZ, Z_{max} (27 September 2012) = -24.2 dBZ, Z_{max} (27 October 2011) = -27.3 dBZ, Z_{max} (01

June 2012) = -24.9 dBZ.

(A9.2) The minimum of detectable radar reflectivity (Z sensitivity in Cloudnet) ranges from -88dBZ at the lowermost level ($\sim 150m$) to -40dBZ at the topmost level ($\sim 15.500m$).

(C10) *2.2 p. 5140 lines 6- 19: why not provide your own estimate of the uncertainty in $\Gamma_{ad}(T,p)$? you can estimate the cloud base temperature for your 4 cases. given the poor NWP estimate of cloud top temperature, this would provide a stronger argument for a smaller Γ_{ad} uncertainty than what you provide here.*

(A10.1) For the calculation of N_d we actually estimated Γ_{ad} for each timestep using T_{cth} and p_{cth} from the satellite, since this can be applied when there is no accomponying ground-based data. We agree that according to the higher uncertainties in satellite derived cloud top temperature and pressure, we could make use of cloud base temperature and pressure instead to calculate Γ_{ad} in this study. We recalculated the results for the 4 cases. This resulted also in a small change of the statistical numbers in our comparison (see revised manuscript [attachment]).

(A10.2) The Γ_{ad} uncertainty of 24% is the value given by Janssen et al. (2011) when they considered the whole seasonal variability of the cloud base temperature. If we compare Γ_{ad} calculated from satellite cloud top temperature and pressure with the one calculated from cloud base values we find an uncertainty of 15% considering all 4 cases. As we see some deviations in the cloud top height, we believe that this can be mainly attributed to uncertain satellite estimates of cloud top properties.

(C11) *p. 5142 line 9: please clarify what the beta index is for the reader rather than referencing other papers.*

(A11) We rephrased the paragraph: **Thereby it is assumed that the droplet size distribution can be described by a gamma distribution with parameter β, where β is the index of the gamma function following the size distribution definition in (Fox and Illingworth, 1997; Martucci and O'Dowd, 2011):**

$$N(r) \propto Ar^{\beta} \exp\left(-Br\right) \tag{1}$$

Thereby B is the rate parameter and A a function of the rate parameter.

(C12) *3.3.2: please explain why we should care about f_{ad} to the exclusion of other factors. this should go in the introduction. among other factors worth considering Id also suggest the radar vertical resolution and radar sensitivity, and the beta index, which serves as a measure of the droplet spectral width. how confident are you in the ground-based H retrievals?*

(A12) According to comments of referee #2 we decided to limit the investigation to the OE1 method. This method does not require the assumption of an linear increasing liquid water content profile, but N_d is considered vertically constant. The OE method includes error estimates from Cloudnet, also including radiometric noise (in the discussion paper stated ambigiously as observation errors) and forward model error. Only the representativeness error is neglected. The forward model error is estimated as described in the paper by an estimate of the standard deviation when different values for β are assumed. We tried to state this more clearly in the revised manuscript:

The observation error covariance can be split up into individual contributing parts such as forward model error, radiometric noise error, and representativeness error. In this study the representativeness error is neglected, since observations and state variables are on the same grid. Radiometric noise errors are given by the Cloudnet algorithm. The forward model error is estimated by applying values of β in the range of 1 to 6 to the radar forward model and taking the variance of the resulting reflectivity values for a sample cloud profile with a geometrical extent of 700 m and linearly increasing q_{L} in steps of 0.1 gm^{-2} per 100 m.

(C13) *3.3.2: doesnt the radar Z profile give you some information about f_{ad} ? do all the cases show a Z profile that increases with height, as one would expect for a non- drizzling cloud? I cannot tell from the figures.*

(A13.1) In Fig. 1 of the revised manuscript we added some sample Z profiles to give a better impression than from the Z time-height-plots alone. Here the increase of Z with height can be seen clearly especially for the homogeneous cases.

(A13.2) We can estimate the adiabatic factor by relating the observed Z profile to an adiabatic Z profile. The latter means that we could use the adiabatic liquid water content profile and use the relationship in Fox and Illingworth (1997) to simulate the adiabatic Z profile. This would further require an assumption about cloud droplet number concentration. We use our N_d^{OE} to cross-check the adiabatic factor using this method and the one applying Q_L and H_{cloud}. The results can be seen in the added scatter plots (3) to the revised manuscript. We see that overall both independent methods give results in the same range with good correlation. But also it is observed that the method using H and Q_L gives slightly higher values for the adiabatic factor. Explanations for this difference could be due to the uncertainty in H, but also in retrieved N_d which still has larger uncertainties as our OE method points out.

We added the following paragraph to the ch. 2.2.2 of the revised manuscript:

Given the retrieved $N_{\mathrm{d}}^{\mathrm{OE}}$ and the theoretical adiabatic liquid water content for the observed cloud geometrical depth, we are able to calculate an adiabatic radar profile applying the relationship of q_{L}, Z and N_{d} of Fox and Illingworth (1997). If we relate Z_{ad} to the Z_{obs} from the cloud radar we obtain a second method to calculate the adiabatic factor ($f_{\mathrm{ad}}^{\mathrm{OE}}$):

$$f_{\mathrm{ad}}^{\mathrm{OE}} = \frac{\int Z_{\mathrm{obs}} dz}{\int Z_{\mathrm{ad}} dz} \tag{2}$$

We also added the following discussion to ch. 4.1.1 of the revised manuscript:

For cross-checking with an independent approach, we also calculate the adiabatic factor using the information of the radar reflectivity profile. We see in Fig. 3 that the mean adiabatic factor calculated from the radar profiles is generally a bit lower, and that the correlation for all four cases is quite good with 62 % to 95 %, and root mean square differences between 0.14 and 0.24. This difference is likely explained by uncertainties in $H_{\mathrm{obs}}^{\mathrm{ground}}$ and Q_{L}, but also in Z obtained from the cloud radar and the retrieved N_{d}. In the following we will use the adiabatic factor calculated from Q_{L} and $H_{\mathrm{obs}}^{\mathrm{ground}}$.

(C14) *3.3.2 p. 5143 lines 23-26: only now are the readers told the methodological constraints imposed upon this study. these need to go into the introduction and motivated better.*

(A14) We tried to state our methodology and the required assumptions more clear in the revised manuscript.

(C15) *4.1.1. p. 5145 lines 8-9: please be more specific about the contribution to enhanced* Q_L *by drizzle and the underestimation of actual* H_{cloud}. *perhaps subsample your dataset further to exclude such cases? further on on p 5146 you mention it is primarily the* $H < 400\,m$ *clouds that are superadiabatic. is this because the radar doesnt see the upper radar range gates? estimate the resulting uncertainty.*

(A15.1) Indeed, drizzle should not enhance Q_L for the thin clouds considered here, and the cloud radar should be able to see the upper range gates. The cloud radar is known to have issues with the cloud base, but this is covered by the use of a ceilometer. But still, the uncertainties of the MWR of $20\,gm^{-2}$ and of H of $60\,m$ due to the instruments vertical resolution, can easily add up to errors in the adiabatic factors that lead to superadiabatic artefacts. We outlined the uncertainty estimate in the discussion paper on page 5146 for such thin clouds, but move this discussion further up in the revised manuscript.

(A15.2) Since we want to point out the uncertainty in the adiabatic factor due to thin clouds when ground based measurements are taken into account, we will keep the discussion about superadiabatic artefacts but exclude $f_{ad} > 1$ in our further investigation ($f_{ad} > 1.5$ previously).

(C16) *4.1.1. p. 5146, line 12-15: finally, a quantitative assessment of* Q_L *and* H *uncertainty. I would suggest subsetting your sample to reduce the relative size of these contributions.*

(A16) See answer A15.

(C17) *p. 5148 line 7-10: I cannot see this feature in fig. 1b.*

For adiabatic clouds the radar reflectivity profile should increase linearly. For the time-period mentioned here the radar profiles shows two peaks due to a more multi-layer-like cloud structure, which can be seen in Fig. 1b.

(C18) *p. 5150 line 4:I would be surprised if drizzle is strongly contributing to a higher microwave-derived* Q_L. *see Zuidema et al., 2005 (JGR) Appendix A for a quantification, to develop your intuition on this. But if drizzle is apparent in the radar reflectivity profile, that profile doesnt meet the selection criteria and should not be considered, no?*

(A18) We agree with the referee that profiles containing drizzle do not meet the selection criteria. Indeed, none of our considered profiles did exceed the drizzle treshold of -20dBZ. Therefore the explanation for the difference is not found in drizzle as we already tried to point out. The observed difference could as well be attributed to the satellite retrieved value. Since at the same time period also the the CDNC shows larger differences the explanation might be found in problems of the satellite retrieval of τ and r_e.

(C19) *4.2.2: do you find modis-seviri differences in re and tau as a function of sza? if not previously reported, it would be useful to do so.*

(A19) Since only 4 cases with very few MODIS data points were considered in this study we are not able to draw statistically robust conclusion in this direction. But since a large solar zenith angle is known to lead to biases in the CPP retrieval for SEVIRI, we believe that it plays a role especially for the late autumn case of 2011-10-27. It definitely would be useful to investigate the MODIS-SEVIRI differences of r_e and τ as a function of the solar zenith angle for a larger dataset. This is currently investigated, but we feel that this is beyond the scope of the current study.

(C20) *4.2.2. page 5153, end: please, somewhere you need to discuss your drizzle reflectivity threshold and your sensitivity to that threshold.*

(A20) See answer A9.

(C21) *conclusions: it seems to me that the main contribution of the study could be to suggest a subadiabaticity factor for the satellite retrievals, or a way of incorporating subadiaticity into the satellite retrievals based on the initial retrieval of H and Nd. do the authors have any thoughts on how to do this? it is mentioned at the end but rather vaguely. or is a good take-away point that the SEVIRI re retrievals appear to be too low - is this an original finding? you mention solar radiation observations - are those available at the cloudnet sites?*

(A21.1) Adressing the suggestion of the adiabatic factor that can be used for satellite retrievals of H and N_d, we added the following paragraphs to the conclusion:

For 3 out of 4 cases we obtained similar median values around 0.65 ± 0.2 at different seasons. Although larger datasets are required to draw robust conclusions about a typical adiabtic factor, this value could be a first guess for homogeneous stratocumulus clouds as they occur over Central Europe.

So far only four cases were analyzed, but given the network of Cloudnet/ACTRIS in Central Europe this offers the opportunity to investigate the climatology of the adiabatic factor and investigate its regional, seasonal or synoptical dependency. Using more data from a greater network would give statistically more robust insights.

(A21.2) Regarding solar radiation measurements: Cloudnet sites generally require only a instrument set including cloud radar, microwave radiometer and ceilometer. At the LACROS site and also many other Cloudnet sites also solar radiation measurements (e.g. from a shadowband radiometer) are available.

(C22) *figures: the figures 1-2 are very difficult to read. perhaps in final form they will be a larger format? I would at least suggest using the plot size better, e.g., selecting y-ranges in fig 1 that show more of the data. could they perhaps be shown as 2x2 panels rather than one row of 4?*

(A22) We revised the figures. See revised figures below.

(C23) *fig. 1 a: I dont believe I saw the Seviri CTH overestimate discussed anywhere... fig. 6: modis and seviri are difficult to distinguish. fig. 7: extremely difficult to read. please find a way of enlarging.*

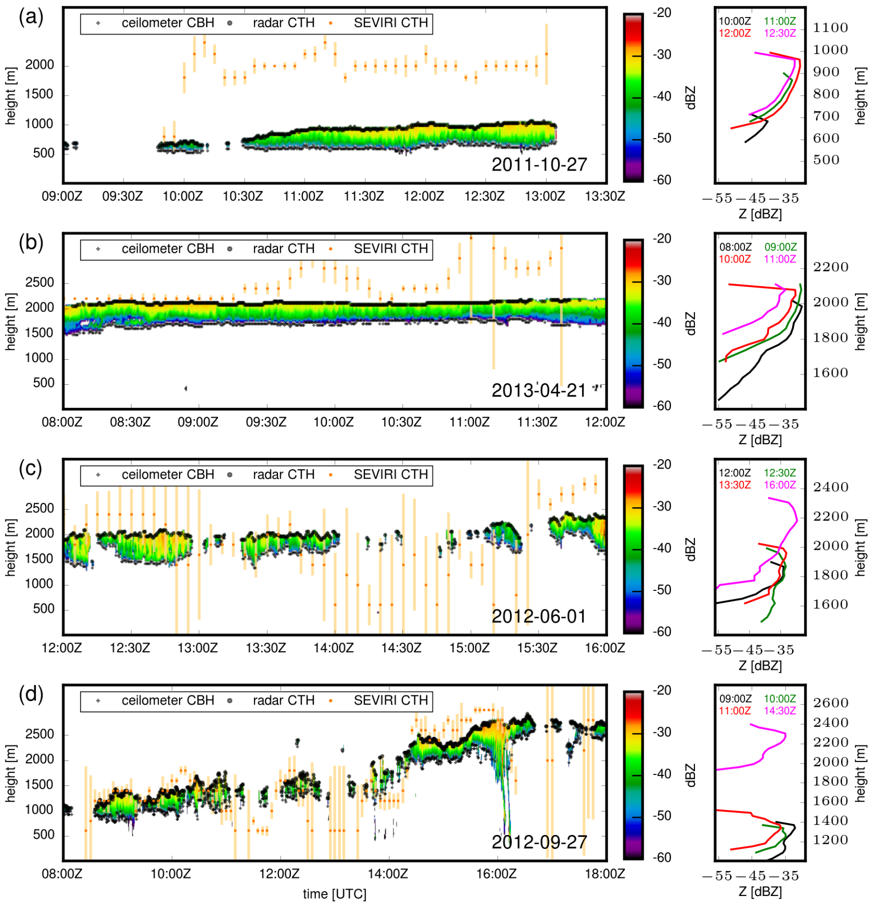

Figure 1: Time series of radar reflectivity (in dBZ) and cloud borders for the 4 cases; (a) 27 October 2011, (b) 21 April 2013, (c) 1 June 2012, (d) 27 September 2012. Cloud borders are shown as detected by Cloudnet with black dots and by SEVIRI using NWCSAF in orange dots. Sample profiles of radar reflectivity are shown for each case at different times.

(A23.1) We added the discussion of CTH differences (see answer A7). (A23.2) We also revised these figures. See revised figures below.

References

Ahmad, I., Mielonen, T., Grosvenor, D., Portin, H., Arola, A., Mikkonen, S., Kühn, T., Leskinen, A., Juotsensaari, J., Komppula, M., Lehtinen, K., Laaksonen, A., and Romakkaniemi, S.: Long-term measurements of cloud droplet concentrations and aerosol-cloud interactions in continental boundary layer clouds, Tellus B, 65, URL `http://www.tellusb.net/index.php/tellusb/article/view/20138`, 2013.

Derrien, M., Gléau, H., Daloze, J.-F., and Haeffelin, M.: Validation of SAFNWC/MSG cloud products with one year of SEVIRI data, in: 2005 EUMETSAT Meteorological Satellite Conference, pp. 95–103, 2005.

Fox, N. I. and Illingworth, A. J.: The Retrieval of Stratocumulus Cloud Properties by Ground-Based Cloud Radar, Journal of Applied Meteorology, 36, 485–492, doi:10.1175/1520-0450(1997)036¡0485:TROSCP¿2.0.CO;2, URL `http://dx.doi.org/10.1175/1520-0450(1997)036<0485:TROSCP>2.0.CO;2`, 1997.

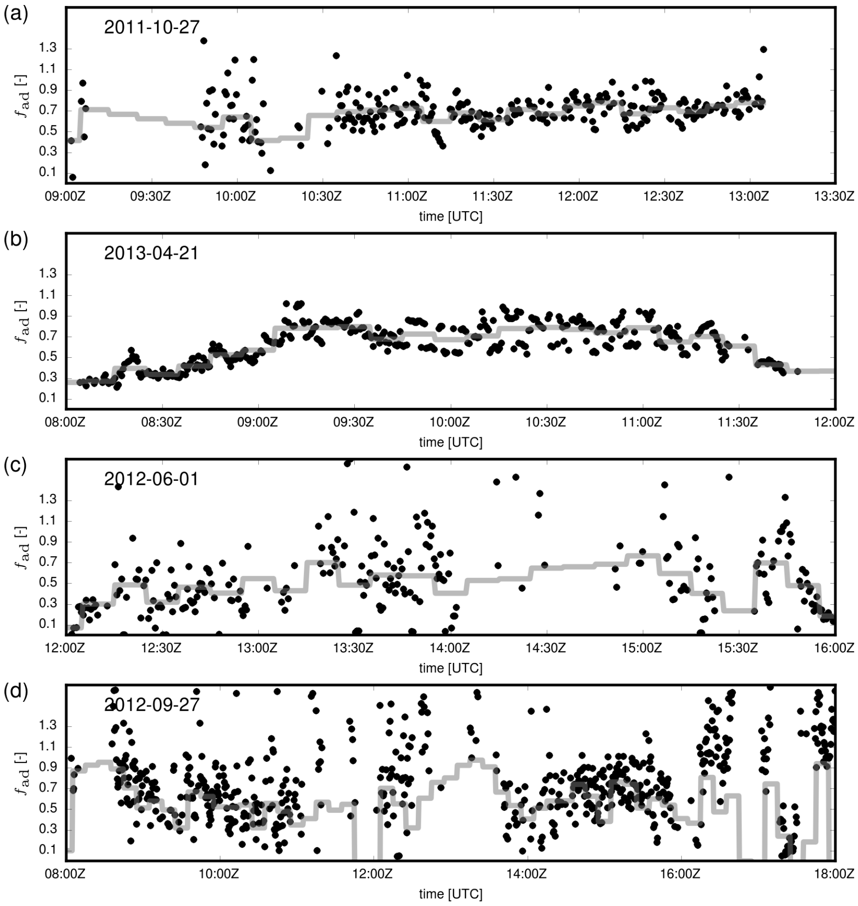

Figure 2: Adiabatic factor for all four cases. Black dots represent the adiabatic factor derived using ground-based geometrical depth and liquid water path from the microwave radiometer. The gray line represents the 10-min averaged and interpolated adiabatic factor neglecting superadiabatic values.

Janssen, R. H. H., Ganzeveld, L. N., Kabat, P., Kulmala, M., Nieminen, T., and Roebeling, R. A.: Estimating seasonal variations in cloud droplet number concentration over the boreal forest from satellite observations, Atmospheric Chemistry and Physics, 11, 7701–7713, doi:10.5194/acp-11-7701-2011, URL `http://www.atmos-chem-phys.net/11/7701/2011/`, 2011.

Mace, G. G. and Sassen, K.: A constrained algorithm for retrieval of stratocumulus cloud properties using solar radiation, microwave radiometer, and millimeter cloud radar data, Journal of Geophysical Research: Atmospheres, 105, 29 099–29 108, doi:10.1029/2000JD900403, URL `http://dx.doi.org/10.1029/2000JD900403`, 2000.

Marshak, A., Platnick, S., Várnai, T., Wen, G., and Cahalan, R. F.: Impact of three-dimensional radiative effects on satellite retrievals of cloud droplet sizes, Journal of Geophysical Research: Atmospheres, 111, n/a–n/a, doi:10.1029/2005JD006686, URL `http://dx.doi.org/10.1029/2005JD006686`, d09207, 2006.

Martucci, G. and O'Dowd, C. D.: Ground-based retrieval of continental and marine warm cloud microphysics, Atmospheric Measurement Techniques, 4, 2749–2765, doi:10.5194/amt-4-2749-2011, URL `http://www.atmos-meas-tech.net/4/2749/2011/`, 2011.

Min, Q., Joseph, E., Lin, Y., Min, L., Yin, B., Daum, P. H., Kleinman, L. I., Wang, J., and Lee, Y.-N.: Comparison of MODIS cloud microphysical properties with in-situ measure-

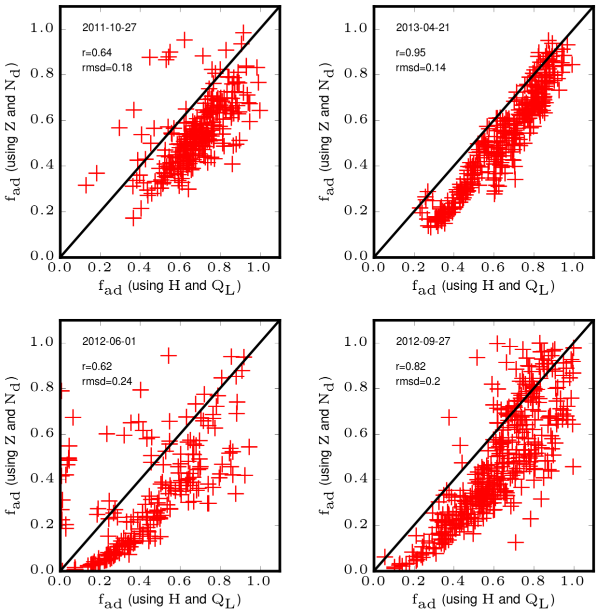

Figure 3: Adiabatic factor calculated from ground-based observations using H and Q_{L} (x-axis) and from Z and N_{d} (y-axis). Superadiabatic values are omitted. The graphs correspond to our four investigated cases.

ments over the Southeast Pacific, Atmospheric Chemistry and Physics, 12, 11 261–11 273, doi: 10.5194/acp-12-11261-2012, URL `http://www.atmos-chem-phys.net/12/11261/2012/`, 2012.

Painemal, D. and Zuidema, P.: Microphysical variability in southeast Pacific Stratocumulus clouds: synoptic conditions and radiative response, Atmospheric Chemistry and Physics, 10, 6255–6269, doi:10.5194/acp-10-6255-2010, URL `http://www.atmos-chem-phys.net/10/6255/2010/`, 2010.

Painemal, D. and Zuidema, P.: Assessment of MODIS cloud effective radius and optical thickness retrievals over the Southeast Pacific with VOCALS-REx in situ measurements, Journal of Geophysical Research: Atmospheres, 116, n/a–n/a, doi:10.1029/2011JD016155, URL `http://dx.doi.org/10.1029/2011JD016155`, 2011.

Rémillard, J., Kollias, P., and Szyrmer, W.: Radar-radiometer retrievals of cloud number concentration and dispersion parameter in nondrizzling marine stratocumulus, Atmospheric Measurement Techniques, 6, 1817–1828, doi:10.5194/amt-6-1817-2013, URL `http://www.atmos-meas-tech.net/6/1817/2013/`, 2013.

Roebeling, R., Placidi, S., Donovan, D., Russchenberg, H., and Feijt, A.: Validation of liquid cloud property retrievals from SEVIRI using ground-based observations, Geophysical Research Letters, 35, L05 814, 2008a.

Roebeling, R. A., Deneke, H. M., and Feijt, A. J.: Validation of Cloud Liquid Water Path Retrievals from SEVIRI Using One Year of CloudNET Observations, Journal of Applied Meteorology and Climatology, 47, 206–222, doi:10.1175/2007JAMC1661.1, URL `http://dx.doi.org/10.1175/2007JAMC1661.1`, 2008b.

Zeng, S., Riedi, J., Trepte, C. R., Winker, D. M., and Hu, Y.-X.: Study of global cloud droplet number concentration with A-Train satellites, Atmo-

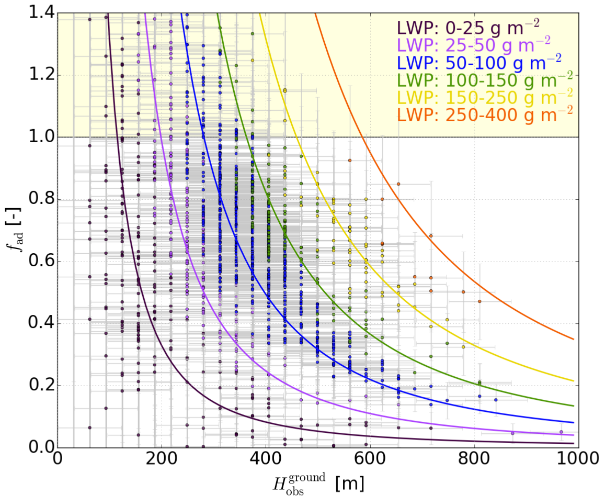

Figure 4: Adiabatic factor as a function of observed cloud geometrical depth ($H_{\mathrm{obs}}^{\mathrm{ground}}$) including data of all four cases. Colors indicate different liquid water path bins. The range with $f_{ad} > 1$ is shaded with light yellow. This superadiabatic range is neglected for the further study. The solid lines represent the theoretical relationship for bin mean liquid water path and $\Gamma_{\mathrm{ad}} = 1.9 \cdot 10^{-3}\mathrm{gm}^{-4}$.

spheric Chemistry and Physics, 14, 7125–7134, doi:10.5194/acp-14-7125-2014, URL http://www.atmos-chem-phys.net/14/7125/2014/, 2014.

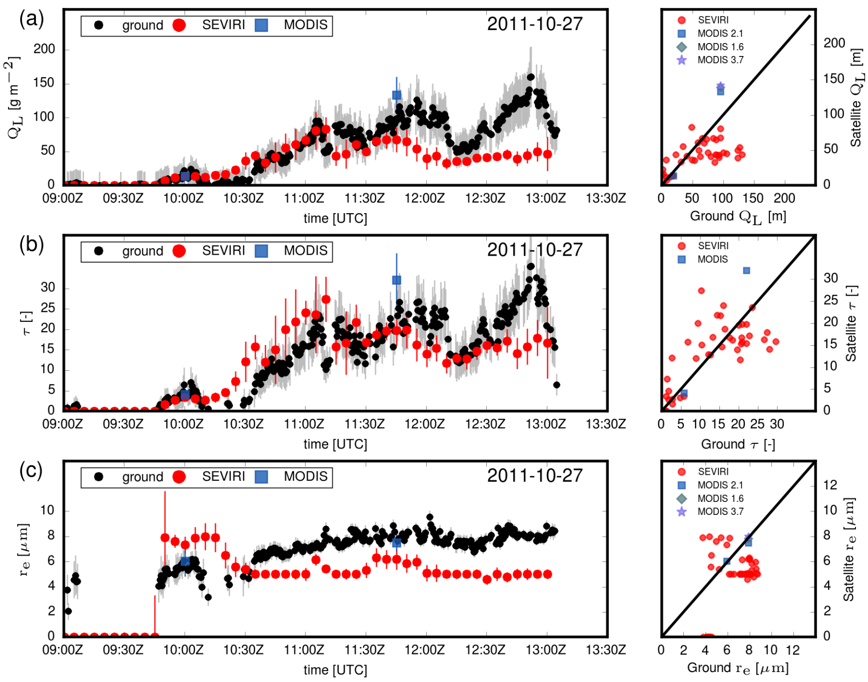

Figure 5: (a) Liquid water path for 27 October 2011 as obtained from the microwave radiometer (black dots), adiabatically from SEVIRI (red dots), and MODIS (green dots), respectively. For MODIS the effective radius obtained with three different channels is shown in the scatter plot with different symbols (square: 2.1 μm, diamond: 1.6 μm, star: 3.7 μm). (b) Time series of optical depth as obtained from SEVIRI (red), MODIS (green), and calculated from ground retrievals, respectively (black). (c) Time series of effective radius with the same colors. The variability of SEVIRI- and MODIS-derived values is given in terms of standard deviation of the surrounding area of ± 1 and ± 9 pixels, respectively.

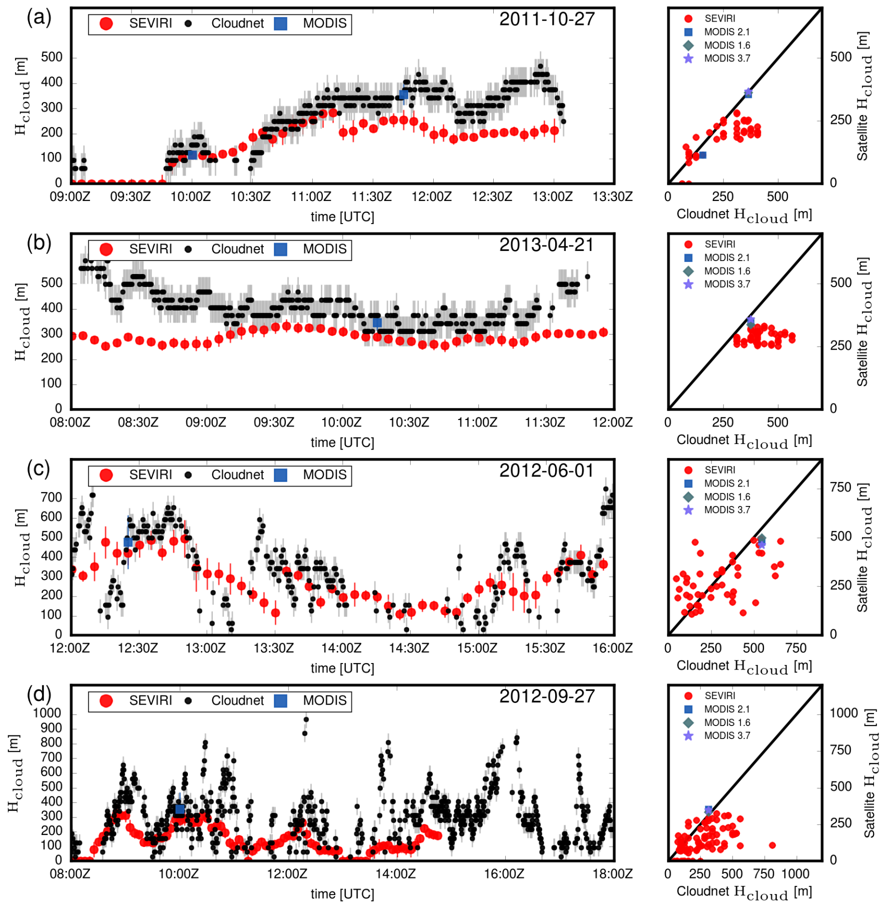

Figure 6: H_{cloud} for the four cases. Black dots represent the geometrical cloud depth observed from ground, red dots the SEVIRI adiabatically derived values, and green dots the MODIS adiabatically derived values. The uncertainties for the ground-based values are shown as shaded areas. The uncertainty estimates of MODIS and SEVIRI are represented in the same way as described in Fig. 5. In the scatter plots diamonds and stars represent the MODIS adiabatically derived values using available channels 1.6 μm and 3.7 μm, respectively.

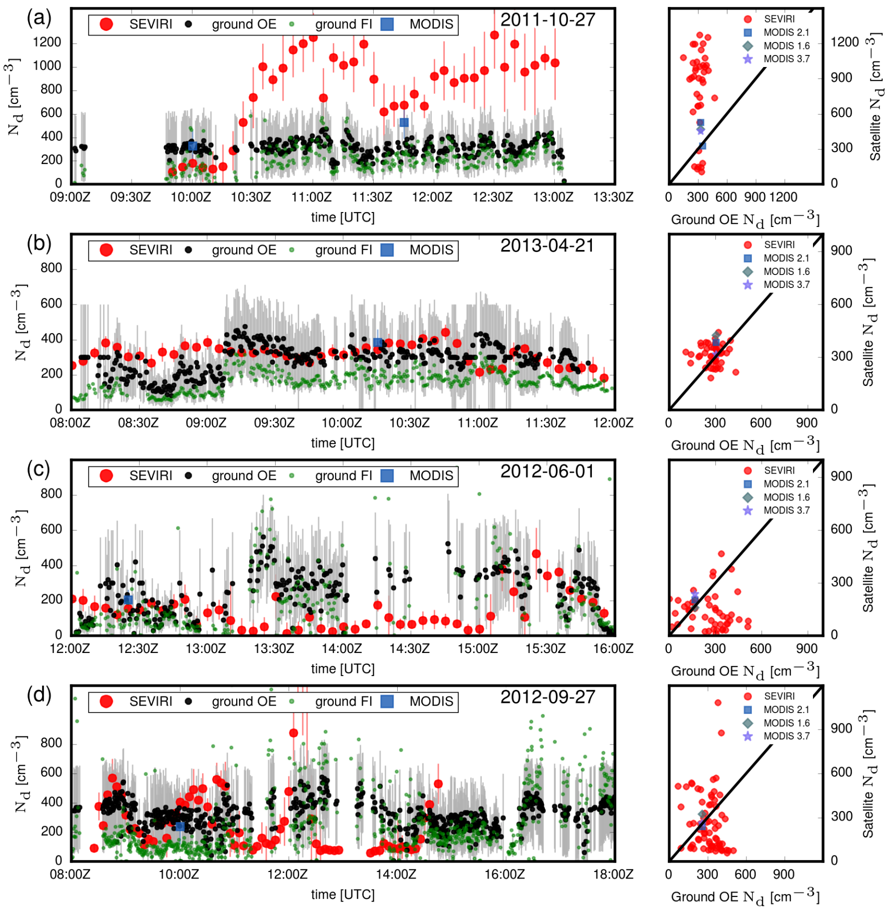

Figure 7: Time series of retrievals of the estimated cloud droplet number concentration. Black dots represent the OE method, using ground-based data (N_d^{OE}). The gray shaded area illustrates the uncertainty, calculated from the error covariance matrix of OE. Blue dots represent the retrieval with the FI method applied to ground site data (N_d^{FI}). Red dots represent the adiabatically derived values from SEVIRI (N_d^{SEVIRI}), while green dots those from MODIS (N_d^{MODIS}). Different MODIS channels used in the retrieval are denoted with the same symbols as in the figures before. Variability for SEVIRI and MODIS is given in terms of standard deviation of the surrounding area of ± 1 and ± 9 pixels, respectively.

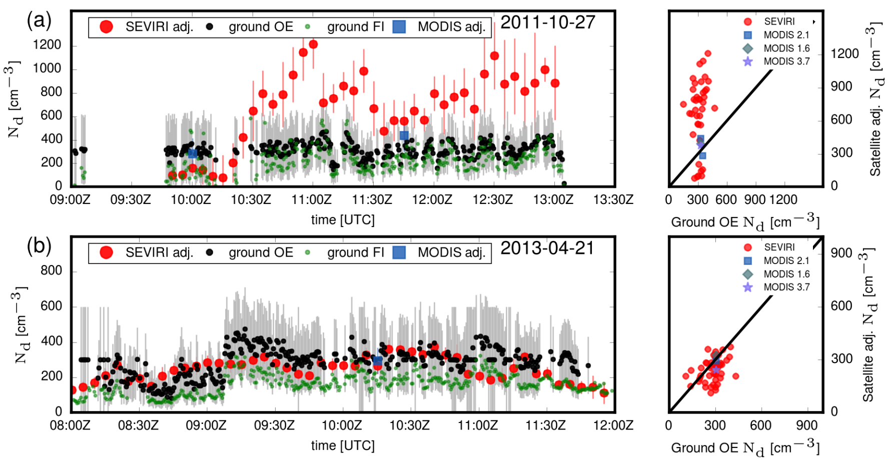

Figure 8: Adjusted cloud droplet number concentration from SEVIRI and MODIS applying f_{ad} from ground-based observations for the two homogeneous cases. Colors and symbols are the same as in Fig. 7.

Answers to Anonymous Referee #2

We thank anonymous referee #2 for his/her helpful comments and suggestions. We revised the manuscript according to his/her comments and the comments of anonymous referee #1. In the following answer to the referee we decided to give

- *referee comments in italic*
- our answers in normal format and
- **textual changes in the manuscript in bold format.**

We revised our manuscript according to the comments of anonymous referee #1 and #2, of which the main changes are as follows:

(1) Revision of the theory section: the equations for the sub-adiabatic model do now consider the sub-adiabatic state as the general case and can be transformed to the adiabatic case by setting $f_{ad} = 1$.

(2) The order of the theory and data section was reversed, so that the reader first gets a clear picture of the methods that are used and of the observed data that are available from the satellite and ground perspective. The following results section starts with an overview of parameters observed and used for the retrievals of key parameters which then can be compared to each other.

(3) A comprehensive revision of the introduction to introduce the goals earlier, and give a more focused overview of previous studies that use similar instruments and methods.

(4) We added an overview table of parameters considered in other studies that applied the sub-adiabatic model, to give a better comparison and motivation to what is done in this work.

(5) We omitted the presentation of method OE2, which led to some confusion. Instead we added a comparison of the adiabatic factor as derived from ground based observations using (a) the observed cloud geometrical depth from radar and ceilometer as well as the liquid water path from the microwave radiometer and (b) the observed radar profile and the adiabatic radar profile which can be calculated from the results of the OE1 method.

(6) To avoid confusion by introducing a "virtual adiabatic cloud geometrical depth" calculated from the ground-base microwave radiometer, we splitted the comparison of satellite and ground into Q_L and H. This means the following new structure of the results section: (a) comparison of ground-based parameters: f_{ad} and f_{ad}^{OE} (b) comparison of ground-based parameters: N_d^{FI} and N_d^{OE} (c) comparison of ground- and satellite-based parameters: Q_L (d) comparison of ground- and satellite-based parameters: H (e) comparison of ground- and satellite-based parameters: N_d

(7) We completely redid the figures for this study and hope that these are easier to read now.

We adress more specific remarks in the following:

(C1) *The theory is spread out over several subsections: 3.1, 3.2, 3.3 and 3.4. It applies the adiabatic assumption as the rule and the sub-adiabatic state as the exception. So we get Eq (1) and (2) about the adiabatic state, and then the sub-adiabatic state as an afterthought on line 204 and beyond.*

(A1) We did a comprehensive revision of our theory section. We now introduce the sub-adiabatic state as the rule and the adiabatic state as a special case with $f_{ad} = 1$.

- In Eq (4), (5) and (6) it is unclear whether we are dealing with an adiabatic state or a sub-adiabatic state.

The equations in the theory section now always consider the general sub-adiabatic case.

(C2) *- The following lines do nothing to clarify, as they would be largely incomprehensible to most readers: According to the authors, the factors A1 and A2 are both dependent on the adiabatic factor (line 219), and then in the next line they are not (line 220). In fact, if (6) considers the adiabatic value for the cloud depth, then A2 cannot be dependent on the adiabatic factor.*

(A2) We clarified this issue by avoiding A1 and A2 and give the factors in the equations explicitely.

(C3) *- In the next line (221) it mentions that the uncertainty in A2 is discussed elsewhere, but they do not quantify it. Instead they jump to the factor k in the next line (line 222) and specify its uncertainty.*

(A3) We rephrased the discussion about uncertainties and moved it from the theory section to the discussion of our results. Since we listed all the factors in Eq (4), (5) and (6) explicitely, the discussion about uncertainties of the individual factors should become more clear.

(C4) *- In 3.3.1 they discuss the Remillard retrieval method but its assumptions are unclear: adiabatic? Sub adiabatic?*

(A4) We assume the referee is referring to the Fox and Illingworth (1997) (FI) retrieval method. The Fox and Illingworth (1997) (FI) retrieval method, which is discussed in sect. 2.2.1 in the revised manuscript, is based on the assumption of a gamma-shaped droplet size distribution. It is assumed that N_d is constant with height, but no explicit assumptions about the liquid water content profile are necessary. We added the following sentence to clarify this issue: **Due to the relationship $N \propto \sqrt{Z}$, this retrieval method does not require the assumption of a linearly increasing liquid water content profile.**

(C5) *- In 3.3.2 there are two OE techniques, one which seems to be describing a sub adiabatic model (OE1), the other an adiabatic model (OE2), although it takes a long time to figure that out. - Eq (9) and (10) come out of a Wood (2006) reference, but this reference is not sufficiently specified at the back of the paper in the bibliography.*

(A5.1) According to the suggestions, we only discuss the OE1 method in the revised manuscript to avoid confusion of to many different approaches.

(A5.2) The reference of Wood2006 was corrected in the typeset manuscript.

(C6) - *Furthermore, (9) and (10) have an implicit assumption about the cloud structure (inhomogeneous mixing, or homogeneous mixing, see the Boers 2006 paper) but the authors say nothing about it. This type of unstructured introduction into the theory does not help the reader understand the overall content. It would be much preferable to redo the theory entirely as a separate section (possibly before the data) and start with a set of general equations (such as a general version of (9) and (10), plus the sub adiabatic version of (1)) and derive all the other equations from it.*

(A6) We revised the theory section and moved it before the data section. As suggested we now introduce a general set of equations from which the adiabatic state can be derived by setting $f_{ad} = 1$. We also clarified that we are assuming the homogeneous mixing model for our study.

(C7) *Next, discuss the adiabatic structure as the exception to the general sub adiabatic state. In that way it becomes clear that the power laws (4), (5) and (6) are transparent evolutions from these basic equations.*

(A7) This is done in the revised manuscript.

(C8) *Next the data: the list you have is : cloud base [ceilometer], cloud top[radar], N [OE or Remillard], LWP from microwave data, and (τ, r_e) from satellite. It then would become clear that there is only a single method to derive the adiabatic factor, namely through equation (8) by using the radar and lidar to get cloud dimension and using LWP from the microwave radiometer. This is the key. Next a discussion of parameters you want to compare: a) N_OE with $N_{Remillard}$, b) f_{ad} with f_{OE} [the latter you should be able to derive from OE1 is it not?] c) N and h [ground-based and sat-based] And so on.*

(A8) We revised the results section according to the suggestions. We also added the comparison of f_{ad} with f_{ad}^{OE}. Instead of comparing two differently calculated cloud geometrical depths from ground with cloud geometrical depth from satellite, we decided to compare (a) Q_L^{sat} and Q_L^{ground} and (b) H_{ad}^{sat} and H_{obs}^{ground} in two steps. In this way we were able to clear out H_{ad}^{sat} completely. We hope that this makes the discussion more clear.

The introduction to the results section now reads as follows:

The following investigation is built on the observations from ground (cloud base height from ceilometer, cloud top height and Z from cloud radar, Q_L from the microwave radiometer) and from passive satellites (τ, r_e).

We will first focus on ground-based retrievals and evaluate the adiabatic factor, followed by a comparison of ground-based CDNC retrieval results using the FI and OE method. Aftewards the key quantities H, N_d, Q_L obtained from satellite observations of SEVIRI and MODIS will be evaluated against the respective ground-based observations. We calculate the cloud droplet number concentration and cloud geometrical depth from the passive satellite-derived τ, r_e, assuming in the first step $f_\mathrm{ad} = 1$ and in a second step the f_ad calculated from the ground-based observations.

(C9) *THE USE OF OE2 OE2 is introduced on page 10 in a very unclear fashion. It is in fact almost incomprehensible to me. I gather between the lines that it is an linear adiabatic* *version of OE1. So it begs the question why one wants to use it, if the assumption on which it is based, namely the adiabatic state, is manifest incorrect. In my opinion OE2 should not be used, so that the section that deals with the intercomparison between OE1 and OE2 can be cleared out almost entirely (in section 4.1.2, and figure 5, which is only partly explained anyway).*

(A9) According to the suggestion we dropped OE2 in the revised manuscript.

(C10) *IMPRECISION OF STATEMENTS a) Line 13: The best match between satellite and ground perspectives. . .. .: No idea what this means; possibly: When satellite-based and ground-based retrievals are compared the best agreement was found for one of the homogeneous cloud cases, namely a 15% . . . in cloud geometric depth and a 27% . . . in cloud droplet concentration.*

(A10) Corrected to: **When satellite-based and ground-based retrievals are compared, the best agreement was found for the 21 April 2013 homogeneous case, namely a ...**

(C11) *b) Line 16: The estimation of ...... is especially sensitive to radar reflectivity for ... and to effective radius. . ... for the satellite retrieval. This should be: The estimation of . . .. . . is especially sensitive to variations in radar reflectivity for . . . and to variations in effective radius. . ... for the satellite retrieval.*

(A11) According to referee #1 this sentence is changed to **For all evaluated cases, the current SEVIRI retrieval seems to underestimate the effective radius relative to ground-based and MODIS measurements for unfavourable solar zenith angles of above approximately** 60°**. This deviation strongly propagates to the derived cloud droplet number concentration.**

(C12) *c) Line 360: . . ...points to thicker clouds in general. No idea what this means.*

(A12) This sentence is left out in the revision of the discussion, using Q_L instead of H^{ad}_{ground}.

(C13) *d) Line 366 369: These lines form an unclear introduction to the next set of lines because line 370 starts with the adiabatic factor, not with H or with a vertical velocity.*

(A13) The paragraph is restructured. The discussion about uncertainties of the adiabatic factor went to the discussion of superadiabatic points further above. Afterwards we first investigate the adiabatic factor as a function of cloud geometrical depth and second as a function of Doppler vertical velocity.

(C14) *e) Lines 453 455. . . ..the largest differences in adiabatic cloud depth .. show up as differences in QL. . . as both differences are linearly linked: Cloud depth differences show up as differences in QL, that is apples and oranges for me. In fact, read 453 465 out aloud and you will appreciate that this is an incomprehensible set of statements. Former and latter are used incorrectly too.*

(A14) This sentence is removed in the revision of the discussion, using Q_L instead of H^{ad}_{ground}.

(C15) *f) Line 483: never start an complete new section with the word Also. Also is used when you have already discussed something else.*

(A15) Corrected.

(C16) *g) Again, lines 503 513: A complete chaos: real cloud do not follow this relationship. What relationship? What are real clouds? What are pure adiabatic clouds? Do you have impure adiabatic clouds?*

(A16) Corrected the sentence, which now reads as follows: **Cloud observations do not always show an increase of effective radius from channel 1.6 μm over 2.1 μm to 3.7 μm as is expected for plane-parallel, adiabatic clouds (Platnick, 2000; King et al., 2013).** We avoided the use of the adjective pure for adiabatic. The terms adiabatic clouds ($f_{ad} = 1$) and sud-adiabatic clouds ($f_{ad} < 1$) are used troughout the whole manuscript.

(C17) *Line 510: The smallest mean absolute difference of effective radius of all channels? What is that?*

(A17) The sentence is rephrased to: **Comparing mean differences of effective radius from SEVIRI and each of the three available MODIS channels, we find the smallest difference in r_e considering the MODIS channel at 1.6 μm. The mean difference in this case is 0.86 μm.**

(C18) *Line 513: Intercomparison . . ..only results in . . .differences with 0.68 m and 0.51.. Differences with what?*

(A18) The sentence is rephrased to: **Intercomparing the effective radii retrieved from the three MODIS channels results in slightly smaller differences. The difference of MODIS channels at 2.1 μm and at 1.6 μm is 0.68 μm, while the difference of the retrieval at MODIS channels at 2.1 μm and at 3.7 μm is 0.51 μm.**

(C19) *h) Line 531: Why would you want to multiply N seviri by an adiabatic factor? No theoretical background is provided. [This should follow out of a complete revamp of the theory, though.]*

(A19) From the revised theory and eq. (5) it should become clear now how the adiabatic factor is applied for the retrieval of N_d. Revised eq. 5:

$$N_d = \frac{\sqrt{10}}{4\pi\rho_w^{0.5}k}(f_{ad}\Gamma_{ad})^{0.5}\tau^{0.5}r_e^{-2.5} \tag{1}$$

(C20) *i) Line 542: A blending of received signals: no idea what you mean.*

(A20) We revised the sentence: **The underestimation of $N_\mathrm{d}^\mathrm{SEVIRI}$ comprared to N_d^OE can likely be attributed to broken-cloud effects on the SEVIRI retrieval. For broken clouds within the SEVIRI pixel the satellite receives a combined signal from the clouds but also from the surface.**

(C21) *j) Line 545: Destroys the reliability? What is that?*

(A21) We revised the sentence: **It remains open to which extent the subpixel surface contamination leads to a bias in the retrieved cloud parameters especially for**

inhomogeneous cloud scenes when the brightness temperature actually does not represent the cloud radiative temperature.

(C22) *k) Line 561: both perspectives. What do you mean?*

(A22) We revised the sentence; **Considering the number of uncertainties for both the satellite and ground perspective, and those originating from the issue of representativity of the two perspectives ...**

(C23) *l) Line 571: Virtual adiabatic one? Besides a pure adiabatic one, we now have a virtual adiabatic one? What does that mean?*

(A23) The phrase virtual adiabatic cloud geometrical depth was meant to describe a geometrical depth that was not actually observed, but calculated from the adiabatic theory, meaning that this is only an auxiliary tool. To avoid confusion we stick to the terminology: adiabatic ($f_{ad} = 1$) and sub-adiabatic ($f_{ad} < 1$). For our revised discussion we also avoided this theoretical tool and instead compare directly the liquid water path from ground and satellite.

(C24) *m) Line 588: Ground retrieved one. What?*

(A24) Corrected.

(C25) *And on it goes. In conjunction with the co-authors, the principal author should carefully evaluate each and every sentence they write down and screen on its significance, style and coherence and logical placement in the whole text. This was clearly not done in preparation of this manuscript.*

(A25) We did a major revision of both the structure and discussion style, of our manuscript.

(C26) *OTHER: a) Unless I missed it, it seems that Cahalans work on homogeneity is introduced in the table 1 only, not in the text.*

(A26) We now also introduce the definition of the Cahalan inhomogeneity parameter in the text.

(C27) *Furthermore, you have homogeneous / inhomogeneous clouds, and the homogeneous mixing and the inhomogeneous mixing assumption. These terms are mixed throughout the paper and it is not always clear what is meant by what.*

(A27) In the paper the term homogeneous / inhomogeneous clouds is used in terms of temporally homogeneous / inhomogeneous clouds. If the mixing process is meant, we explicitely mention homogeneous mixing or inhomogeneous mixing. To clarify that we also added the following sentence to the revised manuscript: **In the following the terms homogeneous and inhomogeneous clouds always refer to the temporal homogeneity if not stated otherwise.**

(C28) *b) In the print-out that I made, Table 1 and table 2 appear in the text, rather than at the end of it.*

(A28) This should not be the case in the typeset discussion paper. This issue occured only in the first version of the uploaded manuscript.

(C29) *c) Acronyms are not always introduced: SEVIRI, MODIS, MIRA, HATPRO. They are mixed with acronyms that are introduced: LACROS, DFOV etc etc.*

(A29) We went trough the paper again and checked for acronyms not correctly introduced.

(C30) *d) Equation (13) this is not an equation when you use the sign :*

(A30) Corrected in the revised manuscript.

(C31) *e) The colors in the figures are insufficiently separated. Green en blue hues, then something yellow or reddish. The result is that one needs a microscope to see the differences*

(A31) We revised the colors and size of the figures. See revised figures below:

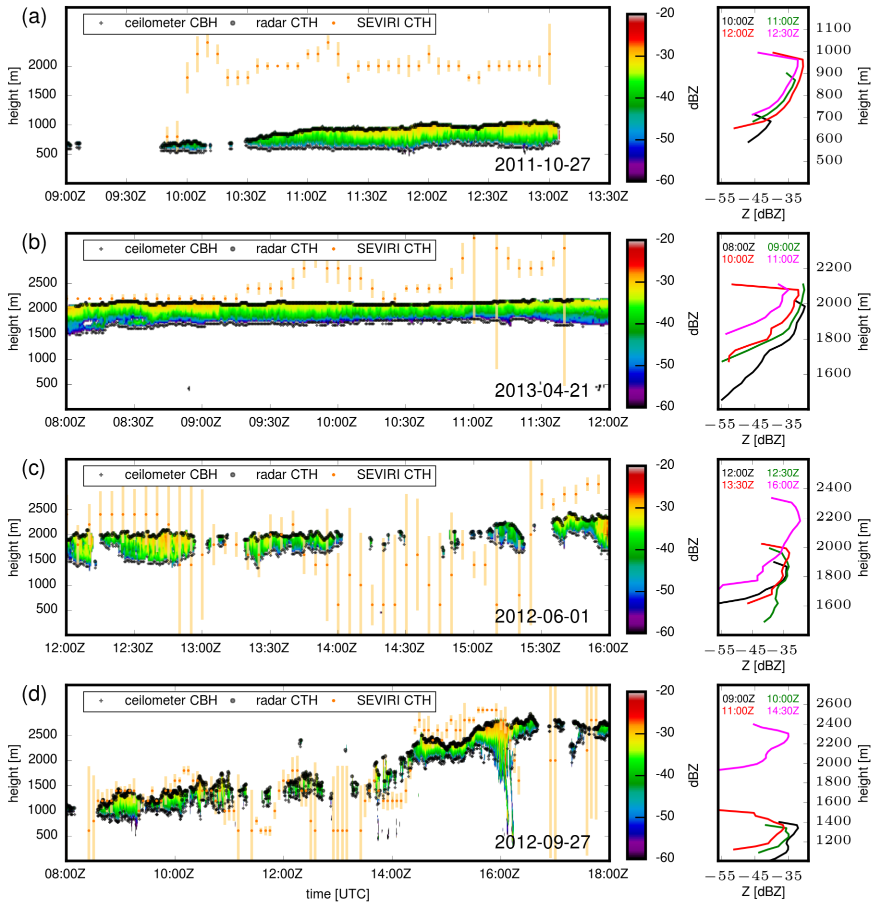

Figure 1: Time series of radar reflectivity (in dBZ) and cloud borders for the 4 cases; (a) 27 October 2011, (b) 21 April 2013, (c) 1 June 2012, (d) 27 September 2012. Cloud borders are shown as detected by Cloudnet with black dots and by SEVIRI using NWCSAF in orange dots. Sample profiles of radar reflectivity are shown for each case at different times.

References

Fox, N. I. and Illingworth, A. J.: The Retrieval of Stratocumulus Cloud Properties by Ground-Based Cloud Radar, Journal of Applied Meteorology, 36, 485–492, doi:10.1175/1520-0450(1997)036¡0485:TROSCP¿2.0.CO;2, URL `http://dx.doi.org/10.1175/1520-0450(1997)036<0485:TROSCP>2.0.CO;2`, 1997.

King, N. J., Bower, K. N., Crosier, J., and Crawford, I.: Evaluating MODIS cloud retrievals with in situ observations from VOCALS-REx, Atmospheric Chemistry and Physics, 13, 191–209, doi:10.5194/acp-13-191-2013, URL `http://www.atmos-chem-phys.net/13/191/2013/`, 2013.

Platnick, S.: Vertical photon transport in cloud remote sensing problems, Journal of Geophysical Research: Atmospheres, 105, 22 919–22 935, doi:10.1029/2000JD900333, URL `http://dx.doi.org/10.1029/2000JD900333`, 2000.

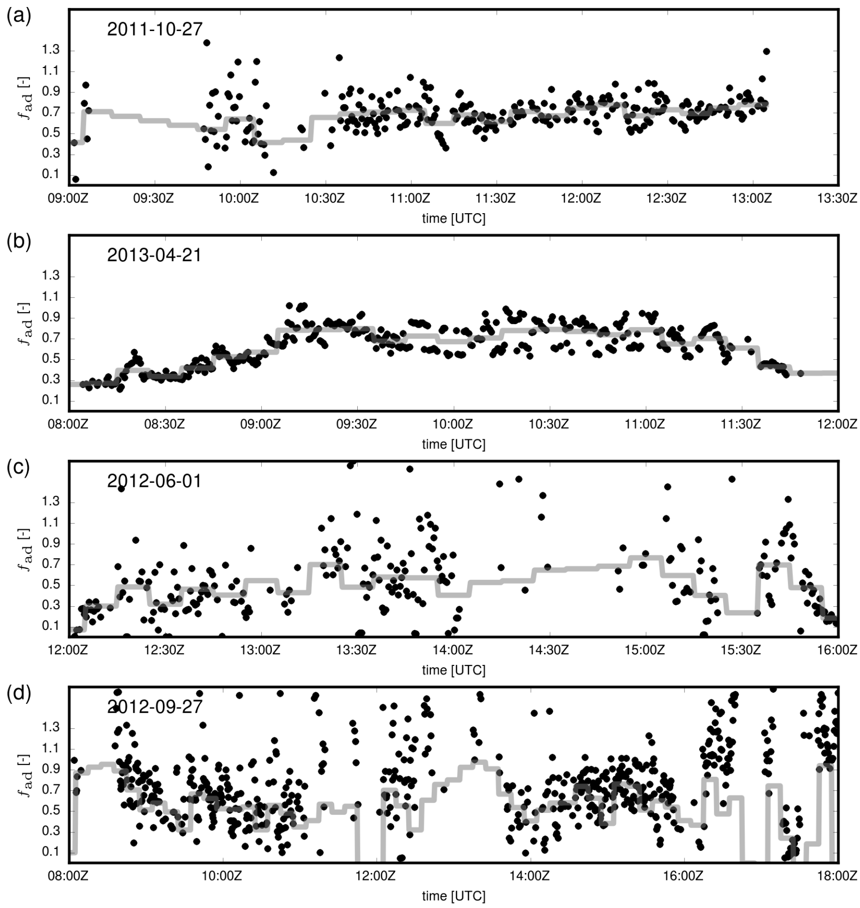

Figure 2: Adiabatic factor for all four cases. Black dots represent the adiabatic factor derived using ground-based geometrical depth and liquid water path from the microwave radiometer. The gray line represents the 10-min averaged and interpolated adiabatic factor neglecting superadiabatic values.

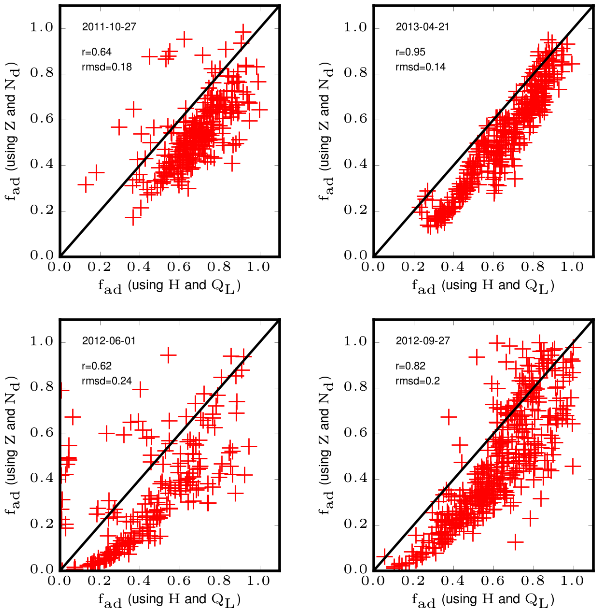

Figure 3: Adiabatic factor calculated from ground-based observations using H and Q_{L} (x-axis) and from Z and N_{d} (y-axis). Superadiabatic values are omitted. The graphs correspond to our four investigated cases.

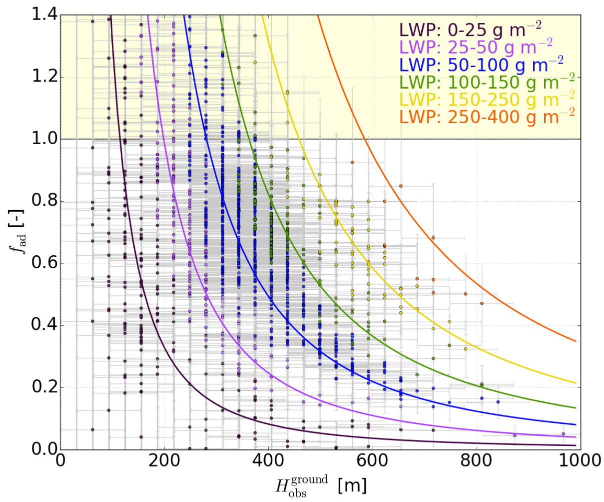

Figure 4: Adiabatic factor as a function of observed cloud geometrical depth ($H_{\mathrm{obs}}^{\mathrm{ground}}$) including data of all four cases. Colors indicate different liquid water path bins. The range with $f_{ad} > 1$ is shaded with light yellow. This superadiabatic range is neglected for the further study. The solid lines represent the theoretical relationship for bin mean liquid water path and $\Gamma_{\mathrm{ad}} = 1.9 \cdot 10^{-3}\mathrm{gm}^{-4}$.

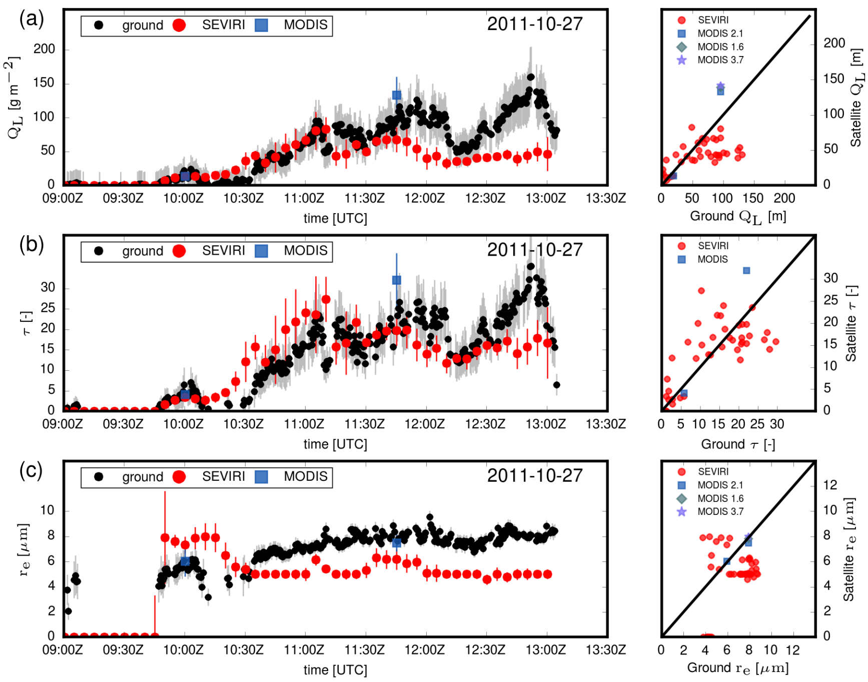

Figure 5: (a) Liquid water path for 27 October 2011 as obtained from the microwave radiometer (black dots), adiabatically from SEVIRI (red dots), and MODIS (green dots), respectively. For MODIS the effective radius obtained with three different channels is shown in the scatter plot with different symbols (square: 2.1 μm, diamond: 1.6 μm, star: 3.7 μm). (b) Time series of optical depth as obtained from SEVIRI (red), MODIS (green), and calculated from ground retrievals, respectively (black). (c) Time series of effective radius with the same colors. The variability of SEVIRI- and MODIS-derived values is given in terms of standard deviation of the surrounding area of ± 1 and ± 9 pixels, respectively.

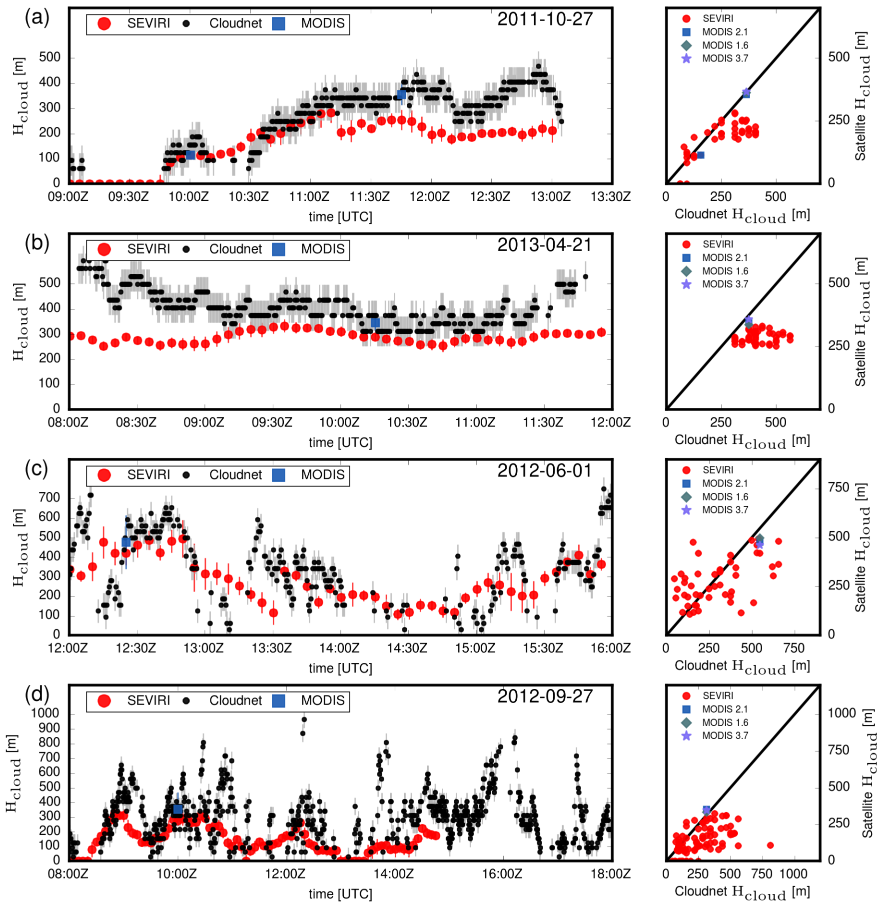

Figure 6: H_{cloud} for the four cases. Black dots represent the geometrical cloud depth observed from ground, red dots the SEVIRI adiabatically derived values, and green dots the MODIS adiabatically derived values. The uncertainties for the ground-based values are shown as shaded areas. The uncertainty estimates of MODIS and SEVIRI are represented in the same way as described in Fig. 5. In the scatter plots diamonds and stars represent the MODIS adiabatically derived values using available channels 1.6 μm and 3.7 μm, respectively.

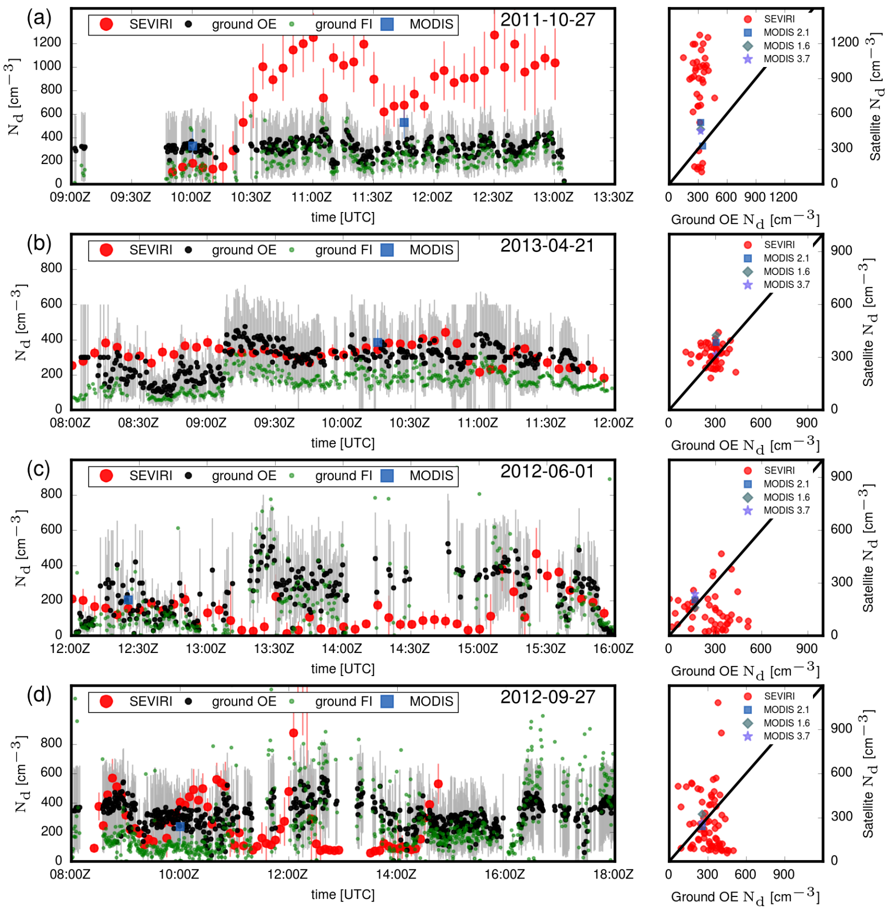

Figure 7: Time series of retrievals of the estimated cloud droplet number concentration. Black dots represent the OE method, using ground-based data (N_d^{OE}). The gray shaded area illustrates the uncertainty, calculated from the error covariance matrix of OE. Blue dots represent the retrieval with the FI method applied to ground site data (N_d^{FI}). Red dots represent the adiabatically derived values from SEVIRI (N_d^{SEVIRI}), while green dots those from MODIS (N_d^{MODIS}). Different MODIS channels used in the retrieval are denoted with the same symbols as in the figures before. Variability for SEVIRI and MODIS is given in terms of standard deviation of the surrounding area of ±1 and ±9 pixels, respectively.

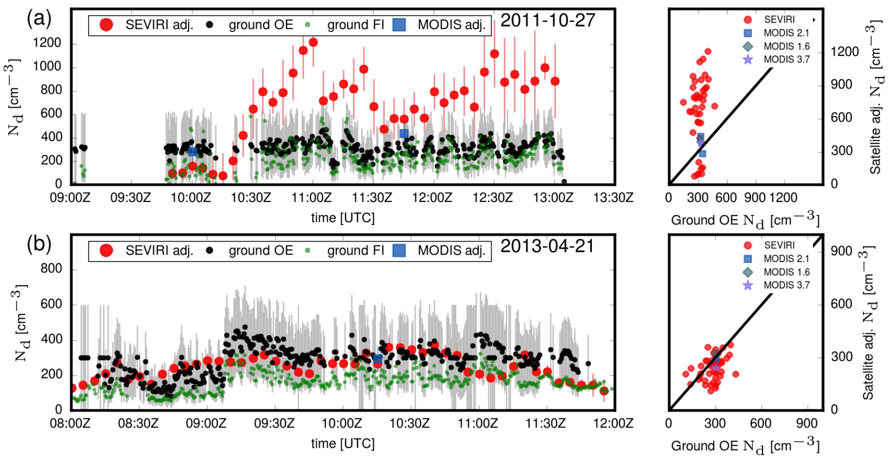

Figure 8: Adjusted cloud droplet number concentration from SEVIRI and MODIS applying f_{ad} from ground-based observations for the two homogeneous cases. Colors and symbols are the same as in Fig. 7.

Manuscript prepared for Atmos. Chem. Phys.
with version 2014/09/16 7.15 Copernicus papers of the LaTeX class copernicus.cls.
Date: 29 May 2015

Investigation of the adiabatic assumption for estimating cloud micro- and macrophysical properties from satellite and ground

D. Merk[1], H. Deneke[1], B. Pospichal[2], and P. Seifert[1]

[1]Leibniz Institute for Tropospheric Research, Leipzig, Germany
[2]Leipzig Institute for Meteorology, Leipzig, Germany

Correspondence to: D. Merk (merk@tropos.de)

Abstract. In this study ~~we investigate~~ the accuracy of quantities relevant for diagnosing the first indirect aerosol effect ~~, with focus on the~~ with satellite is investigated by comparing co-located ground-based and spaceborne observations. The focus is set on retrievals of cloud droplet number concentration and cloud geometrical depth. ~~The adiabatic cloud model~~ For the study we considered the sub-adiabatic cloud model which is commonly applied to retrieve cloud micro- and macrophysical quantities from passive satellite sensors like SEVIRI or MODIS. As reference we use ground-based observations from a cloud radar, a microwave radiometer and a ceilometer ~~. The cloud geometrical depth is obtained directly from these measurements. An~~ from which cloud droplet number concentration is derived with a newly developed optimal estimation technique~~was developed to retrieve profiles of droplet number concentration~~. Although the ground-based observations contain detailed information about the cloud vertical structure, ~~there are also large uncertainties~~ large uncertainties in the retrieved cloud microphysical properties were found. We investigate four different cases (27 October 2011, 1 June 2012, 27 September 2012 and 21 April 2013) of temporally homogeneous and inhomogeneous liquid cloud layers observed over Germany. Considering uncertainties for both ground-based and satellite-based retrievals~~we found~~ , we find a good agreement ~~for observations under suitable conditions. Overall~~when temporally homogeneous single-layer clouds are considered. Overall, cloud layers were ~~subadiabatic with values of the subadiabatic factor consistent with previous studies. The best match between satellite and ground perspective is found for one of the homogeneous cases where we obtained a~~ sub-adiabatic with medians of the adiabatic factor around 0.65 for 3 cases and around 0.45 for one case. When satellite-based and ground-based retrievals are compared, the best agreement was found for the 21 April 2013 homogeneous case, namely a 4 % relative mean difference of ~~adiabatic~~ cloud geometrical depth ~~of~~ and a 15 % ~~and a~~ rel-

ative mean difference of cloud droplet number concentration ~~of 27. The estimation of cloud droplet number concentration is especially sensitive to radar reflectivity for the~~ when the sub-adiabatic factor obtained from ground-based ~~retrieval and to effective radius for the satellite retrieval.~~ observations is considered. For all evaluated cases, the current SEVIRI retrieval seems to underestimate the effective radius relative to ground-based and MODIS measurements for unfavourable solar zenith angles of above approximately 60°. This deviation strongly propagates to the derived cloud droplet number concentration.

1 Introduction

Low-level liquid clouds play an important role in the energy balance of the ~~earth~~Earth, and are found in many areas around the globe. Their microphysical and optical properties are strongly influenced by aerosol particles that act as cloud condensation nuclei (CCN). Twomey (1974) first postulated the effect of an increased aerosol number concentration in clouds~~as~~, which is commonly referred to as the first indirect aerosol effect, as a climatically relevant process. The ~~quantitifcation~~ quantification of such aerosol indirect effects remains one of the main uncertainties in climate projections (Boucher et al., 2013).

If the liquid water content as well as the geometrical depth of the cloud are considered constant, a higher aerosol load ~~directly~~ results in an enhanced cloud albedo. This effect is observed in particular by means of ship tracks that form in marine stratocumulus cloud decks (e.g. Ackerman et al., 2000). The chain of interactions of cloud microphysics and dynamics is complex and not yet fully understood. However, to quantify the effect of a change in the aerosol load on cloud albedo, it is necessary to consider both microphysics and macrophysics, which are influenced by cloud dynamical processes. Brenguier et al. (2000) noted that a 15 % change in the cloud geometrical depth (~~H_{cloud}~~H_{cloud}) can have a similar effect on cloud albedo as a doubling of the cloud droplet number concentration (~~N_{d}~~N_{d}). Already Han et al. (1998) suggested to investigate a column cloud droplet number concentration which combines ~~H_{cloud} and N_{d}~~H_{cloud} and N_{d}. These two quantities ~~turn~~ turned out to be the key parameters for quantifying the aerosol effect on cloud albedo.

~~While both in-situ and remote sensing~~ The aim of the current study is to gain a better understanding of the current possibilities and shortcomings when H_{cloud} and N_{d} of clouds are retrieved from satellite observations, by evaluating existing retrievals with ground-based observations performed over Germany. We combine observations from SEVIRI (Spinning Enhanced Visible and InfraRed Imager) onboard Meteosat Second Generation (MSG) and MODIS (Moderate-Resolution Imaging Spectroradiometer) onboard Terra and Aqua with ground-based remote sensing data obtained with ceilometer, microwave radiometer and 35-GHz cloud radar at Leipzig, Germany (51.35 N, 12.43 E) and at Krauthausen, Germany (50.897 N, 6.46 E). Those ground-based instruments are operated in the framework of Cloudnet (Illingworth et al., 2007) and ACTRIS (Aerosols, Clouds and Trace gases Research InfraStructure Network).

The combination of ground-based ceilometer and cloud radar is able to provide reliable detection of cloud geometric borders (Boers et al., 2000; Shupe, 2007; Illingworth et al., 2007; Martucci et al., 2010) . To derive N_d with this set of ground-based instruments Rémillard et al. (2013) recently suggested a radar-radiometer retrieval based on a condensational growth model taking the vertical velocity into account and allowing small variations of N_d with height, while it is assumed vertically constant in most other studies. Since Cloudnet does not provide N_d, we developed and apply an optimal estimation technique to obtain N_d, based on the method introduced by Fox and Illingworth (1997) , similarly also applied in Rémillard et al. (2013) . Given other instrument combinations such as those including lidar measurements (Schmidt et al., 2014a) , (Martucci and O'Dowd, 2011) or solar radiation measurements (Dong et al., 1997, 2002) would give alternative opportunities to derive N_d. Due to the under-constrained nature and assumptions made in such retrieval methods, substantial differences for the obtained microphysical parameters may occur, as pointed out by Turner et al. (2007) , who intercompared several ground-based retrieval methods for one case study.

While remote sensing observations from ground ~~do not cover large areas with high spatial resolution~~are always column measurements, passive satellite observations ~~, although costly,~~ from, e.g., SEVIRI or MODIS, show a good spatio-temporal coverage and are therefore suitable to investigate the first indirect aerosol effect on a larger scale. Active satellite sensors on the other hand, such as the cloud profiling radar onboard CloudSat (Stephens et al., 2002) or the Cloud-Aerosol-Lidar with Orthogonal Polarization (CALIOP) onboard CALIPSO ~~(Winker et al., 2009)~~ (Winker et al., 2009, Cloud-Aerosol Lidar and Infrared Pathfinder are able to provide vertically resolved cloud observations over larger areas that can be used to investigate aerosol effects on cloud properties (e.g. Christensen and Stephens, 2011) , but lack highly-resolved temporal coverage and have a smaller scanning swath than passive sensors onboard polar-orbiting satellites. ~~For geostationary satellites,~~

Despite their coarser spatial resolution, geostationary satellite observations benefit from the high temporal ~~resolution~~ coverage of up to 5 ~~is a big advantage, despite the reduced spatial resolution.~~

~~This motivated the evaluation of cloud parameters such as liquid water path (Q_L)as in Roebeling et al. (2008b, a); Hünerbein et al.~~ ~~H_cloud as in Roebeling et al. (2008a) obtained from SEVIRI~~ minutes in conjunction with a high spatial coverage. This can be considered as an advantage for the determination of large-scale first indirect aerosol effects. Within this study the capabilities of geostationary satellites for cloud retrievals will be further evaluated. Validation of satellite-derived cloud parameters, such as (Q_L), with ground-based observations ~~. To retrieve micro- and macrophysical properties of homogeneous liquid clouds from passive satellite instruments, commonly the adiabatic model is applied (e.g. Schueller et al., 2003; Boers et al., 2006; Bennartz,~~ ~~Therefore it is important to investigate its validity. The comparison of N_d and H_cloud~~ has only infrequently been performed Roebeling et al. (2008b, a); Hünerbein et al. (2014) . Especially the comparison of N_d and H_cloud from both space and ground has not yet been carried out intensively for different regions of the Earth, although Placidi et al. (2007) pointed out that their combined retrieval of N_d and H_cloud would give the opportunity to derive the first indirect effect with high spatial and temporal resolution. ~~The validation of retrieved N_d and H_cloud from passive sensing satellite instruments remains a challenging task.~~ In this study, we contrast ~~such~~ satellite retrievals with the ~~same cloud parameters retrieved independently~~ independently retrieved properties from ground-based remote sensing. To our knowledge such evaluations from the SEVIRI instrument for the indirect aerosol effects' key parameters have been rarely carried out (e.g. in Roebeling et al. (2008a)). Previous satellite retrieval studies, retrieving N_d and/or H_cloud, usually apply a (sub-)adiabatic cloud model with a presumed adiabatic factor (e.g. Schueller et al., 2003; Boers et al., 2006; Bennartz, 2007) . Only Min et al. (2012) calculated this factor in advance. With that, we can assess the influence of cloud sub-adiabaticity on N_d and H_cloud as well as the agreement between the retrieved properties from ground and satellite. Apart from assumptions about the adiabatic factor, also uncertainties in the retrieval of optical depth and effective radius determine the accuracies of the results and will be discussed in this context.

~~Remote sensing methods from ground are able to provide reliable detection of cloud geometric borders through the combination of ceilometer and radar (Boers et al., 2000; Shupe, 2007; Illingworth et al., 2007; Martucci et al., 20~~ ~~Several retrieval methods have been developed over the last years combining different instruments or exploiting novel techniques to retrieve information about the vertical microphysical structure of the cloud. Given only the cloud radar measurements, a common approach is to relate~~ The paper is structured as follows. In Sect. 2 we introduce the adiabatic model, relevant for the satellite-based retrieval of key parameters, as well as the retrieval methods from ground. Afterwards we describe the instruments and data processing tools used within this study in Sect. 3. In Sect. 4 these retrievals are applied to four different cases which are then used to evaluate the satellite-based observations. Finally, a conclusion and outlook is given in Sect. 5.

2 Cloud microphysical retrieval methods

In this section we present the theory of the (sub-)adiabatic cloud model and retrieval strategies for the cloud droplet number concentration from the suite of ground-based instruments.

2.1 Retrievals using the (sub-)adiabatic cloud model

For a moist rising air parcel liquid water content ~~with the radar reflectivity via a power-law relationship. A short overview of studies applying such methods is given in Löhnert et al. (2001) . With additional measurements by a microwave radiometer, more accurate retrievals of q_L (e.g. Frisch et al., 1998; Dong and Mace, 2003) and even N_d become possible. Rémillard et al. (2013) suggests a radar-radiometer~~ $q_\mathrm{L}(z)$ increases linearly with height (Albrecht et al., 1990) and can be related to $N_\mathrm{d}(z)$ and the mean volume droplet radius

$r_v(z)$:

$$q_L(z) = f_{\rm ad}\Gamma_{\rm ad}(T,p)z = \frac{4}{3}\pi\rho_{\rm w} r_{\rm v}^3(z) N_{\rm d}(z) \quad (1)$$

Here z is the height above cloud base, $\rho_{\rm w}$ is the density of water. $f_{\rm ad}$ represents the sub-adiabatic fraction of liquid water content, in the following simply called adiabatic factor. It can be explained by the reduction of liquid water due to evaporation influenced by the entrainment of drier air masses and leads to $f_{\rm ad} < 1$ (sub-adiabatic). $\Gamma_{\rm ad} = A_{\rm ad}(T,p)\rho_{\rm a}(T,p)$ is the adiabatic rate of increase of liquid water content, with $\rho_{\rm a}$ the air density and $A_{\rm ad}$ the adiabatic increase of the liquid water content mixing ratio. In general, for the adiabatic factor $f_{\rm ad}$ a range of $[0.3, 0.9]$ is seen as common (Boers et al., 2006) . From eq. (1) it is clear that either $N(z)$ or $r_{\rm v}(z)$ can be affected by evaporation. Boers et al. (2006) considers two extremes: (a) homogeneous mixing, where $N_{\rm d}(z)$ stays constant in the vertical layer, but the droplet radius ($r_{\rm v}(z)$) is changed due to evaporation, (b) inhomogeneous mixing, where the number of droplets change (dilution of whole droplets), but the droplet radius profile is unchanged. In nature, a mixture of both processes may likely occur (Lehmann et al., 2009) . For our study we only consider homogeneous mixing.

In remote sensing usually the effective radius is retrieved. It is defined as the third over the second moment of the droplet size distribution (Hansen and Travis, 1974) and can be linked to the mean volume radius ($r_{\rm v}$) with the following relationship:

$$r_{\rm e}^3 = k^{-1} r_{\rm v}^3 \quad (2)$$

The factor k depends on the cloud type and corresponding typical droplet size distributions. Typical values for marine and continental liquid water clouds are 0.67 and 0.80, respectively (Brenguier et al., 2000) .

This leads to the following two equations for optical depth τ and effective radius $r_{\rm e}$ (compare Eq. A12, A14 in Boers et al. (2006)):

$$\tau = \frac{6}{5}\pi^{1/3}\left(\frac{4}{3}\rho_{\rm w}\right)^{-2/3}(\Gamma_{\rm ad} f_{\rm ad})^{2/3}(kN_{\rm d})^{1/3} H^{5/3} \quad (3)$$

and

$$r_{\rm e} = \left(\frac{4}{3}\pi\rho_{\rm w}\right)^{-1/3}(kN_{\rm d})^{-1/3}(\Gamma_{\rm ad} f_{\rm ad})^{1/3} H^{1/3} \quad (4)$$

Without entrainment, we find $f_{\rm ad} = 1$ (adiabatic clouds) in all the equations above.

The typically obtained products from passive satellite remote sensing are τ and r_e using the Nakajima and King (1990) retrieval method. The (sub-)adiabatic cloud model can be used to derive cloud properties such as liquid water path (Q_L), cloud droplet number concentration (N_d) and geometrical depth (H) by inserting eq. 4 into eq. 3 and solving for the desired quantity.

$$N_\mathrm{d} = \frac{\sqrt{10}}{4\pi\rho_\mathrm{w}^{0.5}k}(f_\mathrm{ad}\Gamma_\mathrm{ad})^{0.5}\tau^{0.5}r_\mathrm{e}^{-2.5} \tag{5}$$

$$H = \sqrt{\frac{10}{9}(f_\mathrm{ad}\Gamma_\mathrm{ad})^{-1}\rho_\mathrm{w}\tau r_\mathrm{e}} \tag{6}$$

$$Q_\mathrm{L} = \frac{5}{9}\rho_\mathrm{w}\tau r_\mathrm{e} \tag{7}$$

Various different values considered for k, Γ_ad and f_ad can be found in previous studies (Table 1) due to different climatic and geographical regions on Earth (e.g. continental vs. maritime). Often even adiabatic clouds are considered ($f_\mathrm{ad} = 1$) (e.g. Quaas et al., 2006) . In this study we take a constant value for k ($k = 0.8$), and $\Gamma_\mathrm{ad}(T,p)$ using pressure and temperature obtained for cloud base height. The adiabatic factor is initially set to $f_\mathrm{ad} = 1$ for the satellite-derived values of N_d and H, but is also calculated from ground-based observations in a further step. Following Wood (2006) the adiabatic factor is given by the following relationship:

$$f_\mathrm{ad} = \frac{2Q_\mathrm{L}}{(H_\mathrm{obs}^\mathrm{ground})^2\Gamma_\mathrm{ad}(T,p)} \tag{8}$$

We use Q_L from the ground-based microwave radiometer, $H_\mathrm{obs}^\mathrm{ground}$ as the difference of cloud top height from the cloud radar and cloud base height from the ceilometer, and $\Gamma_\mathrm{ad}(T_\mathrm{cbh}, p_\mathrm{cbh})$ using numerical weather prediction (NWP) data.

2.2 Ground-based retrieval of cloud droplet number concentration

2.2.1 Radar-radiometer based retrieval method

With the given observations, the retrieval of ~~N_d based on a condensational growth model taking the vertical velocity into account and allowing small variations of N_d with height, while it is assumed vertically constant in most other studies. Accompanying lidar extinction measurements have been used to retrieve q_L, effective radius (r_e)~~ cloud droplet number concentration can be based on a combination of the cloud radar and the microwave radiometer. This mainly requires an assumption about the droplet size distribution. Cloud microphysical quantities can then be described in terms of moments of this droplet size distribution. The cloud droplet number concentration is equivalent to the zeroth moment, the mean radius to the first moment, the liquid water content is proportional to the third moment, while the effective radius is the third over the second moment, and the radar reflectivity factor is proportional to the sixth moment. Relating these moments gives the chance to fully describe a unimodal distribution following either a gamma or lognormal shape and therefore calculating other moments of the size distribution which are not directly observed (Rémillard et al., 2013) . Following Fox and Illingworth (1997) , we relate the measured radar reflectivity (Z) to q_{L} and ~~N_{d} in parallel (Martucci and O'Dowd, 2011) , although the fast extinction within the first few decameters of~~ N_{d}. Thereby it is assumed that the droplet size distribution can be described by a gamma distribution with parameter β, where β is the index of the ~~cloud. Also observation of solar radiation can be included as additional independent information (Dong et al., 1997, 2002) . Recently, a technique to derive profiles of q_{L}, r_{e}, and N_{d} was developed based on measurements with dual-field-of-view (DFOV) Raman lidar (Schmidt et al., 2013) . The amplitude of the aerosol cloud interaction was investigated similar to the approach presented by Feingold et al. (2003) by relating the measured aerosol extinction coefficient below cloud base to the retrieved cloud microphysical properties of the same profile. Taking co-located Doppler lidar measurements of vertical velocity into account, it was found that for small temporal and spatial scales the strength of updrafts considerably determines the intensity of~~ gamma function following the size distribution definition in (Fox and Illingworth, 1997; Martucci and O'Dowd, 2011) :

$$N(r) \propto Ar^{\beta}\exp\left(-Br\right) \tag{9}$$

Thereby B is the rate parameter and A a function of the rate parameter. A similar method has been applied in (Rémillard et al., 2013) , but using a lognormal size distribution. Although N_{d} may vary vertically, it is commonly suspected that it stays nearly constant throughout the vertical column of a nonprecipitating cloud (Bennartz, 2007; Brenguier et al., 2000) . To retrieve the column cloud droplet number concentration from the available single-layer observations, we integrate q_{L} over the cloud column and can therefore use Q_{L} from the microwave radiometer (compare Rémillard et al., 2013) :

$$N_{\mathrm{d}}^{\mathrm{FI}} = \frac{9}{2\pi^2 k\rho^2}\frac{(\beta+6)!}{(\beta+3)!(\beta+3)^3}\frac{Q_L^2}{(\int\sqrt{Z}dz)^2} \tag{10}$$

Due to the ~~aerosol cloud interaction especially at cloud base (Schmidt et al., 2014a) . On large spatial and temporal scales and in the cloud-top region the impact of up- and downdrafts on~~ relationship $N \propto \sqrt(Z)$, this retrieval method does not require the assumption of a linearly increasing liquid water content profile. Both, homogeneous and inhomogeneous mixing with dry air (Lehmann et al., 2009) can easily alter the microphysical quantities in clouds in ways not adequately adressed within such a retrieval scheme. For example, the ~~aerosol cloud interaction levels out and approaches values similar to those obtained from measurements of passive spaceborne sensors (Schmidt et al., 2014b) . At this time,~~ size distribution may become skewed and not be accurately described with a gamma-shape anymore. However, Boers et al. (2006) and Janssen et al. (2011) found out, that both assumptions about the mixing process result in nearly the same vertically averaged N_d.

2.2.2 Optimal Estimation method

The Optimal Estimation (OE) method, presented in the following, aims on finding the most likely state given the observations, the a-priori and the error estimates. Therefore we try to minimize a cost function following Rodgers (2000) . The OE retrieval of cloud droplet number concentration (N_d^OE) and the liquid water content profile is based on the radar-radiometer method.

We further assume a vertically constant N_d, a gamma-shaped droplet size distribution with parameter β. As before, q_L, N_d, and Z are nonlinearly related. We include error estimates for the observed quantities as well as an a-priori state together with its error estimate.

Our observation vector ($\boldsymbol{y}$) contains the radar reflectivity Z and the ~~DFOV Raman lidar technique can only be applied during nighttime, which hinders its application for the evaluation of measurements by spaceborne sensors such as SEVIRI or MODIS that rely on daylight conditions for the retrieval of liquid-cloud microphysical properties.~~ microwave radiometer Q_L. Our state vector ($\boldsymbol{x}$) contains the vertically-constant N_d and the natural logarithm of the vertical q_L profile. The logarithm is used to avoid the occurence of unphysical negative liquid water contents in the minimization process.

$$\boldsymbol{y} = (Z, Q_\mathrm{L})^T ; \boldsymbol{x} = (N_\mathrm{d}, \ln(q_\mathrm{L}))^T \tag{11}$$

~~Our aim is to gain a better understanding of the current possibilities and shortcomings when these key quantities of clouds are retrieved, by simultaneously adopting the space and ground perspective, and by contrasting them to each other. Due~~ The forward model ($F(\boldsymbol{x})$) for OE consists of two separate parts: a model (Eq. (12)) for the calculation of Q_L, and a model (Eq. (10)) for the calculation of N_d given the state vector $\boldsymbol{x}$.

$$Q_\mathrm{L} = \int \exp(\ln(q_\mathrm{L}(z))\mathrm{d}z \tag{12}$$

The Jacobians are calculated numerically using finite differences for both methods as follows:

$$H(x) = \frac{\delta y_i}{\delta x_j} = \frac{F(x_i + dx_i) - F(x_i)}{dx_i} \tag{13}$$

We apply the Levenberg-Marquardt minimization method until convergence is reached (Hewison, 2007) . Only profiles with all required input data are processed. Only 0.1 % of all the valid input profiles failed convergence within 30 iteration steps.

For the a-priori state vector, we assume that the liquid water profile follows the adiabatic scaled profile. For the a-priori N_d we set a value of $300\,\mathrm{cm}^{-3}$ which is a typical value for continental sites (Miles et al., 2000) . We assume that there are no correlations between the elements in the covariance matrix, implying no correlations of the q_L uncertainties at different height levels and no correlations between q_L and N_d uncertainties. This is a rather simplistic assumption, but the variances are set reasonably large. The standard deviation for N_d is set to $300\,\mathrm{cm}^{-3}$ and for $\ln(\mathrm{q_L})$ to $2.5\,\ln(\mathrm{gm}^{-2})$.

Just as for the background error covariance matrix, we assume for the observation error covariance matrix that there is no cross-correlation, and that all off-diagonal terms are thus zero.

The observation error covariance can be split up into individual contributing parts such as forward model error, radiometric noise error, and representativeness error. In this study the representativeness error is neglected, since observations and state variables are on the same grid. Radiometric noise errors are given by the Cloudnet algorithm. The forward model error is estimated by applying values of β in the range of 1 to 6 to the ~~under-constrained nature and assumptions made in retrieval methods, substantial differences for the obtained microphysical parameters may occur, as pointed outby Turner et al. (2007) , who investigated several ground-based retrieval methods for one case study of ground-based observations. We use a synergistic dataset combining SEVIRI, MODIS and Cloudnet (Illingworth et al., 2007) to address these problems. We investigate how close the adiabatic assumption matches the observations from ground and if the satellite retrievals can benefit from information about cloud adiabacitity retrieved from the ground.~~

~~The paper is structured as follows. In Sect. 3, we describe the instruments and data processing tools and algorithms used within this study. The retrieval methods based on an adiabatic description of clouds are presented in Sect. 2. Therein also a new optimal estimation retrieval of N_d using ground-based radar and microwave radiometer are presented. In Sect. 4 these retrievals are applied to four different cases which are then used to evaluate the satellite-based observations. Finally, a conclusion and outlook is given in Sect. 5.~~ radar forward model and taking the variance of the resulting reflectivity values for a sample cloud profile with a geometrical extent of 700 m and linearly increasing q_L in steps of 0.1 gm^{-2} per 100 m.

Given the retrieved N_d^OE and the theoretical adiabatic liquid water content for the observed cloud geometrical depth, we are able to calculate an adiabatic radar profile applying the relationship of q_L, Z and N_d of Fox and Illingworth (1997) . If we relate Z_ad to the Z_obs from the cloud radar we obtain a second method to calculate the adiabatic factor ($f_\mathrm{ad}^\mathrm{OE}$):

$$f_\mathrm{ad}^\mathrm{OE} = \frac{\int Z_\mathrm{obs} dz}{\int Z_\mathrm{ad} dz} \tag{14}$$

3 Data

3.1 Instruments and retrievals

~~For our study we combine observations from SEVIRI (Spinning Enhanced Visible and InfraRed Imager) onboard Meteosat Second Generation (MSG) and MODIS (Moderate-Resolution Imaging Spectroradiometer) onboard Terra and Aqua with ground-based remote sensing data obtained with~~

~~the same mobile instruments at sites at Leipzig, Germany (51.35, 12.43) and during a three month campaign at Krauthausen, Germany (50.897, 6.46).~~

Data from SEVIRI (Schmetz et al., 2002) are used for the geostationary satellite perspective. SEVIRI provides 12 spectral channels covering the visible, the near infrared, and the infrared spectrum. The channels used here have a nadir resolution of 3 km ~~×~~x 3 km. The spatial resolution decreases towards the poles and is about 4 km ~~×~~x 6 km over our region of interest (Central Europe). In this study we use the ~~5~~5-min temporal resolution data from the Rapid Scan Service (RSS). The SEVIRI radiances in the different channels are used as input for the Nowcasting Satellite Application Facility (NWCSAF) algorithm (Derrien, 2012) which provides a cloud mask, cloud top height, and cloud classification.

~~This~~ The NWCSAF cloud mask is used for deriving cloud phase, cloud optical depth, and effective radius with the KNMI (Royal Netherlands Meteorological Institute) cloud physical properties (CPP) algorithm (Roebeling et al., 2006), developed in the context of the satellite application facility on climate monitoring ~~(CMSAF, Schulz et al., 2009)~~ (CMSAF, Schulz et al., 2009) . To derive the cloud mask, different multispectral tests using SEVIRI channels are applied in order to discriminate cloudy from cloud-free pixels. The cloud top height for low, liquid clouds is obtained by using a ~~-~~best fit between measured brightness temperatures in the 10.8 μm channel and simulated values using the RTTOV radiative transfer model (Saunders et al., 1999) applied to atmospheric profiles from the ECMWF NWP model. Using a channel in the visible spectrum (0.6 μm) together with an absorbing channel in the near infrared (1.6 μm) (Nakajima and King, 1990), the CPP algorithm retrieves cloud optical depth as well as effective radius which are representative for the uppermost cloud part. As this method relies on solar channels it works only during daytime.

MODIS is an imaging spectrometer onboard the satellites Terra (descending node) and Aqua (ascending node) which probe the Earth's atmosphere from a polar orbit that results in one daytime overpass per satellite per day over the region of interest. MODIS measures in 36 bands in the visible, near-infrared, and infrared spectrum, with some bands having a spatial resolution of up to 250 m. The cloud physical properties (Platnick et al., 2003) are retrieved in a similar manner as for SEVIRI, but at 1 km spatial resolution using the channels 0.6 μm (band 1~~) over land~~, over land) and 2.1 μm (band 7, over land and sea). In addition, effective radius retrievals are available using the channels at 1.6 μm (band 6) and 3.7 μm (band 20) together with band 1. Note that band 6 on the Aqua satellite suffers from a stripe-problem (Meirink et al., 2013). In this study MODIS collection 5.1 is used for the retrieved cloud optical depth and effective radius.

The ground remote sensing instruments of the Leipzig Aerosol and Cloud Remote Observations System (LACROS) comprise a~~35~~ 35-GHz ~~MIRA~~ MIRA-35 cloud radar, a HATPRO (Humidity And Temperature PROfiler) microwave radiometer, and a CHM15X ceilometer, which are used also for field campaigns. All instruments are operated in a vertically pointing mode. The raw measurements are processed with the Cloudnet algorithm package (Illingworth et al., 2007). The output data is available in an unified temporal resolution of 30 s and a vertical grid of 30 m. Cloudnet uses further information from a ~~numerical weather prediction (NWP)~~ NWP model (here: COSMO-DE). In this study we use the attenuation-corrected radar reflectivity from the cloud radar, together with its error estimate, the liquid water path obtained from the microwave radiometer, as well as the cloud base and top height retrieved from ceilometer and cloud radar, respectively. ~~Also the~~ The vertical Doppler velocity from the cloud radar is also utilized. Furthermore Cloudnet provides a target classification applying a series of tests to discriminate cloud phase, drizzle or rain, and aerosols or insects.

3.2 ~~Synoptic conditions~~Cases

For this study, we focus on four ideal cases to gain a better understanding of the microphysical processes within the cloud by ruling out side-effects accompanying complicated cloud scenes ~~as good as~~ such as multi-layer clouds as well as possible. We ~~picked time periods for several days~~ consider single-layer cloud systems which are entirely liquid and non-drizzling as ideal. We chose cases in a way that ~~the most interesting cloud deck was covered by all ground instruments as well as~~ cloud layers are well-observed by all ground-based instruments and by MODIS and SEVIRI. ~~Ideal cases are single-layer cloud systems which are entirely liquid and non-drizzling. For this studywe selected two~~ In this study, we present, selected from the LACROS observationsm, two temporally rather homogeneous cases (27 October 2011 observed at Leipzig, and 21 April ~~2013~~observed at Krauthausen), and two more inhomogeneous cases (1 June 2012, 27 September 2012~~) in time which were observed by the instruments from LACROS at either Leipzigor Krauthausen. A~~ , both observed at Leipzig). In the following the terms homogeneous and inhomogeneous clouds always refer to the temporal homogeneity unless stated otherwise. For the ±15 surrounding SEVIRI pixels of the ground observations, we calculate the spatial inhomogeneity parameter following Cahalan et al. (1994) , which can be interpreted also in terms of temporal inhomogeneity (χ) if the frozen turbulence hypothesis is applied:

$$\chi = \frac{\exp(\overline{\ln\tau})}{\overline{\tau}} \tag{15}$$

A short overview of the cloud layer characteristics is given in Table ~~-~~2. The cloud boundaries are shown along with the cloud radar reflectivity profile in Fig. ~~1.~~ 1. Although we do not focus on the satellite cloud tops in this study we included these in Fig. 1. While for some time periods a good agreement can be seen, also periods with large discrepancies are found. Differences may result from semitransparent cirrus cloud layers (21 April 2013), inversion layers (27 October 2011) or broken cloud conditions (1 June 2012 and 27 September 2012). In the following we ~~describe~~ sum up the synoptic conditions for each case.

A ~~-~~high pressure system dominates the synoptic weather pattern on 27 October 2011 (Fig. ~~-~~1a). The temperature at the 850 hPa pressure level over Leipzig is around 5 °C. Therefore the stratocumulus cloud layer that is observed between 10:30 and 13:00 UTC consists entirely of water droplets. Its geometrical depth increases in the beginning of the observation period. The Cloudnet classification indicates a cloud deck even before (not shown), although the radar is not sensitive enough to detect the thin cloud layer between 10:00 and 10:30 UTC.

The weather pattern on 21 April 2013 (Fig. ~~-~~1b) is quite similar compared to the first case with the high pressure influence being stronger. The temperatures at the 850 hPa pressure level are slightly positive. During the whole observation period at Krauthausen a closed cloud deck is visible. The ~~ground-obtained~~ ground-based observation of cloud top height shows only small variability, while the cloud base is more inhomogeneous during the beginning of the observation period. A ~~-thin overlying Cirrus~~ thin overlying cirrus cloud deck can be observed around 10:00 UTC and between 11:~~00–12~~00 - 12:00 UTC.

An upper-level ridge covers Central Europe on 1 June 2012 (Fig. ~~-~~1c), but the area around Leipzig is also influenced by a ~~-~~surface low. Temperatures at 850 hPa lie around 10 °C. The stratocumulus cloud deck with the cloud tops slightly below 2000 m between 12:00 and 16:00 UTC is broken with some cloudy periods in the early afternoon that are not well detected by the cloud radar.

The weather pattern for the 27 September 2012 (Fig. ~~-~~1d) shows Leipzig directly in front of a well pronounced trough. Temperatures at ~~850~~850 hPa lie again around 10 °C and the cloud types vary between stratocumulus and shallow cumulus. The cloud base height increases throughout the day. After 16:00 UTC also some precipitation can be observed for a short time~~by means of virga that did not reach the ground~~.

4 ~~Cloud microphysical retrieval methods~~Results

~~To investigate aerosol indirect effects from satellite the adiabatic cloud model is commonly applied in state-of-the-art retrievals. It describes the distribution of microphysical parameters within the cloud. In this section we present the background of the adiabatic model, followed by a description of the retrieval methods applied in this study.~~

4.1 ~~Adiabatic cloud model~~

~~The behavior of a rising moist air parcel can be described as an adiabatic process if no entrainment takes place. Above the lifted condensation level, condensation begins and droplets start to grow with height. Condensation provides additional liquid water that is distributed over the number of droplets (N_d) in the volume. The liquid water content profile $q_\mathrm{L}(z)$ increases linearly with height (Albrecht et al., 1990) and can be related to $N_\mathrm{d}(z)$ and the mean volume droplet radius $r_\mathrm{v}(z)$:~~

$$q_\mathrm{L}(z) = \Gamma_\mathrm{ad}(T,p)z = \frac{4}{3}\pi r_\mathrm{v}^3(z)\rho_\mathrm{w} N_\mathrm{d}(z)$$

~~Here z is the height above cloud base, ρ_w is the density of water and $\Gamma_\mathrm{ad}(T,p)$ describes the adiabatic liquid water content gradient as a function of temperature and pressure. Restructuring this relationship and considering N_d constant with height yields the following mean cloud droplet radius profile ($r_\mathrm{v}(z)$):~~

$$\underline{r_\mathrm{v}(z) = \left(\frac{3\Gamma_\mathrm{ad}(T,p)}{4\pi\rho_\mathrm{w}N_\mathrm{d}}\right)^{1/3} z^{1/3}}$$

~~In remote sensing the effective radius (r_e) is more relevant, as it can be obtained from reflected solar radiation measurements. The effective radius is defined as the third over the second moment of the droplet size distribution (Hansen and Travis, 1974) and can be linked to the mean volume radius (r_v) with the following relationship:~~

$$\underline{r_\mathrm{e}^3(z) = k^{-1} r_\mathrm{v}^3(z)}$$

~~The factor k depends on the cloud type and corresponding typical droplet size distributions. Typical values for marine and continental liquid water clouds are 0.67~~ The following investigation is built on the observations from ground (cloud base height from ceilometer, cloud top height and ~~0.80, respectively (Brenguier et al., 2000) .~~

~~Deviations from a pure adiabatic cloud can be accounted for by replacing $\Gamma_\mathrm{ad}(T,p)$ by $\Gamma_\mathrm{eff} = \Gamma_\mathrm{ad}(T,p) f_\mathrm{ad}(z)$, introducing the so-called adiabatic factor $f_\mathrm{ad}(z)$. It can have values between 0 and 1, where a pure adiabatic cloud would correspond to $f_\mathrm{ad} = 1$. The deviation from the pure adiabatic q_L profile can result from mixing with dry air by either reducing the N_d (inhomogeneous mixing), reducing the radius (homogeneous mixing) or a mixture of both processes (Lehmann et al., 2009) . In general, for the adiabatic factor $f_\mathrm{ad}(z)$ a range of $[0.3, 0.9]$ is seen as common (Boers et al., 2006) . In the following we assume $f_\mathrm{ad}(z)$ to be constant for the whole vertical profile and write it as f_ad.~~

4.1 ~~Satellite retrievals~~

~~The adiabatic model can be used to relate Q_L (Eq. 7), N_d (Eq. 5) as well as the adiabatic cloud depth H_ad (Eq. 6) to the effective radius (r_e) and optical depth (τ). The latter two can be retrieved from satellite remote sensing using the method described in Nakajima and King (1990) :~~

$$\underline{Q_\mathrm{L}^\mathrm{SEVIRI} = \frac{5}{9}\rho_\mathrm{w}\tau r_\mathrm{e}}$$

$$\underline{N_\mathrm{d}^\mathrm{SEVIRI} = A_1 \tau^{0.5} r_\mathrm{e}^{-2.5}}$$

$$\underline{H_\mathrm{ad}^\mathrm{SEVIRI} = A_2 \tau^{0.5} r_\mathrm{e}^{0.5}}$$

~~These equations are also applied for MODIS τ and r_e. The factors A_1 and A_2 are variable (Janssen et al., 2011) . They depend on $\Gamma_\mathrm{ad}(T,p)$ and the adiabatic factor. Often they are considered to be constant. In doing so pure adiabatic clouds with a representative $\Gamma_\mathrm{ad}(T,p)$ are assumed (e.g. Quaas et al., 2006) .~~

~~The uncertainty of the different parameters contained in A_{I} are discussed by Janssen et al. (2011) . They estimated the uncertainty of k to be negligible (around 3). When considering the whole seasonal variability of cloud base temperature, they obtained an error of 24for the adiabatic lapse rate of liquid water mixing ratio ($\Gamma_{\mathrm{ad}}(T,p)$). In our case, this error is supposed to be considerably smaller since we use NWP data to constrain the cloud top temperature. Janssen et al. (2011) were further assuming an uncertainty in the adiabatic factor of 0.3. This resulted in a numerically evaluated error of around 26considering typical values of effective radius and optical depth. We will discuss the applicability and shortcomings of the adiabatic model in Sect. 4.~~

4.1 ~~Ground-based retrievals~~

~~Ground-based retrievals usually combine several remote sensing techniques. From the ceilometer extinction profile it is possible to obtain the cloud base height , because the laser beam is strongly attenuated by liquid droplets and photons are only able to penetrate the lowest part of the cloud (Martucci et al., 2010) . The radiation of the cloud radaris, on the other hand, able to penetrate clouds and the strong gradient of the range-corrected radar reflectivity profile is used to determine the cloud top height. For the derivation of the cloud top we further use the Cloudnet target classification, so that the cloud top and base heights refer only to the liquid cloud layer and ignore overlaying cirrus clouds. This difference between cloud top and cloud base height is referred to as the observed cloud geometrical depth ($H_{\mathrm{obs}}^{\mathrm{ground}}$). The adiabatic scaled cloud depth ($H_{\mathrm{ad}}^{\mathrm{ground}}$) is obtained by assuming a linear q_{L} profile which integral matches the observed Q_{L}~~ Z from cloud radar, Q_{L} from the microwave radiometer~~, starting from the cloud base while accounting for $\Gamma_{\mathrm{ad}}(T,p)$ at cloud base:~~

$$\cancel{H_{\mathrm{ad}}^{\mathrm{ground}} = \sqrt{2 \cdot \frac{Q_{\mathrm{L}}}{\Gamma_{\mathrm{ad}}(T,p)}}}$$

) and from passive satellites (τ, r_{e}).

~~To calculate the adiabatic factor (f_{ad})we relate the $H_{\mathrm{obs}}^{\mathrm{ground}}$ to Q_{L} obtained from the microwave radiometer (Wood, 2006) .~~

$$\cancel{f_{\mathrm{ad}} = \frac{2Q_{\mathrm{L}}}{\left(H_{\mathrm{obs}}^{\mathrm{ground}}\right)^2 \Gamma_{\mathrm{ad}}(T,p)}}$$

~~Cloud microphysical quantities can be described in terms of moments of the droplet size distribution. The cloud droplet number concentration is equivalent to the zeroth moment, the mean radius to the first moment, the liquid water content is proportional to the third moment, while the effective radius is the third over the second moment and the radar reflectivity factoris proportional to the sixth moment. Relating these moments gives the chance to fully describe a unimodal distribution following either a gamma or lognormal shape and therefore calculating other moments of the size distribution which are not directly observed (Rémillard et al., 2013) . This is the basis for most~~

~~retrieval methods. In the next section, we present a retrieval combining microwave radiometer and cloud radar observations,~~ We will first focus on ground-based retrievals and evaluate the adiabatic factor, followed by a ~~description of two optimal estimation approaches. These use the same observations but also account for the instrument uncertainties and prior assumptions of adiabatic liquid cloud profiles.~~

~~Given $H_{\mathrm{obs}}^{\mathrm{ground}}$ and $N_{\mathrm{d}}^{\mathrm{OE1}}$ (described in the following Sect. 2.2.2) we can calculate the~~ comparison of ground-based ~~optical depth (τ^{ground}, Eq. 3) and effective radius ($r_{\mathrm{eff}}^{\mathrm{ground}}$, Eq. 4) (Wood, 2006) which are also used for comparison with the satellite obtained values later on.~~

$$\tau^{\mathrm{ground}} = 0.0145 \cdot \left(\Gamma_{\mathrm{ad}}(T,p) f_{\mathrm{ad}}\right)^{\frac{2}{3}} \left(k N_{\mathrm{d}}^{\mathrm{OE1}}\right)^{\frac{1}{3}} \left(H_{\mathrm{obs}}^{\mathrm{ground}}\right)^{\frac{5}{3}}$$

$$r_{\mathrm{e}}^{\mathrm{ground}} = 0.0620 \cdot \left(\Gamma_{\mathrm{ad}}(T,p) f_{\mathrm{ad}}\right)^{\frac{1}{3}} \left(k N_{\mathrm{d}}^{\mathrm{OE1}}\right)^{-\frac{1}{3}} \left(H_{\mathrm{obs}}^{\mathrm{ground}}\right)^{\frac{1}{3}}$$

4.0.1 ~~Radar-radiometer retrieval of cloud droplet number concentration~~

~~Following Fox and Illingworth (1997) , we relate the measured radar reflectivity (Z), q_{L} and N_{d}. Thereby it is assumed that the droplet size distribution can be described by a gamma distribution with index β (Fox and Illingworth, 1997; Martucci and O'Dowd, 2011) . A similar method has been applied in (Rémillard et al., 2013) , but using a lognormal size distribution. Although N_{d} may vary vertically, it is commonly suspected that it stays nearly constant throughout the vertical column of a nonprecipitating cloud (Bennartz, 2007; Brenguier et al., 2000) . To retrieve the column cloud droplet number concentration from the available single-layer observations , we integrate q_{L} over the cloud column and can therefore use Q_{L} from the microwave radiometer (compare Rémillard et al., 2013) :~~

$$N_{\mathrm{d}}^{\mathrm{FI}} = \frac{9}{2\pi^2 k \rho^2} \frac{(\beta+6)!}{(\beta+3)!(\beta+3)^3} \frac{Q_{\mathrm{L}}^2}{(\int \sqrt{Z} \mathrm{d}z)^2}$$

~~Both, homogeneous and inhomogeneous mixing (Lehmann et al., 2009) can easily alter the microphysical quantities in clouds in ways not adequately adressed within the retrieval schemes. For example, the size distribution may become skewed and not be accurately described with a gamma-shape anymore. However, Boers et al. (2006) and Janssen et al. (2011) found out, that both assumptions about the mixing process result in nearly the same vertically averaged N_{d}.~~

4.0.1 ~~Optimal Estimation of cloud droplet number concentration~~

~~The Optimal Estimation (OE) technique allows to derive~~ N_{d} retrieval results using the FI and OE method. Aftewards the key quantities H, N_{d}, Q_{L} obtained from satellite observations of SEVIRI and MODIS will be evaluated against the respective ground-based observations. We calculate the cloud droplet number concentration and ~~the liquid water content profile considering also observation~~

~~uncertainties. We introduce here two different strategies in order to better address the topic of cloud adiabacity.~~

~~Both approaches are based on the assumptions mentioned above, i.e. a vertically constant N_d, a gamma-shaped droplet size distribution with parameter β and a nonlinear relationship between q_L, N_d, and Z. We include error estimates for the observed quantities as well as an a-priori state together with its error estimate. The optimal estimation method aims on finding the most likely state given the observations. Therefore we try to minimize a cost function following Rodgers (2000) .~~

~~The main difference of the two approaches lies in the degree of freedom for the q_L profile. For the first method, we allow the q_L profile to take any shape and therefore deviate from the adiabatic model (referred to as OE1), while the second method enforces a linear increase of q_L with height (OE2). The cost function of OE2 can thus be used as a measure of deviation from the adiabatic assumption.~~

~~Our observation vector ($\boldsymbol{y}$) for OE1 contains the radar reflectivity Z and the microwave radiometer Q_L. Our state vector ($\boldsymbol{x}$) for OE1 contains the vertically-constant N_d and the natural logarithm of the vertical q_L profile. The logarithm is used to avoid the occurence of unphysical negative liquid water contents in the minimization process.~~

$$\boldsymbol{y} = (Z, Q_\mathrm{L})^T; \quad \boldsymbol{x} = (N_\mathrm{d}, \ln(q_\mathrm{L}))^T$$

~~The forward model ($F(\boldsymbol{x})$) for OE1 consists of two separate parts: a model H_1 (Eq. 12) for the calculation of Q_L, and a model H_2 (Eq. 10) for the calculation of N_d given the state vector $\boldsymbol{x}$.~~

$$H_1 : Q_\mathrm{L} = \int \exp(\ln(q_\mathrm{L}(z)))\mathrm{d}z$$

~~The main difference for OE2 lies in the state vector, which does not contain the q_L profile since this is fixed by the observation of Q_L using the adiabatic scaled q_L profile.~~

$$\boldsymbol{x} = (N_\mathrm{d})^T$$

~~The observation vector remains the same (Eq. 11). The forward model for OE2 only consists of the N_d calculation in the same way as for OE1 (Eq. 10).~~

~~The Jacobians are calculated numerically using finite differences for both methods as follows:~~

$$H(x) = \frac{\delta y_i}{\delta x_j} = \frac{F(x_i + \mathrm{d}x_i) - F(x_i)}{\mathrm{d}x_i}$$

~~We apply the Levenberg-Marquardt minimization method until convergence is reached (Hewison, 2007) . Only profiles with all required input data was processed. Only 0.1failed convergence within 30 iteration steps.~~

~~For the prior state vector of OE1 we assume that the liquid water profile follows the adiabatic sealed profile. For OE2~~ cloud geometrical depth from the passive satellite-derived τ, r_e, assuming in the first step $f_\mathrm{ad} = 1$ and in a second step the f_ad calculated from the ~~q_L profile is always set equal~~

~~to the adiabatic scaled profile. For the a-priori N_d we set a value of 300which is a typical value for continental sites (Miles et al., 2000) . We assume that there are no correlations between the elements in the covariance matrix, implying no correlations of the q_L uncertainties at different height levels and no correlations between q_L and N_d uncertainties. This is a rather simplistic assumption, but the variances are set reasonably large. The SD for N_d is set to 300and for $\ln(q_\mathrm{L})$ to 2.5~~ground-based observations.

~~Just as for the background error covariance matrix, we assume for the observation error covariance matrix that there is no cross-correlation, and that all off-diagonal terms are thus zero.~~

~~The observation error covariance could be split up into individual contributing parts such as forward model error, radiometric noise error, and representativeness error. Here only forward model errors and the observation errors are considered. Observation errors are given by the Cloudnet algorithm. The forward model error is estimated by applying values of β in the range of 1 to 6 to the radar forward model and taking the variance of the resulting reflectivity values for a sample cloud profile with a geometrical extent of 700and linearly increasing q_L in steps of 0.1per 100.~~

5 ~~Results~~

~~The retrieval methods described in the previous section have been applied to the case studies introduced in Sect. 3.2. We investigate differences for cloud key parameters for four cases, two being more homogeneous and two showing more temporal variability in cloud cover. Those key parameters are important for further investigation of the first indirect effect. Deviations resulting from two different perspectives on the same cloud scene have to be kept in mind for the interpretation.~~

4.1 Retrieval of cloud properties from ground

~~We first evaluate the results from the ground-based perspective before comparing those to the satellite retrieved values.~~

4.1.1 Cloud adiabatic factor

4.1.2 ~~Cloud geometrical depth and cloud adiabacity~~

~~From ground we have the opportunity to compare $H_\mathrm{obs}^\mathrm{ground}$ observed with radar and lidar with the virtual adiabatic $H_\mathrm{ad}^\mathrm{ground}$ derived from Q_L measurements (Eq. ??).~~

~~Differences between $H_\mathrm{obs}^\mathrm{ground}$ and $H_\mathrm{ad}^\mathrm{ground}$ can be mainly explained by subadiabaticity (Roebeling et al., 2008a) .~~ Entrainment of dry air leads to deviations from the linearly increasing ~~q_L~~ q_L profile. The cloud adiabatic factor as calculated from Eq. ~~(~~(8) using ~~Q_L~~ Q_L from the microwave radiometer and ~~$H_\mathrm{obs}^\mathrm{ground}$~~ $H_\mathrm{obs}^\mathrm{ground}$ can quantify such deviations.

~~Comparing the time series of $H_\mathrm{obs}^\mathrm{ground}$ and $H_\mathrm{ad}^\mathrm{ground}$ for the two homogeneous cases (Fig. 2a and b), we find a correlation of 0.96 on 27 October 2011. For 21 April 2013 we find a correlation of 0.56~~

~~after 09:00UTC. Before 09:00UTC the adiabatic scaled cloud depth is considerably smaller than the values obtained by the observed cloud depth. The radar reflectivity measurements (Fig. 1b) reveal that the cloud base is more inhomogeneous during this time period than later on. On average, $H_{\mathrm{obs}}^{\mathrm{ground}}$ is larger than $H_{\mathrm{ad}}^{\mathrm{ground}}$, 284versus 238for 27 October 2011, and 404vs. 313for 21 April 2013.~~

~~The time~~ The time series of the adiabatic factor calculated for the two homogeneous cases is shown in Fig. ~~3aand~~ 2a,b. The adiabatic factor at 27 October 2011 lies in the range from 0.4 to 0.9. Short time periods with ~~$f_{\mathrm{ad}} > 1$~~ $f_{\mathrm{ad}} \geq 1$ occur. These ~~superadiabatic~~“superadiabatic” points are likely to be artefacts, since the occurence of ~~superadiabatic~~“superadiabatic” cloud profiles in nature is physically implausible. Such artefacts may easily arise due to ~~enhanced Q_{L} by drizzle or an underestimation of actual H_{cloud}~~uncertainties in Q_{L} and H_{cloud} for thin clouds. In contrast to the original Cloudnet code, our calculation of the adiabatic factor allows for values greater than one. Within Cloudnet ~~superadiabatic~~“superadiabatic” profiles are avoided by increasing the cloud top height if the adiabatic integrated ~~q_{L}~~ q_{L} is smaller than ~~Q_{L}~~ Q_{L} measured by the microwave radiometer. We omitted adiabatic factors with ~~$f_{\mathrm{ad}} > 1.5$~~ $f_{\mathrm{ad}} > 1.0$ since we believe that those are most likely affected by the measurement uncertainties. ~~At~~ This can be seen when considering the uncertainties that influence the adiabatic factor. For example, consider a cloud with $Q_{\mathrm{L}} = 100\,\mathrm{g\,m^{-2}}$ and $H_{\mathrm{obs}}^{\mathrm{ground}} = 324\,\mathrm{m}$ that is adiabatic ($f_{\mathrm{ad}} = 1$). The Q_{L} retrieval uncertainty (microwave radiometer instrument error + retrieval error) is approximately $20\,\mathrm{g\,m^{-2}}$ and the $H_{\mathrm{obs}}^{\mathrm{ground}}$ uncertainty of the ceilometer and the cloud radar is at least $\pm\,60\,\mathrm{m}$ due to the vertical resolution. Accounting for the maximum uncertainty ($Q_{\mathrm{L}} = 120\,\mathrm{g\,m^{-2}}$, and $H_{\mathrm{obs}}^{\mathrm{ground}} = 64\,\mathrm{m}$) or ($Q_{\mathrm{L}} = 80\,\mathrm{g\,m^{-2}}$ and $H_{\mathrm{obs}}^{\mathrm{ground}} = 384\,\mathrm{m}$), the resulting adiabatic factor would be 1.81 or 0.57, respectively. This shows that with the current uncertainty limits of the ground-based observations the adiabatic factor is still prone to large uncertainties especially for geometrically thin clouds.

For cross-checking with an independent approach, we also calculate the adiabatic factor using the information of the radar reflectivity profile. We see in Fig. 3 that the mean adiabatic factor calculated from the radar profiles is generally a bit lower, and that the correlation for all four cases is quite good with 62 % to 95 %, and root mean square differences between 0.14 and 0.24. This difference is likely explained by uncertainties in $H_{\mathrm{obs}}^{\mathrm{ground}}$ and Q_{L}, but also in Z obtained from the cloud radar and the retrieved N_{d}. In the following we will use the adiabatic factor calculated from Q_{L} and $H_{\mathrm{obs}}^{\mathrm{ground}}$.

On 21 April 2013 we find values of the adiabatic factor f_{ad} between 0.2 and 0.6 before 09:00 ~~corresponding to the larger $H_{\mathrm{obs}}^{\mathrm{ground}}$~~UTC. The radar reflectivity measurements (Fig. 1b) reveal that the cloud base is more inhomogeneous during this time period than later on. After 09:00 UTC the adiabatic factor oscillates between 0.5 and 1.0. Overall, the adiabatic ~~factors~~ factor also found for the ~~homogeneous cases~~ other homogeneous case agrees well with the range of values of $[0.3, 0.9]$ suggested by Boers et al. (2006).

For the two inhomogeneous cases~~(Fig. 2c and d) we find correlations between $H_{\mathrm{obs}}^{\mathrm{ground}}$ and $H_{\mathrm{ad}}^{\mathrm{ground}}$ of 0.63 (1 June 2012) and 0.76 (27 September 2012). Similar to the homogeneous cases, we see that~~

~~$H_{\mathrm{obs}}^{\mathrm{ground}}$ points to thicker clouds in general. The mean of $H_{\mathrm{obs}}^{\mathrm{ground}}$ is 364in contrast to the mean of $H_{\mathrm{ad}}^{\mathrm{ground}}$ which is 244for 1 June 2012 and 314in contrast to 261for 27 September 2012.~~

~~For the two inhomogeneous cases the~~ , the variability of the adiabatic factor (Fig. ~~3cand~~ 2c,d) is larger than for the homogeneous cases considered before (Table 3), but the range of values is similar. This shows that independent from cloud homogeneity ~~many clouds are actually subadiabatic.~~

~~We are furthermore interested in dependencies of the adiabatic factor on the cloud morphology and thermodynamics. For the following investigation, we consider data points from all four cases. We relate the adiabatic factor to $H_{\mathrm{obs}}^{\mathrm{ground}}$ and the median radar-observed vertical velocity of each cloud layer~~the majority of clouds seems to be sub-adiabatic.

Figure 4 reveals a tendency that ~~geometrical~~ geometrically thicker clouds are less adiabatic, while mainly the thin clouds (~~$H_{\mathrm{obs}}^{\mathrm{ground}} < 400\,\mathrm{m}$~~$H_{\mathrm{obs}}^{\mathrm{ground}} < 400\,\mathrm{m}$) are responsible for the ~~superadiabatic~~"superadiabatic" cloud profiles. This supports the findings of Min et al. (2012) , who observed the tendency that thicker clouds are less adiabatic in the Southeast Pacific. The investigation of ~~such~~ thin clouds remains challenging. ~~This can be seen also when considering the uncertainties that influence the adiabatic factor. For example, consider a cloud with $Q_{\mathrm{L}} = 100\,\mathrm{g\,m^{-2}}$ and $H_{\mathrm{obs}}^{\mathrm{ground}} = 324\,\mathrm{m}$ that is purely adiabatic ($f_{\mathrm{ad}} = 1$). The Q_{L} retrieval uncertainty (microwave radiometer instrument error + retrieval error) lies around 20and the $H_{\mathrm{obs}}^{\mathrm{ground}}$ uncertainty is at least ±60due to the vertical resolution. Accounting for the maximum uncertainty ($Q_{\mathrm{L}} = 120\,\mathrm{g\,m^{-2}}$, and $H_{\mathrm{obs}}^{\mathrm{ground}} = 264\,\mathrm{m}$) or ($Q_{\mathrm{L}} = 80\,\mathrm{g\,m^{-2}}$ and $H_{\mathrm{obs}}^{\mathrm{ground}} = 384\,\mathrm{m}$), the resulting adiabaticfactor would be 1.81 or 0.57, respectively. This shows that with the current uncertainty limits of the ground-based observations the adiabatic factor is still prone to large uncertainties.~~ We therefore neglect cloud profiles with $f_{\mathrm{ad}} > 1$ in the following.

Schmidt et al. (2014a) used observations of two cases with homogeneous stratocumulus clouds over Leipzig, Germany, and found that in case of occurence of updrafts in clouds, the q_{L} profile is more adiabatic. To investigate if such a behaviour also occurs for our cases we apply the cloud radar Doppler velocity. The average vertical velocity of each cloud profile is found at ~~−0.1~~-0.1 $\mathrm{ms^{-1}}$ with the majority of points in the range [~~−1,~~-1,1] $\mathrm{ms^{-1}}$. Considering this vertical velocity as function of cloud adiabacity we find a large spread, which makes it difficult to detect a clear dependence of cloud adiabacitity on updraft speed. However if we calculate the median adiabatic factor for the updraft and downdraft regimes individually, we find for each of our ~~case studies that the~~ cases that clouds are slightly more adiabatic in the updraft regime (Table 3). This behaviour is expected from adiabaticity and also supported by the findings of ~~e.g.~~ Schmidt et al. (2014a). They ~~used observations of two cases with homogeneous stratocumulus clouds over Leipzig, Germany, and observed that in case of updrafts in the clouds, the q_{L} profile is more adiabatic. They also~~ report that this effect is strongest at the cloud base and blurs when the data points are averaged over the whole cloud profile.

4.1.2 Cloud droplet number concentration from radar-radiometer retrievals

~~N_d~~ N_d is used as the main parameter in many investigations of the first indirect aerosol effect. Advances have been made over the last two decades to apply retrievals for ~~N_d~~ N_d combining ground-based cloud radar and microwave radiometer. We applied such a method following Fox and Illingworth (1997) (hereafter: FI, see Sect. 2.2.1). Furthermore we compare those results with the newly developed Optimal Estimation ~~approaches~~ approach (see Sect. 2.2.2).

Contrasting the ~~N_d from OE1 and OE2~~ N_d from OE with the FI method, we find that the absolute mean difference of ~~$N_\mathrm{d}^\mathrm{OE1}$ and N_d^FI~~ N_d^OE and N_d^FI considering all cases is ~~smaller with~~ $164\,\mathrm{cm}^{-3}$ (19 %)~~than for $N_\mathrm{d}^\mathrm{OE2}$ and N_d^FI with 271(31)~~. Overall, the FI method tends to yield lower values than the ~~OE1~~ OE method, even though some outliers with ~~unreasonable~~ unreasonably large values can be found (~~$N_\mathrm{d}^\mathrm{OE1} > 2000\,\mathrm{cm}^{-3}$). Outliers also occur for OE2, but can be filtered using the cost function. Neglecting N_d retrievals with cost function values greater than 2, we find a correlation between OE1 and OE2 of 93.~~ $N_\mathrm{d}^\mathrm{OE} > 2000\,\mathrm{cm}^{-3}$). In contrast to the FI method the OE ~~methods are~~ method is also able to give information about the remaining uncertainty by ~~processing~~ considering measurement uncertainties as well as the uncertainty of the background state. With a quite large background uncertainty assumed to be $300\,\mathrm{cm}^{-3}$, we can see that the information (measurement and uncertainties) from the ground observation is able to reduce the final analysis error for ~~N_d~~N_d, but more constraints are required to obtain ~~N_d~~ N_d with even higher accuracy. This would be desirable to better evaluate satellite observations.

~~To investigate the two OE approaches in more detail, we compared them in terms of the remaining cost function (J) of the OE2 approach that allows only adiabatic profiles. As shown in Fig. 5 the agreement of N_d especially for the two homogeneous cases is close for values smaller than 300and $J < 2$. Increasing the cost function leads to a steady disagreement of the $N_\mathrm{d}^\mathrm{OE1}$ and $N_\mathrm{d}^\mathrm{OE2}$. Furthermore $N_\mathrm{d}^\mathrm{OE2}$ gives gradually higher values with increasing N_d. The first point can be interpreted as follows: the cost function remains high if it is not possible within the OE scheme to closely match the observations (i.e. the radar reflectivity profile). Since in the OE2 method an adiabatic profile is always required, higher cost function values can be interpretated as larger deviations of the observation from the adiabatic model if the assumption of a vertical constant CDNC is valid. For e.g. the 21 April 2013 case the deviations of the radar profile from the adiabatic description before 09:00UTC can be clearly observed (compare Fig. 1b) in terms of a thin second layer occuring in the radar profiles closely below the base of the main layer. With a pure adiabatic description as applied for OE2 it is not possible to represent such a structure. This further confirms that even small deviations from the adiabatic assumption can lead to significant differences in the retrieval of key parameters used to investigate the first indirect aerosol effect.~~

4.2 Comparison of cloud properties from satellite and ground

Cloud microphysical retrievals that are based on either satellite or ground-based remote sensing both have their advantages and shortcomings. However, when the results of both approaches are in agreement, it is likely that the corresponding cloud layers are well suited for the investigation of key factors determining the first indirect effect.

By comparing ground-based and satellite observations, we have to consider the different spatial and temporal resolution, different error sources of the instruments as well as the different viewing zenith angle on the cloudy scene. For ~~MSG~~ SEVIRI we have to consider a parallax shift at higher latitudes. The satellite viewing zenith angle for Leipzig is 58.8 °. Within this study the average cloud top height is between 1 km and 3 km (see Table 2). This would result in a horizontal displacement of max. 5 km. Considering the spatial resolution of SEVIRI over Central Europe of 4 km ~~×~~x 6 km, we decided to neglect the parallax correction for our study. To address the uncertainty of the satellite observations from SEVIRI and also MODIS we calculated the ~~SD~~ standard deviation of the surrounding pixels. For SEVIRI ±1 pixel around the central pixel is added, resulting in a field of 9 satellite pixels. To cover a comparable area for MODIS, we add ±9 pixel around the central pixel. For the comparison of the time series obtained from space and ground we applied data averaging only if mentioned. As pointed out in the following discussion for inhomogeneous scenes, omitting temporal averaging can lead to considerable differences of ground and satellite quantities.

4.2.1 ~~Cloud geometrical depth~~Liquid water path

~~Contrasting $H_{\mathrm{ad}}^{\mathrm{SEVIRI}}$ with the $H_{\mathrm{obs}}^{\mathrm{ground}}$ from Cloudnet (Fig. 2), we are able to investigate the same quantity obtained with two independent physical retrieval approaches. The correlation is 0.44 for 21 April 2013 after 09:00~~Considering the uncertainty of 20 ~~UTC, 0.59 for 27 October 2011, 0.44 for 1 June 2012, and 0.15 for 27 September 2012. The correlation increases when temporally averaging is applied (Table 4). The correlations for temporally averaged data are within the range that was also obtained by Roebeling et al. (2008a) . They found correlations of 0.71~~ gm^{-2} in Q_{L} for the ground-based microwave radiometer, the absolute mean difference between SEVIRI and ~~Cloudnet for a homogeneous stratocumulus cloud layer. The improvement of results is not surprising when comparing averaged data as also pointed out in other studies (Deneke et al., 2009) . However, a too long averaging period could smear the original variability of the data.~~

~~Considering the mean difference of $H_{\mathrm{ad}}^{\mathrm{SEVIRI}}$ and $H_{\mathrm{ad}}^{\mathrm{ground}}$ for the homogeneous cases, we find values of 52~~the ground-based MWR is in good agreement. We find mean differences (relative mean difference) of 11 ~~(22~~gm^{-2} (14%) for 21 April 2013, 16 ~~) for~~ gm^{-2} (28%) for 27 October 2011~~(Fig. 2a) and 49~~, 27 ~~(15~~gm^{-2} (62%) for 1 June 2012 and 22 ~~) for 21 April 2013~~ gm^{-2} (~~Fig. 2b) . The temporal pattern is well captured by SEVIRI. As shown~~ 42%) for 27~~October 2011 in Fig. 6a, the largest differences in adiabatic cloud depth also show up as differences in Q_{L} between SEVIRI and Cloudnet as both differences are linearly linked and only depend on $\Gamma_{\mathrm{ad}}(T,p)$ (Eq. ??) . Therefore differences in Q_{L} may be used as an indicator for agreement of cloud geometrical depth if only Q_{L} observations are available.~~ September 2012.

On 27 October 2011 we find larger differences in ~~Q_L~~ Q_L mainly after 12:00 UTC ~~. The largest differences between $H_\mathrm{ad}^\mathrm{SEVIRI}$ and Cloudnet $H_\mathrm{ad}^\mathrm{ground}$ of around 200relate to Q_L differences of~~ with up to 100 ~~. Although some slight drizzle beneath the cloud base is identified by the Cloudnet classification for several short time periods after 12:00UTC, the drizzle signal in the radar reflectivity profile is not very pronounced~~ $\mathrm{g\,m^{-2}}$ (Fig. ~~1a). Generally drizzle could~~ 5). Although rain might be a possible explanation for ~~the higher Q_L~~ higher Q_L observed with the ground-based microwave radiometer~~. The latter is sensitive to the total amount of liquid within the cloud, while the satellite retrieval is based on optical depth and effective radius in the uppermost cloud parts. Although the effective radius at both cloud base and cloud top is affected by drizzle, it has been previously observed that the former is more sensitive to drizzle (Chen et al., 2008) . This can lead to biases in the different retrieval approaches for Q_L.~~ , there are no are no signs for precipitation in both radar signal and satellite observations. The effective radius observed from satellite near cloud top lies clearly below the value of 14 μm which was suggested by Rosenfeld et al. (2012) as the threshold ~~to~~ for drizzle/rain forming clouds.

~~In the following, we contrast the behaviour of the two inhomogeneous cases (Fig. 2c and d) with the homogeneous cases (Fig. 2a and b). The mean differences between $H_\mathrm{ad}^\mathrm{SEVIRI}$ and Cloudnet $H_\mathrm{ad}^\mathrm{ground}$ are 116~~The maximum of the radar reflectivity in each profile did also not -20 ~~(47) and 103(39) for 1 June 2012 and 27 September 2012, respectively. Those values are twice as high as for the homogeneous cases. The Q_L~~ dBZ, which is commonly taken as a drizzle threshold (Rémillard et al., 2013; Mace and Sassen, 2000) . The observed difference might well be attributed to the satellite retrieved Q_L. For the same time period we also find disagreement in N_d from SEVIRI and ground and will discuss possible reasons in this context later.

For the inhomogeneous cases, the Q_L obtained from the ground-based microwave radiometer is highly variable. Especially the Cloudnet observations ~~at~~ on 27 September 2012 show rapid changes of ~~Q_L~~ Q_L with peaks around 400 $\mathrm{g\,m^{-2}}$ and cloud-free periods. The SEVIRI temporal pattern is more smooth, because the satellite signal represents an average over different sub-pixel clouds within the field of view ~~. Within 10a cloud field advected at constant wind speed of 10over the ground site moves 6(spatial resolutionof SEVIRI RSS)~~due to the lower spatial resolution. ~~The comparison of such a 10~~

4.2.2 Cloud geometrical depth

Contrasting $H_\mathrm{ad}^\mathrm{SEVIRI}$ with the $H_\mathrm{obs}^\mathrm{ground}$ (Fig. 6), we are able to investigate the same quantity obtained with two independent physical retrieval approaches. The correlation coefficient is 0.47 for 21 April 2013 after 09:00 ~~averaged $H_\mathrm{ad}^\mathrm{SEVIRI}$ and Cloudnet $H_\mathrm{ad}^\mathrm{ground}$ gives mean differences of 119and 92for~~ UTC, 0.59 for 27 October 2011, 0.41 for 1 June 2012~~and~~ , and 0.12 for 27 September ~~2012, respectively. Longer averaging times lead to slightly improved agreement~~ 2012. The correlation increases when temporally averaging is applied (Table 4). The improvement of correlation is not surprising when comparing averaged data as also pointed out in other studies (Deneke et al., 2009) . However, a longer averaging period could remove the original variability of the data. The correlations for temporally averaged data are within the range of values that were obtained by Roebeling et al. (2008b) , Min et al. (2012) and Painemal and Zuidema (2010) . Roebeling et al. (2008b) found correlations of 0.71 between SEVIRI and Cloudnet for a homogeneous stratocumulus cloud layer. Min et al. (2012) found correlations of 0.62 between in-situ and MODIS retrieved H, and could show a better agreement of H when the adiabatic factor is explicitely calculated and considered. Painemal and Zuidema (2010) found correlations of 0.54 (0.7 for $H < 400\,\mathrm{m}$ with cloud fraction$> 90\,\%$) comparing radiosonde-derived cloud geometrical depth to respective MODIS observations. In their study Painemal and Zuidema (2010) reported that satellite values were higher compared to the ground-based ones. The reason for this can potentially be explained by a bias of MODIS-retrieved r_e but also in the choice of the adiabatic factor in the retrieval of H (Eq. 6). Satellite derived H increases if we choose $f_{ad} < 1$ instead of $f_{ad} = 1$. ~~Averaging over 30~~

If the adiabatic factor obtained from ground is applied to Eq. 6 instead of $f_{ad} = 1$, we find that the mean difference (relative mean difference) for the two homogeneous cases reduces from 87 ~~results in mean differences of 101~~m (~~44~~31 %) ~~and 68~~to 45 m (16 %) for 27 October 2011, and from 87 m (23 %) to 14 m (4 %) for 21 April 2013. The same holds true for the inhomogeneous case at 27 September 2012 with a reduction from 149 m (47 %) to 90 m (29 %), but not for 1 June 2012 ~~and 27 September 2012, respectively.~~ where the mean difference increases from 86 m (24 %) to 216 m (60 %).

For the cases investigated here, we saw a better agreement in H for available MODIS retrievals compared to SEVIRI if $f_\mathrm{ad} = 1$ is choosen. Indeed, clouds are actually sub-adiabatic while the retrieval assumes adiabatic clouds. This could counteract a high bias in MODIS r_e that is reported in previous studies (Marshak et al., 2006) . For the four cases considered in this study, the number of collocated observations with MODIS is not sufficient in order to determine which effect is predominant for the bias. Therefore a larger dataset would be desirable for a more in-depth investigation.

4.2.3 Cloud droplet number concentration

~~Also the retrieval of N_d~~ The retrieval of N_d from passive satellite observations relies on the ~~adiabatic~~ (sub-)adiabatic cloud model. In the following we contrast ~~N_d~~ N_d retrieved from ground with the ~~OE1~~ OE method and the adiabatic ($f_{ad} = 1$) retrieved values from MODIS and SEVIRI. ~~We first consider the two homogeneous cases. The retrieved N_d is~~ The retrieved N_d are shown in Fig. ~~7a and b~~7. At 21 April 2013 the values agree within the uncertainty range with a mean difference ~~of 78~~(relative mean difference) of 29 ~~(27~~cm^{-3} (10%) between SEVIRI and ~~OE1~~ OE retrievals for the whole time period.

For 27 September 2012 and 1 June 2012 we find mean differences (relative mean differences) of 23 cm^{-3}(7%) and 103 cm^{-3} (43 %), respectively. At 27 October 2011 we find larger differences between SEVIRI and the ground-based ~~retrievals~~N_d. At the beginning of the observation period (before 10:30 UTC) the ~~$N_\mathrm{d}^\mathrm{SEVIRI}$~~ $N_\mathrm{d}^\mathrm{SEVIRI}$ values are much lower than the ~~$N_\mathrm{d}^\mathrm{OE1}$~~ N_d^OE ones. After 10:30 UTC ~~$N_\mathrm{d}^\mathrm{SEVIRI}$ gives~~ $N_\mathrm{d}^\mathrm{SEVIRI}$ shows twice as large values as ~~$N_\mathrm{d}^\mathrm{OE1}$~~$N_\mathrm{d}^\mathrm{OE}$, resulting in a mean difference of ~~367~~488 ~~(116~~cm^{-3} (154 %) for the whole day.

To find explanations for the large deviations found on 27 October 2011, we calculated optical depth and effective radius from ~~$N_\mathrm{d}^\mathrm{OE1}$ and $H_\mathrm{obs}^\mathrm{ground}$~~ N_d^OE and $H_\mathrm{obs}^\mathrm{ground}$, respectively, using the adiabatic model (~~Eqs. 3and 4~~Eq. (3) and Eq. (4)). By comparing these to the satellite-retrieved values we are able to attribute the observed differences mainly to differences in effective radius, for which SEVIRI gives lower values (Fig. ~~6~~5c). Before 10:30 UTC the mean difference ~~of~~ in the effective radius is 2.5 μm compared to 3.4 ~~afterwards. Q_L differences~~ μm afterwards. Q_L differences (Fig. 5a) can be attributed mainly to optical depth differences (Fig. 5b), which follows the same temporal pattern. Comparing the two satellite observations of the same cloud scene in the area of around ~~± 100~~± 100 km around Leipzig (not shown), we find spatial inhomogeneities of cloud microphysics that can not be resolved in the same way by SEVIRI as it is possible for MODIS. Furthermore SEVIRI has to deal with a large solar zenith angle (~~$> 60°$~~$> 60°$) under relative azimuth angles close to ~~180°~~ 180° around noon, for which Roebeling et al. (2006) pointed out the lower precision of the ~~CPP retrievalmethod~~retrieval.

Another influencing factor is the difference of the effective radius retrieval due to the different channels used by MODIS (2.1 μm) and SEVIRI (1.6 μm) for the standard retrieval products. From MODIS, additional effective radius retrievals from channels at 1.6 μm and 3.7 μm are available. Theoretically, the 3.7~~-channel~~ -μm channel should represent the effective radius close to the cloud top for ~~pure~~ adiabatic clouds, while the 2.1-μm and 1.6~~-channels~~ -μm channels receive the main signal from deeper layers within the cloud. ~~But real cloud~~ Cloud observations do not always ~~follow this relationship (Platnick, 2000; King et al., 2013) . By comparing all available parallel observations~~ show an increase of effective radius from channel 1.6 μm over 2.1 μm to 3.7 μm as is expected for plane-parallel, adiabatic clouds (Platnick, 2000; King et al., 2013) . Comparing mean differences of effective radius from ~~MODIS and SEVIRI~~ SEVIRI and each of the three available MODIS channels, we find the smallest ~~mean absolute difference of effective radius of all channels between the SEVIRI~~ difference in r_e considering the MODIS channel at 1.6 ~~- and the MODIS 1.6-channel with~~ μm. The mean difference in this case is 0.86 ~~.~~ μm. This is not surprising as both channels cover more or less the same wavelength range. The difference increases when ~~using the~~ MODIS channels 2.1 μm and 3.7 ~~to retrieve the effective radius. Intercomparison of MODIS channels only~~ μm are used. Intercomparing the effective radii retrieved from the three MODIS channels results in slightly smaller differences~~with 0.68and 0.51for MODIS~~ . The difference of MODIS channels at 2.1 ~~compared to~~ μm and at 1.6 ~~and~~ μm is 0.68 μm, while the difference of the retrieval at MODIS channels at 2.1 μm and at 3.7 ~~channels, respectively~~μm is 0.51 μm.

~~By considering the error propagation of the factor A_1 and the optical depth in Eq. (5) for N_d~~Due to the $N \propto r_e^{-2.5}$ relationship (see Eq. 5) even small differences of effective radius result in large uncertainties of N_d. Explicitely considering this error propagation, we find for 27 October 2011 at 11:45 UTC that the observed difference in effective radius of 1.33 $\mu\mathrm{m}$ between MODIS and SEVIRI results in an uncertainty of 306 cm^{-3}. The uncertainty due to differences in effective radius of 0.34 $\mu\mathrm{m}$ between MODIS channels 2.1 $\mu\mathrm{m}$ and 1.6 $\mu\mathrm{m}$ is 57 cm^{-3}.

~~Janssen et al. (2011) found for~~ The importance of r_e for the retrieval of N_d from passive satellite imagers has already been pointed out by previuos studies. Those which were mainly based on MODIS (Painemal and Zuidema, 2010, 2011; Ahmad et al., 2013; Zeng et al., 2014) . Painemal and Zuidema (2010) report a high bias of MODIS-derived r_e, but also state that the choice of the other parameters in the retrieval (namely k, Γ_ad) is able to compensate for this effect so that still a good agreement between MODIS retrieved and in-situ values could be achieved. A high bias of r_e occurs for broken cloud conditions (Marshak et al., 2006) . Zeng et al. (2014) also saw a good agreement for MODIS derived N_d (using $f_\mathrm{ad} = 0.8$) with CALIOP (Cloud-Aerosol Lidar with Orthogonal Polarization), although they found a high bias in r_e compared to POLDER (Polarization and Directionality of the Earth Reflectance). Ahmad et al. (2013) also points out the importance of the effective radius for the N_d retrieval. As mentioned before, for our study only few MODIS observation points are available, but we already see that discrepancies in r_e in comparison to SEVIRI are a major source of uncertainty for N_d.

Janssen et al. (2011) also state for satellite retrievals of ~~N_d~~ N_d (and also ~~H_ad) that f_ad and Γ_ad are~~ H_ad) that f_ad and Γ_ad are the most important uncertainty factors. They estimated the uncertainty of k to be negligible (around 3%). By considering the whole seasonal variability of cloud base temperature, they obtained an error of 24% for the adiabatic lapse rate of liquid water mixing ratio ($\Gamma_\mathrm{ad}(T,p)$). In our study ~~Γ_ad~~ Γ_ad has a smaller contribution to those uncertainties due to the fact that we are using model data to gain more reliable information about cloud ~~top~~ base temperature and pressure instead of considering one constant value like in e.g. Quaas et al. (2006). If we compare Γ_ad calculated from satellite cloud top temperature and pressure with the one calculated from cloud base values observed from gound we find an uncertainty of 15% considering all 4 cases. As we see some deviations in the cloud top height, we believe that this can be mainly attributed to wrong satellite estimates of cloud top temperature and pressure. Janssen et al. (2011) further assumed an uncertainty in the adiabatic factor of 0.3. This resulted in a numerically evaluated error of around 26% considering typical values of effective radius and optical depth. To highlight the importance of considering the actual adiabatic factor for the retrieval process, we calculated the optical depth (Eq. ~~3)~~(3)) and effective radius (Eq. ~~4)~~(4)) from the ground-based observations using ~~$N_\mathrm{d}^\mathrm{OE1}$ and $H_\mathrm{obs}^\mathrm{ground}$~~ N_d^OE and $H_\mathrm{obs}^\mathrm{ground}$ with adiabatic factor ~~$f_\mathrm{ad} = 1$~~ $f_\mathrm{ad} = 1$ or the ground-obtained adiabatic factor. Afterwards we compare it to the satellite-retrieved values obtained with the CPP algorithm. When the adiabatic factor is assumed constant ~~($f_\mathrm{ad} = 1$)~~ of $f_\mathrm{ad} = 1$ the mean difference in optical depth is 9.95 on 21 April 2013. When the adiabatic factor obtained from the ground-based measurements is considered, this mean difference is drastically reduced to 2.90. The mean difference of effective radius is reduced from 1.15 μm to 0.12 μm.

Therefore, we ~~try to adjust N_d^{SEVIRI}~~ aim to adjust N_d^{SEVIRI} Eq. 5 for the homogeneous cases by ~~multiplying with~~ setting the adiabatic factor to the value obtained from the ground-based observation. The results can be seen in Fig. ~~-~~8. On ~~21 April 2013 the adjusted N_d^{SEVIRI}~~ 2013-04-21 the adjusted N_d^{SEVIRI} is generally slightly lower due to the observed ~~subadiabaticity~~sub-adiabaticity. Only before 09:00 ~~the adjustments leads~~ UTC the adjustments lead to a better comparison to ground-obtained values. This case still shows the smallest relative mean difference of SEVIRI and ground-retrieved N_d with 15 %. For 27 October 2011 the retrieved ~~N_d^{SEVIRI}~~ N_d^{SEVIRI} is also generally reduced, diminishing also the mean difference to the ground-retrieved values in this case (relative mean difference is reduced from 154 % to 114 %). The reason that including the adiabatic factor does not ~~generally~~ always lead to a better agreement can ~~be attributed amongst other things to~~ likely be attributed to the uncertainties of ground observations ~~.~~(discussed in Sect. 4.1.1). Although we were not able to see always an improvement in agreement of N_d by considering the ground-based calculated f_{ad}, Min et al. (2012) found a better agreement in N_d when considering it in their study. Since clouds are clearly sub-adiabatic in all our 4 cases independent of season, we believe that applying an adiabatic factor smaller than one is advantageous over considering adiabatic clouds in the retrieval.

For the inhomogeneous cases shown in Fig. ~~7c and~~ 7c,d, a high temporal variability in ~~the optimal estimation retrievals of N_d~~ N_d^{OE} can be seen. ~~N_d^{MODIS} and the N_d^{OE1}~~ N_d^{MODIS} and the N_d^{OE} agree well within the uncertainty range. For the comparison of ~~N_d^{SEVIRI} and N^{OE1}~~ N_d^{SEVIRI} and N_d^{OE} we find good agreement in the beginning and end of the observation period at 1 June 2012, when the clouds are more homogeneous. ~~Underestimation of N^{OE1} by SEVIRI during the more broken cloud scene can be mainly explained by a blending of the received signal from clouds and~~

The underestimation of N_d^{SEVIRI} comprared to N_d^{OE} can likely be attributed to broken-cloud effects on the SEVIRI retrieval. For broken clouds within the SEVIRI pixel the satellite receives a combined signal from the clouds but also from the surface. The same explanation can also be applied to the second inhomogeneous case (27 September 2012). It remains open to which extent the ~~inhomogeneity within a SEVIRI pixel destroys the reliability of retrieved parameters~~subpixel surface contamination leads to a bias in the retrieved cloud parameters especially for inhomogeneous cloud scenes when the brightness temperature actually does not represent the cloud radiative temperature.

While some of the differences between satellite- and ground-based retrievals of ~~N_d~~ N_d can be attributed to the invalidity of the ~~pure~~ adiabatic assumption and coarse spatial resolution of the satellites, it has to be mentioned that the ground-based retrieval strongly relies on the accuracy of the radar reflectivity and therefore also on the radar calibration and attenuation corrections for atmospheric gases and liquid water that are made within the Cloudnet algorithm. Löhnert et al. (2003) points out the strong influence of drizzle on the cloud reflectivity. Errors of ~~30–60~~30-60 % have to be anticipated for ~~q_L~~ q_L profile retrievals. Those retrieval approaches are based on very similar principles as our ~~OE1~~ OE method (Löhnert et al., 2001). In our study we filtered out drizzling profiles as well as possible, but the radar reflectivity still remains very sensitive to few larger droplets in a volume, which can not totally be ruled out. Therefore also the correct radar calibration is an issue.

5 Summary and Conclusions

To investigate the accuracy of satellite-based estimates of aerosol indirect effects, we have studied the validity of the (sub-)adiabatic cloud model as a conceptional tool commonly applied in previous studies (e.g. Bennartz, 2007; Schueller et al., 2003). The ~~adiabatic~~ (sub-)adiabatic cloud model allows indirectly to estimate ~~H_{cloud} and N_{d}~~ cloud geometrical depth (H_{cloud}) and cloud droplet number concentration (N_{d}) from passive satellite observations.

As reference, we used a combination of ground-based active and passive remote sensing instruments with high temporal and vertical resolution to provide detailed information of the cloud vertical structure. We could, however, demonstrate that such retrievals also have ~~large~~ considerable uncertainties.

Considering the number of ~~difficulties for both perspectives and~~ uncertainties for both the satellite and ground perspective, and those originating from the ~~contrast of~~ issue of representativity of the two perspectives, our comparison showed that the temporal evolution of cloud micro- and macrophysical quantities is captured surprisingly well for some cases. We discussed the large uncertainties that may occur depending on the observed scene and observation geometry.

The cloud geometrical depth can be obtained with ground-based remote sensing directly from ceilometer cloud base and radar cloud top heights~~, and by applying the adiabatic method using liquid water path observed with a microwave radiometer~~. The mean difference of SEVIRI and ground-based ~~adiabatic~~ cloud geometrical depth is lowest for the two ~~homogeneous cases~~ presented homogeneous cases when the ground-based adiabatic factor is considered with values down to ~~49~~14 m (~~15~~4 %). ~~The overall larger cloud geometrical depth observed with ground-based ceilometer and radar in contrast to the virtual adiabatic one can be explained by subadiabaticity of the cloud~~ Overall we found sub-adiabatic cloud layers. The adiabatic factor varied ~~temporally~~ in time and attained values similar to those reported by Boers et al. (2006). For 3 out of 4 cases we obtained similar median values around 0.65 ± 0.2 at different seasons. Although larger datasets are required to draw robust conclusions about a typical adiabtic factor, this value could be a first guess for homogeneous stratocumulus clouds as they occur over Central Europe. For thin clouds the uncertainties ~~remain~~ remains large due to the high relative uncertainties of liquid water path and cloud geometrical depth. This also leads to superadiabatic artefacts in the retrieval. With increasing geometrical depth, the clouds become less adiabatic. We also found that clouds are slightly more adiabatic when the cloud profile is dominated by positive ~~Doppler~~ vertical velocity (updrafts). Although a larger dataset would be desirable to draw more robust conclusions~~in this direction~~, our results support those from Schmidt et al. (2014a) and Schmidt et al. (2014b). ~~In general it is desirable to account for subadiabacity in satellite retrievals.~~

We developed ~~two similar~~ an Optimal Estimation (OE) ~~retrievals to estimate N_d~~ retrieval to estimate N_d from ground-based radar and microwave radiometer observations~~. The main difference is found in the degrees of freedom of the~~ , which does not require the assumption of a linear increasing liquid water content profile~~(adiabatic versus nonadiabatic). This results in differences of N_d. We found that applying an adiabatic OE approach from ground leads to larger deviations with increasing N_d. Differences are reflected in the cost function of the adiabatic OE method. Therefore we receive information about which of the retrieved N_d values deviate from the adiabatic model under the assumption that N_d is constant vertically.~~

. While the mean difference of ~~N_d~~ N_d retrieved from SEVIRI and the ground-based ~~nonadiabatic OE was 78~~OE was 29 ~~(27~~cm^{-3} (10 %) for one of the two homogeneous cases, for the second one we saw a large bias of ~~367~~488 ~~(116~~cm^{-3} (154 %)~~, whereby~~ . In these the MODIS retrieval was closer to the ground-retrieved ~~one~~values. We were able to attribute this large bias mainly to an underestimation of the effective radius within the current SEVIRI retrieval. Even small differences in effective radius result in large uncertainties of cloud droplet number concentration due to the $N_\mathrm{d} \propto r_\mathrm{e}^{-2.5}$-relationship. Further research about the influence of observation geometry and spatial resolution effects on effective radius and optical depth differences between MODIS and SEVIRI is required.

The OE approach to retrieve cloud droplet number concentration from ground could be further improved by including more independent observations, e.g. from solar radiation observations (e.g. Brückner et al., 2014), which are available at several ground-based supersites as for LACROS.

Indications have been ~~found~~ detected throughout this study that ~~adjustments to~~ assumptions about cloud subadiabacity may help to ~~reduce~~ explain differences between satellite and ground-based retrievals. ~~For applying such adjustments over larger areas it might be useful to develop a parameterisation~~ Therefore, satellite retrievals should take into account that liquid water clouds are mostly subadiabatic.

So far only four cases were analyzed, but given the network of Cloudnet/ACTRIS in Central Europe this offers the opportunity to investigate the climatology of the adiabatic factor ~~depending on cloud geometrical depth. A combination of satellite-derived cloud top height with cloud base height observations from a ground-based ceilometer network would be very interesting. A comparison for cloud geometrical depth using SEVIRI cloud top height and ceilometer cloud base height was already sucessfully applied by Meerkötter and Bugliaro (2009) for one ground site. Using~~ and investigate its regional, seasonal or synoptical dependency. Using more data from a greater network ~~should be able to gain~~ would give statistically more robust insights.

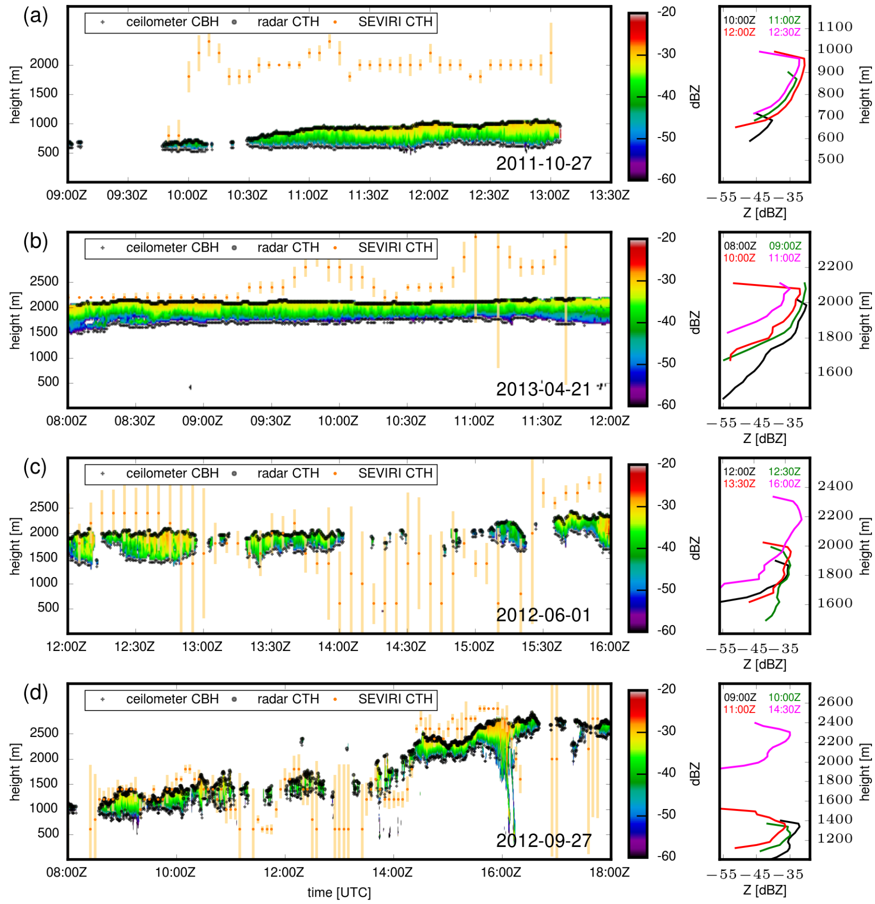

Figure 1. ~~Cases used within this study ordered by date. The minimum cloud base height~~ Time series of radar reflectivity (~~CBHL~~in dBZ) and ~~the maximum~~ cloud ~~top height~~ borders for the 4 cases listed in Table 2; (~~CTHL~~a) ~~of the liquid cloud layer investigated are presented together with the temporal averaged inhomogeneity paramater~~ 27 October 2011, (~~χ~~b) 21 April 2013, (c) 1 June 2012, (d) 27 September 2012. Cloud borders are shown as detected by Cloudnet with black dots and by SEVIRI using NWCSAF in ~~Cahalan et al. (1994) calculated from optical depth~~ orange dots. Sample profiles of ~~the ±15 surrounding SEVIRI pixels~~ radar reflectivity are shown for each ~~observation time. Furthermore the category for each~~ case ~~is listed~~at different times.

Acknowledgements. The first author's work was funded by the Leipzig Graduate School on Radiation (LGS-CAR). We would like to thank the Cloudnet project (European Union Contract EVK2-2000-00611) for providing the ground-based cloud products, and the EUMETSAT SAFS for providing the SEVIRI cloud products, as well as the NASA's Earth-Sun System Division for providing MODIS cloud products. We further acknowledge collegues participating in the HOPE campaign of the HD(CP)^2 project in Juelich. We also thank our collegues Anja Huenerbein, Andreas Macke, Fabian Senf~~and Johannes Quaas~~, Johannes Quaas and two anonymous reviewers for their helpful suggestions and comments.

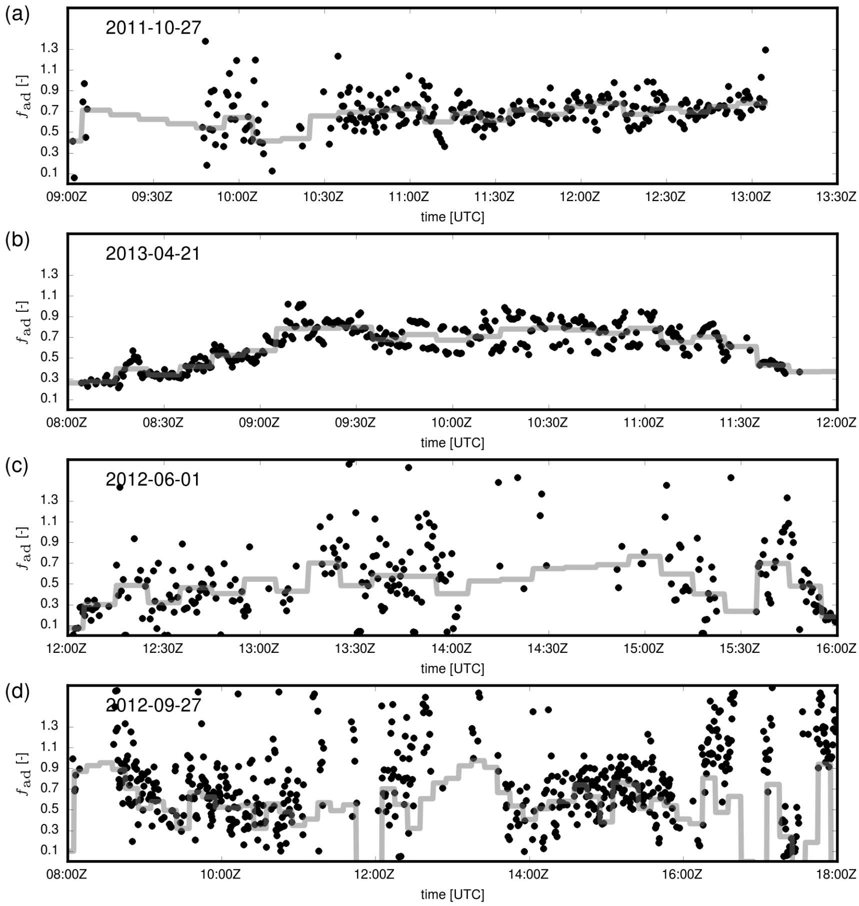

Figure 2. Adiabatic factor for all four cases. Black dots represent the adiabatic factor derived using ground-based geometrical depth and liquid water path from the microwave radiometer. The gray line represents the 10-min averaged and interpolated adiabatic factor neglecting superadiabatic values.

~~Radar reflectivity (in) and cloud borders for the 4 cases listed in Table 2; **(a)** 27 October 2011, **(b)** 21 April 2013, **(c)** 1 June 2012, **(d)** 27 September 2012. Cloud borders are shown as detected by Cloudnet with black dots and by SEVIRI using NWCSAF in orange dots.~~

~~Cloud geometrical depth for **(a)** 27 October 2011 , **(b)** 21 April 2013, **(c)** 1 June 2012, **(d)** 27 September 2012. Dark blue dots represent the ground-based adiabatic scaled values ($H_{\mathrm{ad}}^{\mathrm{ground}}$), green dots the ground-observed values ($H_{\mathrm{obs}}^{\mathrm{ground}}$), yellow dots the SEVIRI adiabatically derived values ($H_{\mathrm{ad}}^{\mathrm{SEVIRI}}$), and red dots the MODIS adiabatically derived values ($H_{\mathrm{ad}}^{\mathrm{MODIS}}$). Red diamonds and stars represent the MODIS adiabatically derived values using available channels 2.1 and 3.7, respectively. The uncertainty for the ground-based values is shown as shaded areas in the same color type as the dots. Variability for SEVIRI and MODIS is given in terms of SD of the surrounding area of ±1 and ±9, respectively.~~

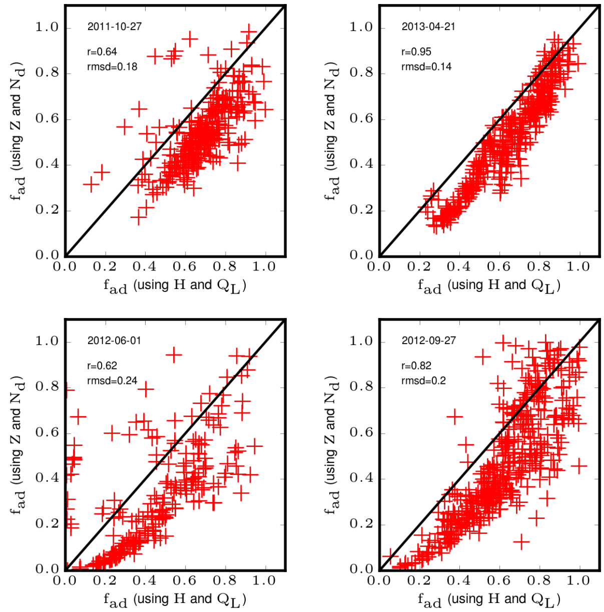

Figure 3. Adiabatic factor calculated from ground-based observations using H and Q_L (x-axis) and from Z and N_d (y-axis). Superadiabatic values are omitted. The graphs correspond to our four investigated cases (see Table 2).

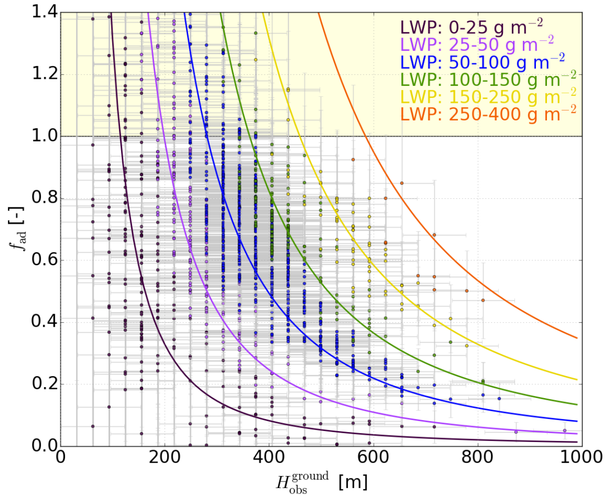

Figure 4. Adiabatic factor as a function of observed cloud geometrical depth (H_{obs}^{ground}) including data of all four cases. Colors indicate different liquid water path bins. The range with $f_{ad} > 1$ is shaded with light yellow. This superadiabatic range is neglected for the further study. The solid lines represent the relationship described in Eq. (8) for bin mean liquid water path and $\Gamma_{ad} = 1.9 \cdot 10^{-3} \mathrm{gm}^{-4}$.

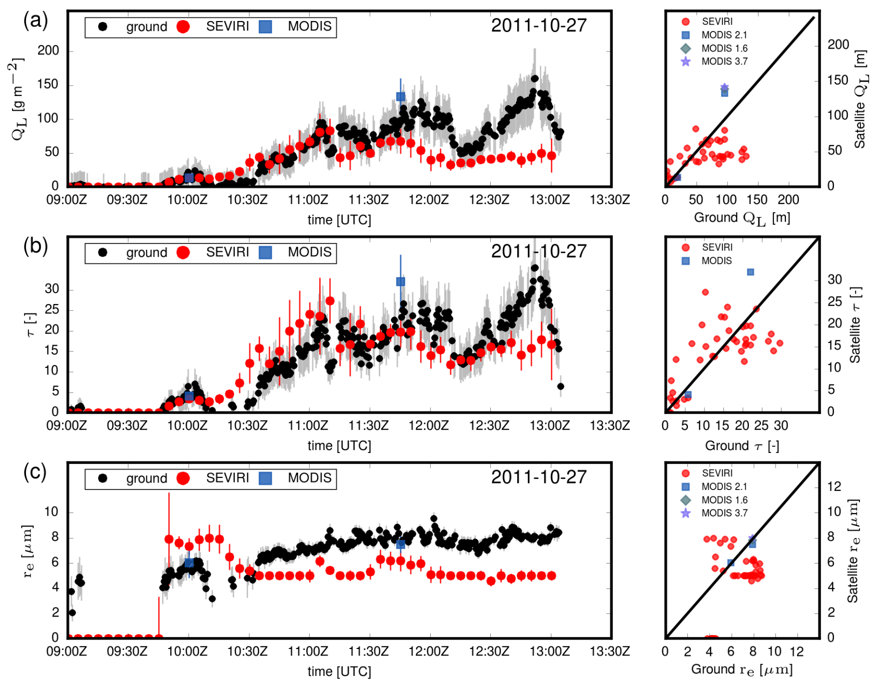

Figure 5. (a) Liquid water path for 27 October 2011 as obtained from the microwave radiometer (black dots), adiabatically from SEVIRI (red dots), and MODIS (green dots), respectively. For MODIS the effective radius obtained with three different channels is shown in the scatter plot with different symbols (square: 2.1 μm, diamond: 1.6 μm, star: 3.7 μm). (b) Time series of optical depth as obtained from SEVIRI (red), MODIS (green), and calculated from ground retrievals, respectively (black). (c) Time series of effective radius with the same colors. The variability of SEVIRI- and MODIS-derived values is given in terms of standard deviation of the surrounding area of ± 1 and ± 9 pixels, respectively.

~~Adiabatic factor for **(a)** 27 October 2011, **(b)** 21 April 2013, **(c)** 1 June 2012, **(d)** 27 September 2012. Blue dots represent the adiabatic factor derived using $H_{\mathrm{obs}}^{\mathrm{ground}}$ and Q_{L} from the microwave radiometer. The blue line represents the interpolated and 10averaged values.~~

~~Adiabatic factor as a function of observed cloud geometrical depth ($H_{\mathrm{obs}}^{\mathrm{ground}}$) including data of all 4 cases. Colors indicate different liquid water path bins. The range with $f_{\mathrm{ad}} > 1$ is shaded with light yellow. The solid lines represent the relationship described in Eq. (8) for bin mean liquid water path and $\Gamma_{\mathrm{ad}} = 1.9 \times 10^{-3}\,\mathrm{g\,m^{-4}}$.~~

~~Comparison of the retrievals of cloud droplet number concentration using OE1 and OE2 method. The color represents the remaining cost function of the OE2 method after the optimization. The black line represents the 1 : 1 relationship.~~

~~**(a)** Liquid water path for 27 October 2012 as obtained from the microwave radiometer (dark blue dots), adiabatically from SEVIRI (yellow dots) and MODIS (red). For MODIS the effective radius obtained with three different channels is shown with different symbols (diamond: 2.1, dot:~~

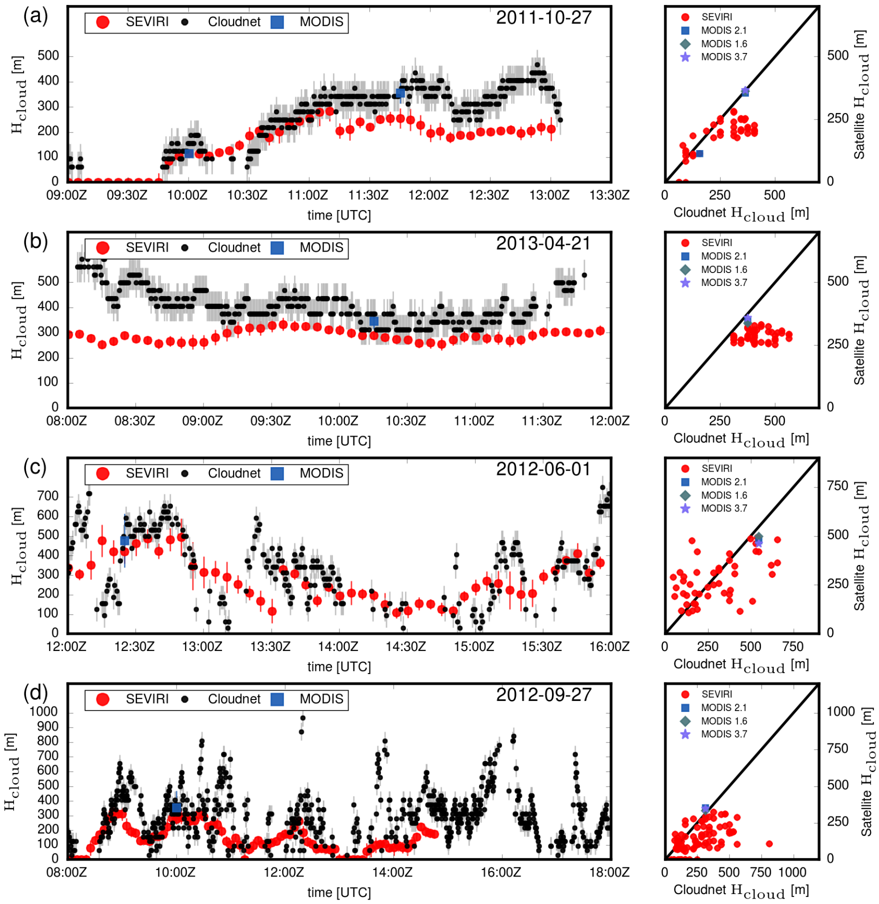

Figure 6. H_{cloud} for the four cases. Black dots represent the geometrical cloud depth observed from ground, red dots the SEVIRI adiabatically derived values, and green dots the MODIS adiabatically derived values. The uncertainties for the ground-based values are shown as shaded areas. The uncertainty estimates of MODIS and SEVIRI are represented in the same way as described in Fig. 5. In the scatter plots diamonds and stars represent the MODIS adiabatically derived values using available channels 1.6 μm and 3.7 μm, respectively.

~~1.6, star: 3.7). The uncertainty estimates are represented in the same way as described in Fig. 2. **(b)** Time series of optical depth as obtained from SEVIRI (yellow), MODIS (red), and calculated from ground retrievals (blue). **(c)** Time series of effective radius with the same colors.~~

~~Time series of retrievals of the estimated cloud droplet number concentration. Blue dots represent the OE1 method, using ground-based data ($N_{\text{d}}^{\text{OE1}}$). The blue shaded area represents the uncertainty, calculated from the error covariance matrix of OE1. Green dots represent the OE2 method ($N_{\text{d}}^{\text{OE2}}$). Gray dots represent the retrieval with the FI method applied to ground site data (N_{d}^{FI}). Orange dots represent the adiabatically derived values from SEVIRI ($N_{\text{d}}^{\text{SEVIRI}}$), while red dots those from MODIS ($N_{\text{d}}^{\text{MODIS}}$). Different MODIS channels used in the retrieval are denoted with the same symbols as in~~

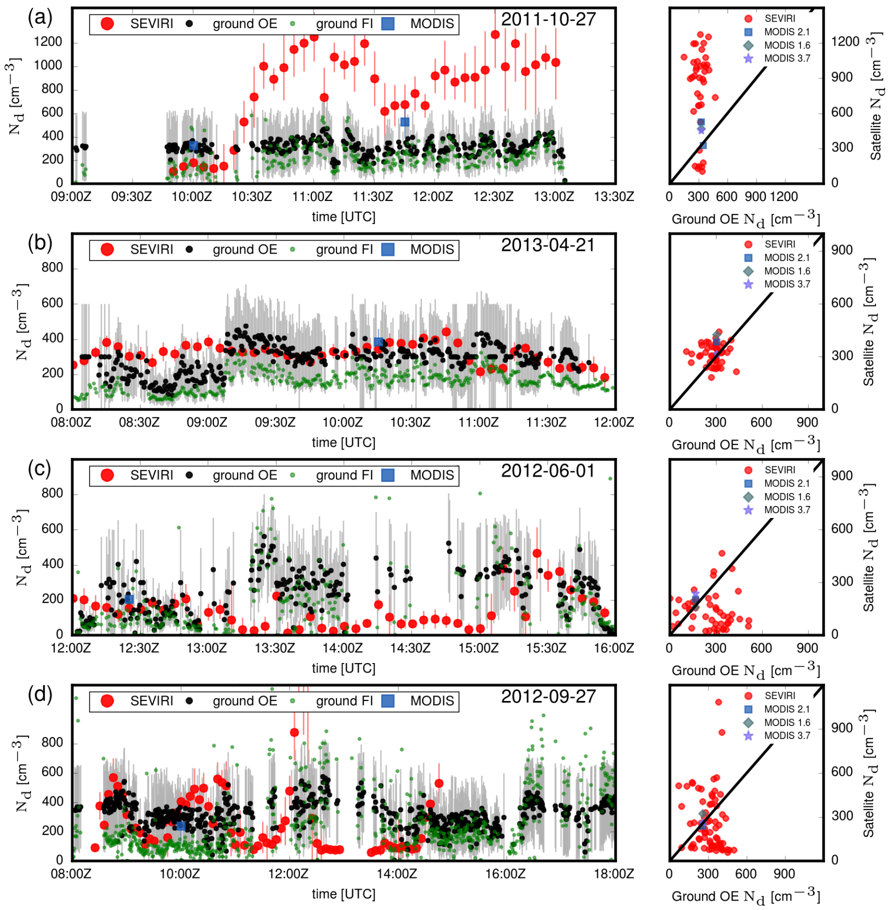

Figure 7. Time series of retrievals of the estimated cloud droplet number concentration. Black dots represent the OE method, using ground-based data (N_d^{OE}). The gray shaded area illustrates the uncertainty, calculated from the error covariance matrix of OE. Blue dots represent the retrieval with the FI method applied to ground site data (N_d^{FI}). Red dots represent the adiabatically derived values from SEVIRI (N_d^{SEVIRI}), while green dots those from MODIS (N_d^{MODIS}). Different MODIS channels used in the retrieval are denoted with the same symbols as in the figures before. Variability for SEVIRI and MODIS is given in terms of standard deviation of the surrounding area of ±1 and ±9 pixels, respectively.

~~the figures before. Variability for SEVIRI and MODIS is given in terms of SD of the surrounding area of ±1 and ±9, respectively.~~

~~10averaged N_d for the two homogeneous cases. As Fig. 7, but with additional $N_\mathrm{d}^{\mathrm{SEVIRI}}$ adjusted by the adiabatic factor (green dots).~~

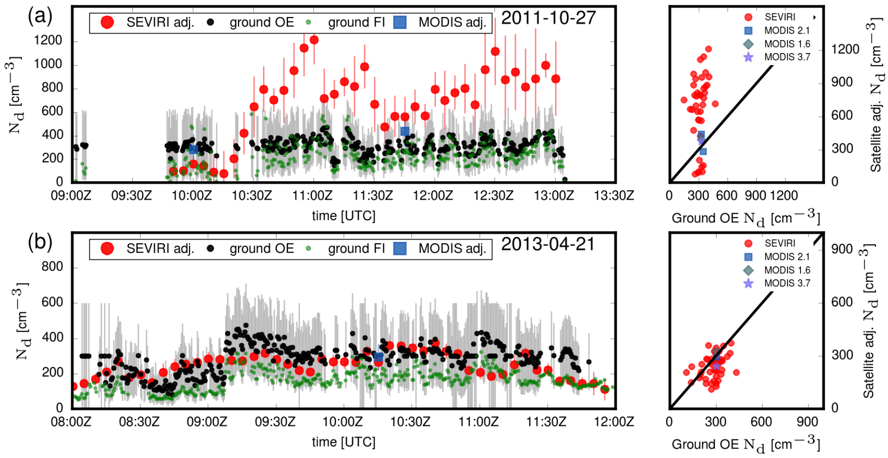

Figure 8. Adjusted cloud droplet number concentration from SEVIRI and MODIS applying f_{ad} from ground-based observations in Eq. 5 for the two homogeneous cases. Colors and symbols are the same as in Fig. 7.

Table 1. Overview of assumptions made for the (sub-)adiabatic cloud model applied to derive N_d and H in literature studies. The table lists the values chosen for Γ_{ad}, f_{ad} (*calc.* refers to explicitely calculated values from additional data) and k according to Eq. 8. The table is sorted by publication year starting with the oldest one.

study	location	instrument(s)	derived quantities	Γ_{ad} [$\cdot 10^{-3} gm^{-4}$]	f_{ad}	k
Szczodrak 2001	Eastern Pacific + Southern Ocean	AVHRR	N_d	2.0	n.a.	n.a.
Schueller 2005	North Atlantic (marine)	MODIS	N_d, H	n.a.	n.a.	n.a.
Boers 2006	Southern Ocean (Cape Grim)	MODIS	N_d, H	const.	0.6	0.87
Quaas 2006, 2008	global	MODIS	N_d	1.9	1.0	0.8
Bennartz 2007	global	MODIS	N_d, H	T-dependent	0.8	0.8
Roebeling 2008	Europe (continental)	SEVIRI	N_d, H	Boers 2006	0.75	Boers 2006
George 2010	Southeast Pacific	MODIS	N_d	1.95	n.a.	n.a.
Painemal 2010	Southeast Pacific	MODIS	N_d, H	2.0	1.0	0.8
Janssen 2011	Finnland (continental)	MODIS	N_d, H	1.44	0.6	0.87
Painemal 2011	Southeast Pacific	MODIS	N_d	2.0	1.0	0.8
Min 2012	Southeast Pacific	MODIS	N_d, H	T-dependent	calc.	0.5-1.0
Ahmad 2013	Puijo (continental)	MODIS	N_d	n.a.	1.0	0.67
Painemal 2013	Southeast Pacific	MODIS, aircraft	N_d	T_{cbh}, p_{cbh}	0.9	0.88
Zeng 2014	global	A-Train	N_d, H	T_{cth}, p_{cth}	1.0	0.6438
this study	Germany (continental)	SEVIRI	N_d, H	T_{cbh}, p_{cbh}	calc.	0.8

References

Ackerman, A. S., Toon, O. B., Taylor, J. P., Johnson, D. W., Hobbs, P. V., and Ferek, R. J.: Effects of Aerosols on Cloud Albedo: Evaluation of Twomey's Parameterization of Cloud Susceptibility Using Measurements of Ship Tracks, Journal of the Atmospheric Sciences, 57, 2684–2695, doi:10.1175/1520-0469(2000)057<2684:EOAOCA>2.0.CO;2, http://dx.doi.org/10.1175/1520-0469(2000)057<2684:EOAOCA>2.0.CO;2, 2000.

Table 2. Cases used within this study ordered by date. The minimum cloud base height (CBHL) and the maximum cloud top height (CTHL) of the liquid cloud layer investigated are presented together with the temporal averaged inhomogeneity paramater (χ) as in Cahalan et al. (1994) calculated from the optical depth of the ± 15 surrounding SEVIRI pixels for each observation time. Furthermore the category for each case is listed.

Date	Time	Location	Min(CBHL) [m]	Max(CTHL) [m]	χ	category
27 Oct 2011	09:00–13:00 UTC	Leipzig	525 m	1056 m	0.87	homogeneous
1 Jun 2012	12:00–16:00 UTC	Leipzig	1336 m	2428 m	0.73	inhomogeneous
27 Sep 2012	08:00–18:00 UTC	Leipzig	775 m	2927 m	0.55	inhomogeneous
21 Apr 2013	08:00–12:00 UTC	~~Juelich~~ Krauthausen	1485 m	2171 m	0.87	homogeneous

Table 3. ~~Correlation~~ Median and standard deviation of ~~observed CGD~~ the adiabatic factor (calculated from ~~Cloudnet~~ Eq. 8) for individual and for all cases, respectively. Furthermore the median of the adiabatic ~~sealed CGD from SEVIRI~~ factor, classified into updraft ($v \geq 0$) and downdraft ($v < 0$) regimes, and the fraction of subadiatic cloud profiles is shown. Adiabatic factors with ~~different averaging periods applied to both datasets~~ $f_{\text{ad}} > 1.0$ are omitted since we believe that those are likely affected by measurement uncertainties.

~~Date unaveraged 10average 20average 30average 21 Apr 2013 (after 09:00) 0.44 0.72 0.66 0.75 27 Sep 2012 0.15 0.39 0.57 0.68 27 Oct 2011 0.59 0.67 0.68 0.75 1 Jun 2012 0.44 0.64 0.74 0.80~~

~~Median and SD of the adiabatic factor for all cases and each case individually. Furthermore the median of the adiabatic factor, classified in updraft ($v > 0$) and downdraft ($v < 0$), and the fraction of subadiatic cloud profiles is shown. Adiabatic factors with $f_{\text{ad}} > 1.5$ are omitted since we believe that those are likely affected by measurement uncertainties.~~

	all	21 Apr 2013	27 Sep 2012	27 Oct 2011	1 Jun 2012
median f_{ad}	~~0.66~~ 0.63	0.64	~~0.72~~ 0.64	~~0.69~~ 0.68	~~0.47~~ 0.44
~~SD~~ stddev f_{ad}	~~0.27~~ 0.22	~~0.19~~ 0.18	~~0.32~~ 0.23	~~0.17~~ 0.15	~~0.31~~ 0.24
median $f_{\text{ad}}\,[v \geq 0]$	~~0.69~~ 0.66	~~0.73~~ 0.71	~~0.74~~ 0.67	0.72	~~0.50~~ 0.46
~~SD~~ stddev $f_{\text{ad}}\,[v \geq 0]$	~~0.27~~ 0.22	0.18	~~0.31~~ 0.21	~~0.16~~ 0.15	~~0.32~~ 0.25
median $f_{\text{ad}}\,[v \leq 0]$	~~0.64~~ 0.61	0.62	~~0.69~~ 0.62	0.66	~~0.44~~ 0.43
~~SD~~ stddev $f_{\text{ad}}\,[v \leq 0]$	~~0.27~~ 0.22	0.18	~~0.32~~ 0.24	~~0.17~~ 0.14	~~0.70~~ 0.24
fraction $f_{\text{ad}} < 1$	0.84	0.99	0.70	0.97	0.85

Table 4. Correlation coefficient of H_{obs} from Cloudnet and H from SEVIRI with different averaging periods applied to both datasets.

Date	30 s unaveraged	10 min average	20 min average	30 min average
21 Apr 2013 (after 09:00 UTC)	0.47	0.68	0.66	0.78
27 Sep 2012	0.12	0.33	0.51	0.63
27 Oct 2011	0.59	0.68	0.68	0.76
1 Jun 2012	0.41	0.59	0.71	0.75

Ahmad, I., Mielonen, T., Grosvenor, D., Portin, H., Arola, A., Mikkonen, S., Kühn, T., Leskinen, A., Juotsensaari, J., Komppula, M., Lehtinen, K., Laaksonen, A., and Romakkaniemi, S.: Long-term measurements of cloud droplet concentrations and aerosol-cloud interactions in continental boundary layer clouds, Tellus B, 65, http://www.tellusb.net/index.php/tellusb/article/view/20138, 2013.

Albrecht, B. A., Fairall, C. W., Thomson, D. W., White, A. B., Snider, J. B., and Schubert, W. H.: Surface-based remote sensing of the observed and the Adiabatic liquid water content of stratocumulus clouds, Geophys. Res. Lett., 17, 89–92, doi:10.1029/GL017i001p00089, http://dx.doi.org/10.1029/GL017i001p00089, 1990.

Bennartz, R.: Global assessment of marine boundary layer cloud droplet number concentration from satellite, Journal of Geophysical Research: Atmospheres, 112, n/a–n/a, doi:10.1029/2006JD007547, http://dx.doi.org/10.1029/2006JD007547, 2007.

Boers, R., Russchenberg, H., Erkelens, J., Venema, V., van Lammeren, A., Apituley, A., and Jongen, S.: Ground-Based Remote Sensing of Stratocumulus Properties during CLARA, 1996, Journal of Applied Meteorology, 39, 169–181, doi:10.1175/1520-0450(2000)039<0169:GBRSOS>2.0.CO;2, http://dx.doi.org/10.1175/1520-0450(2000)039<0169:GBRSOS>2.0.CO;2, 2000.

Boers, R., Acarreta, J. R., and Gras, J. L.: Satellite monitoring of the first indirect aerosol effect: Retrieval of the droplet concentration of water clouds, Journal of Geophysical Research: Atmospheres, 111, n/a–n/a, doi:10.1029/2005JD006838, http://dx.doi.org/10.1029/2005JD006838, 2006.

Boucher, O., Randall, D., Artaxo, P., Bretherton, C., Feingold, G., Forster, P., Kerminen, V., Kondo, Y., Liao, H., Lohmann, U., et al.: Clouds and aerosols, Climate Change, pp. 571–657, 2013.

Brenguier, J.-L., Pawlowska, H., Schüller, L., Preusker, R., Fischer, J., and Fouquart, Y.: Radiative Properties of Boundary Layer Clouds: Droplet Effective Radius versus Number Concentration, Journal of the Atmospheric Sciences, 57, 803–821, doi:10.1175/1520-0469(2000)057<0803:RPOBLC>2.0.CO;2, http://dx.doi.org/10.1175/1520-0469(2000)057<0803:RPOBLC>2.0.CO;2, 2000.

Brückner, M., Pospichal, B., Macke, A., and Wendisch, M.: A new multispectral cloud retrieval method for ship-based solar transmissivity measurements, Journal of Geophysical Research: Atmospheres, 119, 11,338–11,354, doi:10.1002/2014JD021775, http://dx.doi.org/10.1002/2014JD021775, 2014.

Cahalan, R. F., Ridgway, W., Wiscombe, W. J., Bell, T. L., and Snider, J. B.: The Albedo of Fractal Stratocumulus Clouds, Journal of the Atmospheric Sciences, 51, 2434–2455, doi:10.1175/1520-0469(1994)051<2434:TAOFSC>2.0.CO;2, http://dx.doi.org/10.1175/1520-0469(1994)051<2434:TAOFSC>2.0.CO;2, 1994.

Chen, R., Wood, R., Li, Z., Ferraro, R., and Chang, F.-L.: Studying the vertical variation of cloud droplet effective radius using ship and space-borne remote sensing data, Journal of Geophysical Research: Atmospheres, 113, n/a–n/a, doi:10.1029/2007JD009596, http://dx.doi.org/10.1029/2007JD009596, 2008.

Christensen, M. W. and Stephens, G. L.: Microphysical and macrophysical responses of marine stratocumulus polluted by underlying ships: Evidence of cloud deepening, Journal of Geophysical Research: Atmospheres, 116, n/a–n/a, doi:10.1029/2010JD014638, http://dx.doi.org/10.1029/2010JD014638, d03201, 2011.

Deneke, H., Knap, W., and Simmer, C.: Multiresolution analysis of the temporal variance and correlation of transmittance and reflectance of an atmospheric column, J. Geophys. Res., 114, D17 206, doi:10.1029/2008JD011680, http://dx.doi.org/10.1029/2008JD011680, 2009.

Derrien, M.: Algorithm theoretical basis document for cloud products (cma-pge01 v3.2, ct-pge02 v2.2, ctth-pge03 v2.2), Tech. rep., SAFNWC, 2012.

Dong, X. and Mace, G. G.: Profiles of Low-Level Stratus Cloud Microphysics Deduced from Ground-Based Measurements, Journal of Atmospheric and Oceanic Technology, 20, 42–53, doi:10.1175/1520-0426(2003)020<0042:POLLSC>2.0.CO;2, http://dx.doi.org/10.1175/1520-0426(2003)020<0042:POLLSC>2.0.CO;2, 2003.

Dong, X., Ackerman, T. P., Clothiaux, E. E., Pilewskie, P., and Han, Y.: Microphysical and radiative properties of boundary layer stratiform clouds deduced from ground-based measurements, Journal of Geophysical Research: Atmospheres, 102, 23 829–23 843, doi:10.1029/97JD02119, http://dx.doi.org/10.1029/97JD02119, 1997.

Dong, X., Mace, G. G., Minnis, P., Smith, W. L., Poellot, M., Marchand, R. T., and Rapp, A. D.: Comparison of Stratus Cloud Properties Deduced from Surface, GOES, and Aircraft Data during the March 2000 ARM Cloud IOP, Journal of the Atmospheric Sciences, 59, 3265–3284, doi:10.1175/1520-0469(2002)059<3265:COSCPD>2.0.CO;2, http://dx.doi.org/10.1175/1520-0469(2002)059<3265:COSCPD>2.0.CO;2, 2002.

Feingold, G., Eberhard, W. L., Veron, D. E., and Previdi, M.: First measurements of the Twomey indirect effect using ground-based remote sensors, Geophysical Research Letters, 30, n/a–n/a, doi:10.1029/2002GL016633, http://dx.doi.org/10.1029/2002GL016633, 2003.

Fox, N. I. and Illingworth, A. J.: The Retrieval of Stratocumulus Cloud Properties by Ground-Based Cloud Radar, Journal of Applied Meteorology, 36, 485–492, doi:10.1175/1520-0450(1997)036<0485:TROSCP>2.0.CO;2, http://dx.doi.org/10.1175/1520-0450(1997)036<0485:TROSCP>2.0.CO;2, 1997.

Frisch, A. S., Feingold, G., Fairall, C. W., Uttal, T., and Snider, J. B.: On cloud radar and microwave radiometer measurements of stratus cloud liquid water profiles, Journal of Geophysical Research: Atmospheres, 103, 23 195–23 197, doi:10.1029/98JD01827, http://dx.doi.org/10.1029/98JD01827, 1998.

Han, Q., Rossow, W. B., Chou, J., and Welch, R. M.: Global variation of column droplet concentration in low-level clouds, Geophysical Research Letters, 25, 1419–1422, doi:10.1029/98GL01095, http://dx.doi.org/10.1029/98GL01095, 1998.

Hansen, J. E. and Travis, L. D.: Light scattering in planetary atmospheres, Space Science Reviews, 16, 527–610, 1974.

Hewison, T.: 1D-VAR Retrieval of Temperature and Humidity Profiles From a Ground-Based Microwave Radiometer, Geoscience and Remote Sensing, IEEE Transactions on, 45, 2163–2168, doi:10.1109/TGRS.2007.898091, 2007.

Hünerbein, A., Deneke, H., Macke, A., Ebell, K., and Görsdorf, U.: Combining the Perspective of Satellite- and Ground-Based Observations to Analyze Cloud Frontal Systems, Journal of Applied Meteorology and Climatology, 53, 2538–2552, doi:10.1175/JAMC-D-13-0274.1, http://dx.doi.org/10.1175/JAMC-D-13-0274.1, 2014.

Illingworth, A., Hogan, R., O'connor, E., Bouniol, D., Delanoë, J., Pelon, J., Protat, A., Brooks, M., Gaussiat, N., Wilson, D., et al.: Cloudnet: Continuous evaluation of cloud profiles in seven operational models using ground-based observations, Bulletin of the American Meteorological Society, 88, 883–898, 2007.

Janssen, R. H. H., Ganzeveld, L. N., Kabat, P., Kulmala, M., Nieminen, T., and Roebeling, R. A.: Estimating seasonal variations in cloud droplet number concentration over the boreal forest from satellite observations, Atmospheric Chemistry and Physics, 11, 7701–7713, doi:10.5194/acp-11-7701-2011, http://www.atmos-chem-phys.net/11/7701/2011/, 2011.

King, N. J., Bower, K. N., Crosier, J., and Crawford, I.: Evaluating MODIS cloud retrievals with in situ observations from VOCALS-REx, Atmospheric Chemistry and Physics, 13, 191–209, doi:10.5194/acp-13-191-2013, http://www.atmos-chem-phys.net/13/191/2013/, 2013.

Lehmann, K., Siebert, H., and Shaw, R. A.: Homogeneous and Inhomogeneous Mixing in Cumulus Clouds: Dependence on Local Turbulence Structure, Journal of the Atmospheric Sciences, 66, 3641–3659, doi:10.1175/2009JAS3012.1, http://dx.doi.org/10.1175/2009JAS3012.1, 2009.

Löhnert, U., Crewell, S., Simmer, C., and Macke, A.: Profiling Cloud Liquid Water by Combining Active and Passive Microwave Measurements with Cloud Model Statistics, Journal of Atmospheric and Oceanic Technology, 18, 1354–1366, doi:10.1175/1520-0426(2001)018<1354:PCLWBC>2.0.CO;2, http://dx.doi.org/10.1175/1520-0426(2001)018<1354:PCLWBC>2.0.CO;2, 2001.

Löhnert, U., Feingold, G., Uttal, T., Frisch, A. S., and Shupe, M. D.: Analysis of two independent methods for retrieving liquid water profiles in spring and summer Arctic boundary clouds, Journal of Geophysical Research: Atmospheres, 108, n/a–n/a, doi:10.1029/2002JD002861, http://dx.doi.org/10.1029/2002JD002861, 2003.

Mace, G. G. and Sassen, K.: A constrained algorithm for retrieval of stratocumulus cloud properties using solar radiation, microwave radiometer, and millimeter cloud radar data, Journal of Geophysical Research: Atmospheres, 105, 29 099–29 108, doi:10.1029/2000JD900403, http://dx.doi.org/10.1029/2000JD900403, 2000.

Marshak, A., Platnick, S., Várnai, T., Wen, G., and Cahalan, R. F.: Impact of three-dimensional radiative effects on satellite retrievals of cloud droplet sizes, Journal of Geophysical Research: Atmospheres, 111, n/a–n/a, doi:10.1029/2005JD006686, http://dx.doi.org/10.1029/2005JD006686, d09207, 2006.

Martucci, G. and O'Dowd, C. D.: Ground-based retrieval of continental and marine warm cloud microphysics, Atmospheric Measurement Techniques, 4, 2749–2765, doi:10.5194/amt-4-2749-2011, http://www.atmos-meas-tech.net/4/2749/2011/, 2011.

Martucci, G., Milroy, C., and O'Dowd, C. D.: Detection of Cloud-Base Height Using Jenoptik CHM15K and Vaisala CL31 Ceilometers, Journal of Atmospheric and Oceanic Technology, 27, 305–318, doi:10.1175/2009JTECHA1326.1, http://dx.doi.org/10.1175/2009JTECHA1326.1, 2010.

Meerkötter, R. and Bugliaro, L.: Diurnal evolution of cloud base heights in convective cloud fields from MSG/SEVIRI data, Atmospheric Chemistry and Physics, 9, 1767–1778, doi:10.5194/acp-9-1767-2009, http://www.atmos-chem-phys.net/9/1767/2009/, 2009.

Meirink, J. F., Roebeling, R. A., and Stammes, P.: Inter-calibration of polar imager solar channels using SEVIRI, Atmospheric Measurement Techniques, 6, 2495–2508, doi:10.5194/amt-6-2495-2013, http://www.atmos-meas-tech.net/6/2495/2013/, 2013.

Miles, N. L., Verlinde, J., and Clothiaux, E. E.: Cloud Droplet Size Distributions in Low-Level Stratiform Clouds, Journal of the Atmospheric Sciences, 57, 295–311, doi:10.1175/1520-0469(2000)057<0295:CDSDIL>2.0.CO;2, http://dx.doi.org/10.1175/1520-0469(2000)057<0295:CDSDIL>2.0.CO;2, 2000.

Min, Q., Joseph, E., Lin, Y., Min, L., Yin, B., Daum, P. H., Kleinman, L. I., Wang, J., and Lee, Y.-N.: Comparison of MODIS cloud microphysical properties with in-situ measurements over the Southeast Pacific, Atmospheric Chemistry and Physics, 12, 11 261–11 273, doi:10.5194/acp-12-11261-2012, http://www.atmos-chem-phys.net/12/11261/2012/, 2012.

Nakajima, T. and King, M. D.: Determination of the Optical Thickness and Effective Particle Radius of Clouds from Reflected Solar Radiation Measurements. Part I: Theory, Journal of the Atmospheric Sciences, 47, 1878–1893, doi:10.1175/1520-0469(1990)047<1878:DOTOTA>2.0.CO;2, http://dx.doi.org/10.1175/1520-0469(1990)047<1878:DOTOTA>2.0.CO;2, 1990.

Painemal, D. and Zuidema, P.: Microphysical variability in southeast Pacific Stratocumulus clouds: synoptic conditions and radiative response, Atmospheric Chemistry and Physics, 10, 6255–6269, doi:10.5194/acp-10-6255-2010, http://www.atmos-chem-phys.net/10/6255/2010/, 2010.

Painemal, D. and Zuidema, P.: Assessment of MODIS cloud effective radius and optical thickness retrievals over the Southeast Pacific with VOCALS-REx in situ measurements, Journal of Geophysical Research: Atmospheres, 116, n/a–n/a, doi:10.1029/2011JD016155, http://dx.doi.org/10.1029/2011JD016155, 2011.

Placidi, S., Roebeling, R., Donovan, D., Boers, R., and Russchenberg, H.: Evaluation of Meteosat-8/SEVIRI retrieved cloud depth for water clouds using CloudNet sites, in: Joint 2007 EUMETSAT Meteorological Satellite Conference and the 15th Satellite Meteorology & Oceanography Conference of the American Meteorological Society, vol. P.50, pp. s8–s12, EUMETSET, Amsterdam, The Netherlands, 2007.

Platnick, S.: Vertical photon transport in cloud remote sensing problems, Journal of Geophysical Research: Atmospheres, 105, 22 919–22 935, doi:10.1029/2000JD900333, http://dx.doi.org/10.1029/2000JD900333, 2000.

Platnick, S., King, M. D., Ackerman, S. A., Menzel, W. P., Baum, B. A., Riédi, J. C., and Frey, R. A.: The MODIS cloud products: Algorithms and examples from Terra, Geoscience and Remote Sensing, IEEE Transactions on, 41, 459–473, 2003.

Quaas, J., Boucher, O., and Lohmann, U.: Constraining the total aerosol indirect effect in the LMDZ and ECHAM4 GCMs using MODIS satellite data, Atmospheric Chemistry and Physics, 6, 955, http://hal.archives-ouvertes.fr/hal-00328423, 2006.

Rémillard, J., Kollias, P., and Szyrmer, W.: Radar-radiometer retrievals of cloud number concentration and dispersion parameter in nondrizzling marine stratocumulus, Atmospheric Measurement Techniques, 6, 1817–1828, doi:10.5194/amt-6-1817-2013, http://www.atmos-meas-tech.net/6/1817/2013/, 2013.

Rodgers, C.: Inverse methods for atmospheric sounding, vol. 2 of Series on Atmospheric, Oceanic and Planetary Physics, 2000.

Roebeling, R., Placidi, S., Donovan, D., Russchenberg, H., and Feijt, A.: Validation of liquid cloud property retrievals from SEVIRI using ground-based observations, Geophysical Research Letters, 35, L05 814, 2008a.

Roebeling, R. A., Feijt, A. J., and Stammes, P.: Cloud property retrievals for climate monitoring: Implications of differences between Spinning Enhanced Visible and Infrared Imager (SEVIRI) on METEOSAT-8 and Advanced Very High Resolution Radiometer (AVHRR) on NOAA-17, Journal of Geophysical Research: Atmospheres, 111, n/a–n/a, doi:10.1029/2005JD006990, http://dx.doi.org/10.1029/2005JD006990, 2006.

Roebeling, R. A., Deneke, H. M., and Feijt, A. J.: Validation of Cloud Liquid Water Path Retrievals from SEVIRI Using One Year of CloudNET Observations, Journal of Applied Meteorology and Climatology, 47, 206–222, doi:10.1175/2007JAMC1661.1, http://dx.doi.org/10.1175/2007JAMC1661.1, 2008b.

Rosenfeld, D., Wang, H., and Rasch, P. J.: The roles of cloud drop effective radius and LWP in determining rain properties in marine stratocumulus, Geophysical Research Letters, 39, doi:10.1029/2012GL052028, http://dx.doi.org/10.1029/2012GL052028, 2012.

Saunders, R., Matricardi, M., and Brunel, P.: An improved fast radiative transfer model for assimilation of satellite radiance observations, Quarterly Journal of the Royal Meteorological Society, 125, 1407–1425, doi:10.1002/qj.1999.49712555615, http://dx.doi.org/10.1002/qj.1999.49712555615, 1999.

Schmetz, J., Pili, P., Tjemkes, S., Just, D., Kerkmann, J., Rota, S., and Ratier, A.: An introduction to Meteosat Second Generation (MSG)., Bulletin of the American Meteorological Society, 83, 2002.

Schmidt, J., Wandinger, U., and Malinka, A.: Dual-field-of-view Raman lidar measurements for the retrieval of cloud microphysical properties, Appl. Opt., 52, 2235–2247, doi:10.1364/AO.52.002235, http://ao.osa.org/abstract.cfm?URI=ao-52-11-2235, 2013.

Schmidt, J., Ansmann, A., Bühl, J., Baars, H., Wandinger, U., Müller, D., and Malinka, A. V.: Dual-FOV Raman and Doppler lidar studies of aerosol-cloud interactions: Simultaneous profiling of aerosols, warm-cloud properties, and vertical wind, Journal of Geophysical Research: Atmospheres, 119, 5512–5527, doi:10.1002/2013JD020424, http://dx.doi.org/10.1002/2013JD020424, 2014a.

Schmidt, J., Ansmann, A., Bühl, J., and Wandinger, U.: Role of updrafts in aerosol-cloud interactions: lidar observations of layered warm clouds over central Europe, Atmospheric Chemistry and Physics Discussions, 14, 31 409–31 440, doi:10.5194/acpd-14-31409-2014, http://www.atmos-chem-phys-discuss.net/14/31409/2014/, 2014b.

Schueller, L., Brenguier, J.-L., and Pawlowska, H.: Retrieval of microphysical, geometrical, and radiative properties of marine stratocumulus from remote sensing, J. Geophys. Res., 108, 8631, doi:10.1029/2002JD002680, http://dx.doi.org/10.1029/2002JD002680, 2003.

Schulz, J., Albert, P., Behr, H.-D., Caprion, D., Deneke, H., Dewitte, S., Dürr, B., Fuchs, P., Gratzki, A., Hechler, P., Hollmann, R., Johnston, S., Karlsson, K.-G., Manninen, T., Müller, R., Reuter, M., Riihelä, A., Roebeling, R., Selbach, N., Tetzlaff, A., Thomas, W., Werscheck, M., Wolters, E., and Zelenka, A.: Operational climate monitoring from space: the EUMETSAT Satellite Application Facility on Climate Monitoring (CM-SAF), Atmospheric Chemistry and Physics, 9, 1687–1709, doi:10.5194/acp-9-1687-2009, http://www.atmos-chem-phys.net/9/1687/2009/, 2009.

Shupe, M. D.: A ground-based multisensor cloud phase classifier, Geophysical Research Letters, 34, n/a–n/a, doi:10.1029/2007GL031008, http://dx.doi.org/10.1029/2007GL031008, 2007.

Stephens, G. L., Vane, D. G., Boain, R. J., Mace, G. G., Sassen, K., Wang, Z., Illingworth, A. J., O'Connor, E. J., Rossow, W. B., Durden, S. L., Miller, S. D., Austin, R. T., Benedetti, A., Mitrescu, C., and CloudSat Science Team, T.: THE CLOUDSAT MISSION AND THE A-TRAIN, Bulletin of the American Meteorological Society, 83, 1771–1790, doi:10.1175/BAMS-83-12-1771, http://dx.doi.org/10.1175/BAMS-83-12-1771, 2002.

Turner, D. D., Vogelmann, A. M., Johnson, K., Miller, M., Austin, R. T., Barnard, J. C., Flynn, C., Long, C., McFarlane, S. A., Cady-Pereira, K., Clough, S. A., Chiu, J. C., Khaiyer, M. M., Liljegren, J., Lin, B., Minnis, P., Marshak, A., Matrosov, S. Y., Min, Q., O'Hirok, W., Wang, Z., and Wiscombe, W.: Thin Liquid Water Clouds: Their Importance and Our Challenge, Bulletin of the American Meteorological Society, 88, 177–190, doi:10.1175/BAMS-88-2-177, http://dx.doi.org/10.1175/BAMS-88-2-177, 2007.

Twomey, S.: Pollution and the planetary albedo, Atmospheric Environment (1967), 8, 1251 – 1256, doi:10.1016/0004-6981(74)90004-3, http://www.sciencedirect.com/science/article/pii/0004698174900043, 1974.

Winker, D. M., Vaughan, M. A., Omar, A., Hu, Y., Powell, K. A., Liu, Z., Hunt, W. H., and Young, S. A.: Overview of the CALIPSO Mission and CALIOP Data Processing Algorithms, Journal of Atmospheric and Oceanic Technology, 26, 2310–2323, doi:10.1175/2009JTECHA1281.1, http://dx.doi.org/10.1175/2009JTECHA1281.1, 2009.

Wood, R.: Relationships between optical depth, liquid water path, droplet concentration, and effective radius in adiabatic layer cloud, University of Washington, 3, 2006.

Zeng, S., Riedi, J., Trepte, C. R., Winker, D. M., and Hu, Y.-X.: Study of global cloud droplet number concentration with A-Train satellites, Atmospheric Chemistry and Physics, 14, 7125–7134, doi:10.5194/acp-14-7125-2014, http://www.atmos-chem-phys.net/14/7125/2014/, 2014.